71B Antiferroelectric liquid crystals

No. 71B-1 MHPOBC and analogues

L–⬡–⬡–COO–⬡–R

(A) L: $C_nH_{2n+1}O$, R: $COOCH(CH_3)C_mH_{2m+1}$
4-(1-methylalkyl oxycarbonyl)phenyl 4′-alkoxybiphenyl-4-carboxylate
n = 8, m = 6: MHPOBC (4-(1-methylheptyl oxycarbonyl)phenyl 4′-octyloxybiphenyl-4-carboxylate)

1a Antiferroelectricity of 4-(1-methylheptyl oxycarbonyl)phenyl 4′-octyloxybiphenyl-4-carboxylate (MHPOBC) was discovered by Chadani et al. in 1989. 89Cha

b MHPOBC: 97Asa

phase	VI [++])	V	IV	III	II	I	I′
	crystalline solid	smectic C_A^* (Sm C_A^*)	smectic C_γ^* (Sm C_γ^*)	smectic C^* (Sm C^*)	smectic C_α^* (Sm C_α^*)	smectic A (Sm A)	isotropic liquid
state		A	F′ [+])	F	P	P	
Θ [°C]	65 [a])	119.7	120.6	122.1	123.4	148.6	

[a]) 95Kim

[+]) Triple *D-E* hysteresis loop is observed in Sm C_γ^* phase. For this reason the Sm C_γ^* phase is often called "ferrielectric".

[++]) Phase transition between V and VI is sensitive to the optical purity of *R*- or *S*-MHPOBC. Slight reduction of the purity results in the occurrence of Sm I_A^* phase between them [91Tak1]. See Fig. 71B-1-001.

Phase diagram for mixture of *R*- and *S*-MHPOBC: Fig. 71B-1-001.

3b Tilt angle: Fig. 71B-1-002, Fig. 71B-1-003, Fig. 71B-1-004, Fig. 71B-1-005, Fig. 71B-1-006, Fig. 71B-1-007.
Layer spacing: Fig. 71B-1-008; see also Fig. 71B-1-089.
Chevron angle: Fig. 71B-1-009.

5a Dielectric constant: Fig. 71B-1-010.
Dielectric dispersion: Fig. 71B-1-011, Fig. 71B-1-012, Fig. 71B-1-013, Fig. 71B-1-014, Fig. 71B-1-015.
Transition temperatures in regard to electric field: Fig. 71B-1-016.

b Effect of bias electric field on dielectric constant: Fig. 71B-1-017.

c Spontaneous polarization: Fig. 71B-1-018, Fig. 71B-1-019.
D-E hysteresis: Fig. 71B-1-020, Fig. 71B-1-021.

6a Transition heat ΔH and transition entropy ΔS of MHPOBC: 97Asa

	Sm C_A^* → Sm C_γ^* → Sm C^* → Sm C_α^* → Sm A → isotropic liquid				
ΔH [J mol^{-1}]	16.4	18.8	14.6	288	6420
ΔS [J K^{-1}mol^{-1}]	0.042	0.048	0.037	0.733	15.2

Specific heat: Fig. 71B-1-022, Fig. 71B-1-023, Fig. 71B-1-024.
DSC: Fig. 71B-1-025.

9a Birefringence: Fig. 71B-1-026.
Reflection band: Fig. 71B-1-027, Fig. 71B-1-028.

Transmission: Fig. 71B-1-029.
Ellipsometric angle: Fig. 71B-1-030, Fig. 71B-1-031.
Tilt angle of optical axis: Fig. 71B-1-032.
Effect of magnetic field on conoscopic figure: Fig. 71B-1-033, Fig. 71B-1-034.

b Effect of electric field on birefringence: Fig. 71B-1-035.
Hysteresis of transmittance: Fig. 71B-1-036, Fig. 71B-1-037.
Change in transmittance with electric field: Fig. 71B-1-038, Fig. 71B-1-039, Fig. 71B-1-040.
Frequency response of electrooptical properties: Fig. 71B-1-041, Fig. 71B-1-042, Fig. 71B-1-043, Fig. 71B-1-044.
Infrared absorbance: Fig. 71B-1-045.
Response time in a mixture of MHPOBC, TFMHPOBC, TFMHPDBC: see 91Yam

d Optical rotatory power: Fig. 71B-1-046.
Circular dichroism: Fig. 71B-1-047, Fig. 71B-1-048.

10a Raman scattering: Fig. 71B-1-049, Fig. 71B-1-050, Fig. 71B-1-051.

b Photon correlation spectroscopy:
Autocorrelation function: Fig. 71B-1-052.
Relaxation time: Fig. 71B-1-053, Fig. 71B-1-054, Fig. 71B-1-055, Fig. 71B-1-056, Fig. 71B-1-057, Fig. 71B-1-058, Fig. 71B-1-059.
Relaxation time related to orientational elastic constants: Fig. 71B-1-060, Fig. 71B-1-061, Fig. 71B-1-062.
Relaxation time related to twist elastic constant: Fig. 71B-1-063, Fig. 71B-1-064; see also Fig. 71B-1-062.

14a Higher order X-ray Bragg reflections: Fig. 71B-1-065; see also Fig. 71B-1-008 in 3b.
Smectic order parameter: Fig. 71B-1-066.

15 Switching current: Fig. 71B-1-067.

(B) L: C_nH_{2n+1}, R: $COOCH(CH_3)C_mH_{2m+1}$ 4-(1-methylalkyloxycarbonyl)phenyl 4′-alkylbiphenyl-4-carboxylate

n = 8, m = 6: MHPBC (4-(1-methylheptyloxycarbonyl)phenyl 4′-octylbiphenyl-4-carboxylate)

1b MHPBC: 92Oka

phase	V	IV	III	II	I	I′
	smectic C^*_A (Sm C^*_A)	smectic C^*_γ (Sm C^*_γ)		smectic C^*_α (Sm C^*_α)	smectic A (Sm A)	isotropic liquid
state	(A)	(F′) [+])	(A)	(F)	P	
Θ [°C]		64.9	66.4	72.1	76.3	109.0

[+]) "ferrielectric". Two addditional phases, Fl_H and Fl_L, are found above and below the Sm C^*_γ phase: see Fig. 71B-1-068.

Phase diagram for mixture of MHPBC and TFMHPBC: Fig. 71B-1-068.

5a Dielectric constant: Fig. 71B-1-069.
Relaxation frequency and dielectric strength: Fig. 71B-1-070.

(C) L: $C_nH_{2n+1}COO$, R: $COOCH(CH_3)C_mH_{2m+1}$
4-(1-methylalkyloxycarbonyl)phenyl 4′-alkylcarbonyloxy biphenyl-4-carboxylate
n = 8, m = 6: MHPOCBC (4-(1-methylheptyloxycarbonyl)phenyl 4′-octylcarbonyloxy biphenyl-4-carboxylate)
n = 11, m = 6: LC1
n = 14, m = 6: LC2

1b MHPOCBC: 97Asa

phase	V	IV	III	II	I	I′
	crystalline solid	smectic I* (SmI*)	smectic C_A^* (Sm C_A^*)	smectic C_α^* (Sm C_α^*)	smectic A (Sm A)	isotropic liquid
state			A	(F)	P	
Θ [°C]		66.1 [a])	73.3 [a])	100.0	105.3	147.3

[a]) 91Iso

LC1, LC2: 96Gou

phase		VI	V	IV	III	II	I	I′
		crystal-line solid	smectic I* (SmI*)	smectic C_A^* (Sm C_A^*)	smectic C_γ^* (Sm C_γ^*)	smectic C* (Sm C*)	smectic A (Sm A)	isotropic liquid
state				(A)	(F′) [+])	(F)	P	
Θ [°C]	LC1	66.3	(52.0)	108.9	109.6	118.6	137.2	
	LC2	59.9	(53.5)	83.5	92.2	116.0	130.1	

( ): cooling

[+]) "ferrielectric": see 1b of (A).

Phase diagram for mixture of MHPOCBC and MHPOOCBC: Fig. 71B-1-071.

3b Tilt angle: Fig. 71B-1-072, Fig. 71B-1-073.
Layer thickness: Fig. 71B-1-074.

5a Dielectric constant: Fig. 71B-1-075, Fig. 71B-1-076, Fig. 71B-1-077.
See also Fig. 71B-1-073.

b Nonlinear dielectric constants: Fig. 71B-1-078.
Effect of E_{bias}: see Fig. 71B-1-077.

6a Specific heat: Fig. 71B-1-079, Fig. 71B-1-080.
Transition heat ΔH and transition entropy ΔS of MHPOCBC: 97Asa

	Sm C_A^*	→	Sm C_α^*	→	Sm A	→	isotropic liquid
ΔH [J mol^{-1}]	11.6		70.3		6280		
ΔS [J K^{-1}mol^{-1}]	0.031		0.187		14.9		

9a Selective reflection band: Fig. 71B-1-081, Fig. 71B-1-082.

d Liquid crystal induced circular dichroism: Fig. 71B-1-083.

(D) L: $C_nH_{2n+1}OCO$, R: $COOCH(CH_3)C_mH_{2m+1}$
n = 8, m = 6: MHPOOCBC

1b MHPOOCBC: 93Iso2

phase	IV	III	II	I	I′
	crystalline solid	smectic C^*_γ (Sm C^*_γ)	smectic C^* (Sm C^*)	smectic A (Sm A)	isotropic liquid
state		(F′) [+])	F	P	
Θ [°C]	40.0	41.9	87.2	101.3 [a])	[a]) 95LiJ

[+]) Supposed to be "ferrielectric": see 1b of (A). 93Iso2

Phase diagram for MHPOCBC-MHPOOCBC mixture: see Fig. 71B-1-071.

5c $P_s = 1 \cdot 10^{-3}$ C m^{-2}. 91Tak4

9a Selective reflection band: Fig. 71B-1-084.

(E) L: $C_nH_{2n+1}O$, R: $COCH(CH_3)C_mH_{2m+1}$
4-(1,1,1-methylalkylcarbonyl)phenyl 4′-alkoxybiphenyl-4-carboxylate
n = 8, m = 6: MOPBIC (4-(1,1,1-methylheptylcarbonyl)phenyl 4′-octyloxybiphenyl-4-carboxylate)

1b MOPBIC: 91LiJ

phase	III	II	I	I′
	smectic C^*_A (Sm C^*_A)	smectic C^* (Sm C^*)	smectic A (Sm A)	isotropic liquid
state	(A)	F	P	
Θ [°C]	91.6	136.5	156.0	

3b Tilt angle: Fig. 71B-1-085.

5c Spontaneous polarization: Fig. 71B-1-086.

9a Reflection band: see Fig. 71B-1-028.

(F) L: $C_8H_{17}O$, R: $COOCH(CH_3)CH_2COOCH_3$
3MC2PCPOPB (4′-(3-methoxycarbonyl-2-propoxycarbonyl) phenyl 4-(4-(*n*-octyloxy)phenyl) benzoate

1b

phase	VI	V	IV	III	II	I	I′
	crystalline solid	smectic X (Sm X)	smectic C^*_γ (Sm C^*_γ)	smectic C^*_A (Sm C^*_A)	smectic C^* (Sm C^*)	smectic A (Sm A)	isotropic liquid
state			(F′) [+])	A	(F)	P	
Θ [°C]	72	80	85	115	118	165	

93Mor1

[+]) Supposed to be "ferrielectric".

3b Tilt angle: Fig. 71B-1-087.

5a Dielectric constant: see 92Mor
Θ vs. E_{bias}: see 92Mor

(G) L: $C_nH_{2n+1}O$, R: $COOCH(CF_3)C_mH_{2m+1}$
4-(1-trifluoromethyl alkoxycarbonyl) phenyl 4′-alkoxybiphenyl-4-carboxylate
n = 8, m = 6: TFMHPOBC (4-(1-trifluoromethyl heptyloxycarbonyl) phenyl 4′-octyloxybiphenyl-4-carboxylate)
n = 8, m = 8: TFMNPOBC (4-(1-trifluoromethyl nonayloxycarbonyl) phenyl 4′-octyloxybiphenyl-4-carboxylate)

1b

phase		III	II	I	I′	93Mor1
		crystalline solid	smectic C_A^* (Sm C_A^*)	smectic A (Sm A)	isotropic liquid	91LiJ
state			A	P		
Θ [°C]	TFMHPOBC	64	116	125		
	TFMNPOBC	57 [a])	103	114		[a]) 89Suz

Ferroelectric Sm C* phase was reported in a narrow temperature range between phases I and II. 89Suz
Θ for n = 6, 8; m = 6, 8, 10, 12; see also 89Suz
Phase diagram of racemic mixture: Fig. 71B-1-088.

3b Layer thickness: Fig. 71B-1-089.
Rotation angle of smectic layer by voltage pulse: Fig. 71B-1-090, Fig. 71B-1-091.
Helical pitch: see Fig. 71B-1-108 in subsection 9a.

5a Dielectric constant: Fig. 71B-1-092, Fig. 71B-1-093, Fig. 71B-1-094, Fig. 71B-1-095.
Dielectric dispersion: Fig. 71B-1-096, Fig. 71B-1-097, Fig. 71B-1-098, Fig. 71B-1-099, Fig. 71B-1-100.
E–T phase diagram: Fig. 71B-1-101.

b Effect of E_{bias}: Fig. 71B-1-102, Fig. 71B-1-103, Fig. 71B-1-104.
Nonlinear dielectric constant: Fig. 71B-1-105, Fig. 71B-1-106, Fig. 71B-1-107.

c Spontaneous polarization: see Fig. 71B-1-019.

9a Reflection: Fig. 71B-1-108; see also Fig. 71B-1-028.
Transmittance change in field induced phase transition: Fig. 71B-1-109, Fig. 71B-1-110, Fig. 71B-1-111.

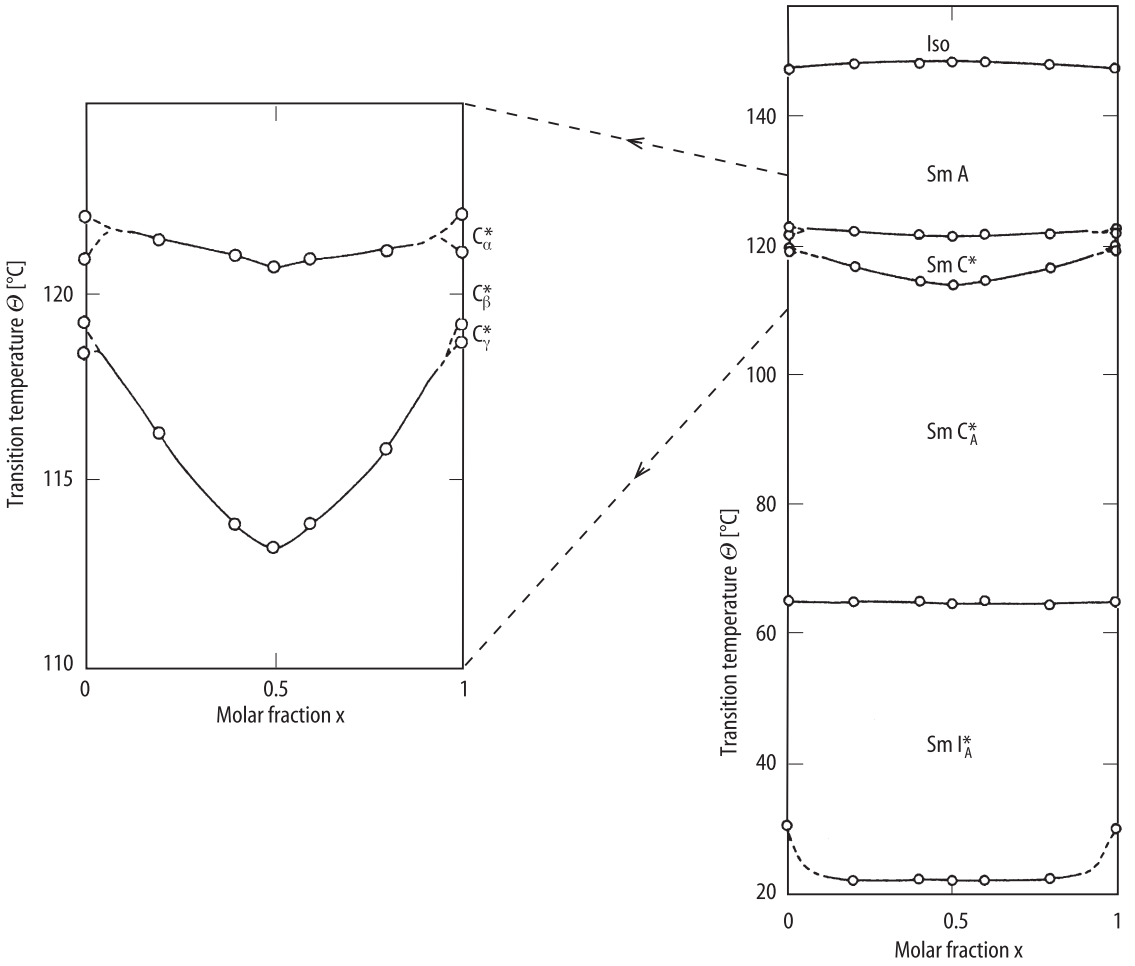

Fig. 71B-1-001. $(R\text{-MHPOBC})_{1-x}(S\text{-MHPOBC})_x$. Θ vs. x [91Tak1]. Phase diagram around Sm C* phase is shown in the left hand figure.

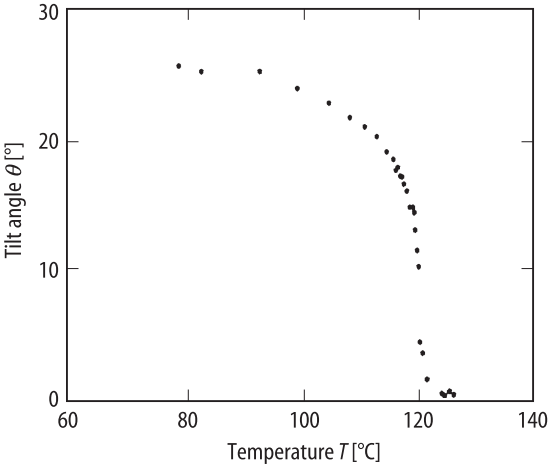

Fig. 71B-1-002. MHPOBC. θ vs. T [93Glo]. θ: tilt angle.

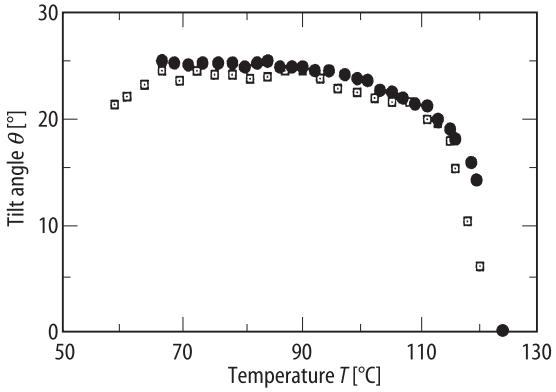

Fig. 71B-1-003. MHPOBC. θ vs. T [94Kim]. θ: tilt angle. Full circle: optical microscope measurement. Square: Raman scattering.

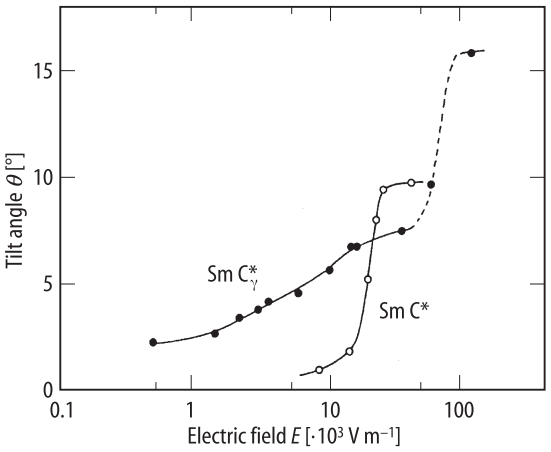

Fig. 71B-1-004. MHPOBC. θ vs. E [90Gor]. θ: tilt angle observed by conoscopic observation. Electric field E was applied parallel to the smectic layer.

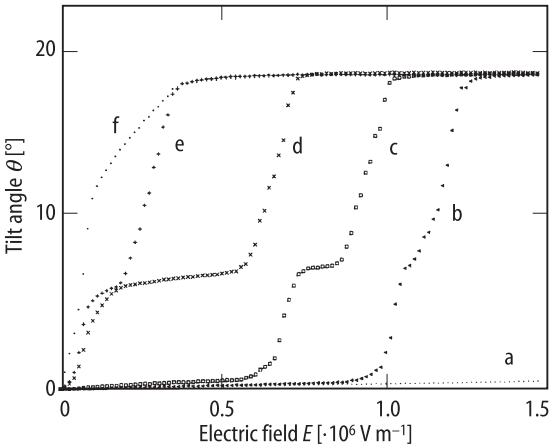

Fig. 71B-1-005. MHPOBC. θ vs. E [91Hir1]. Parameter: T. θ: tilt angle. Sm C_A^* phase: curve a: 113.0 °C, b: 114.7 °C, c: 115.2 °C. Sm C_γ^* phase: curve d: 115.8 °C, e: 116.5 °C. Sm C^* phase: curve f: 116.7 °C.

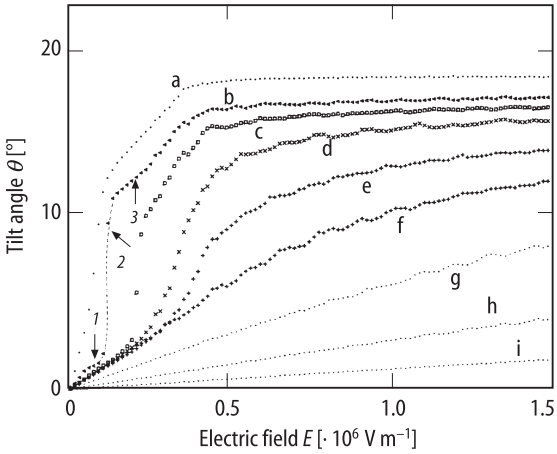

Fig. 71B-1-006. MHPOBC. θ vs. E [91Hir1]. Parameter: T. θ: tilt angle. Sm C* phase: curve a: 116.8 °C. Sm C^*_α phase: curve b: 118.2 °C, c: 118.5 °C, d: 118.8 °C, e: 119.2 °C, f: 119.5 °C. Sm A phase: curve g: 120 °C, h: 121 °C, i: 123 °C. (*1*), (*3*): two kinds of ferrielectric phases. (*2*): transition region between (*1*) and (*3*).

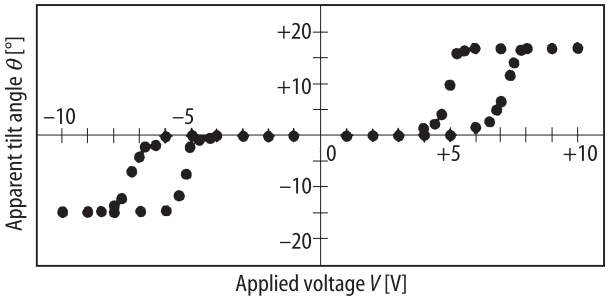

Fig. 71B-1-007. MHPOBC. θ vs. V [88Cha]. T = 107 °C. θ: apparent tilt angle defined as an angle between the layer normal and the extinction direction. V: applied voltage. Cell thickness: 3 μm.

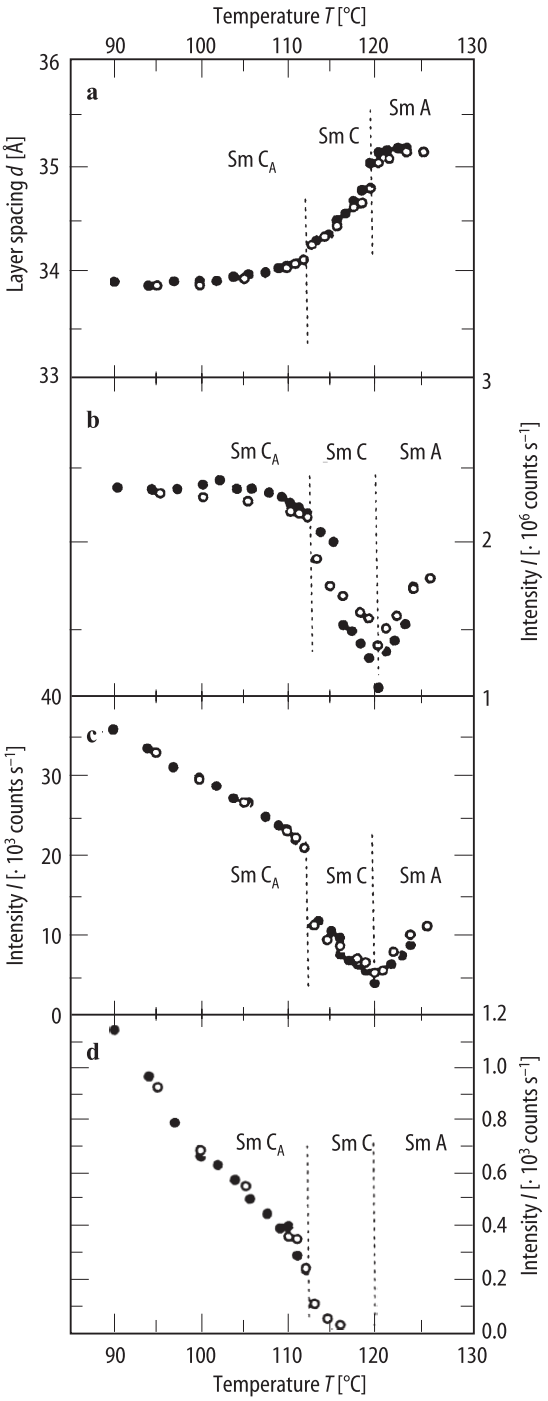

Fig. 71B-1-008. MHPOBC (racemic). (**a**) *d* vs. *T*. (**b**), (**c**), (**d**) *I* vs. *T* [95Tak]. *d*: layer spacing. *I*: integrated X-ray intensity of the first (b), second (c) and third (d) order reflections. Open circle: heating. Full circle: cooling.

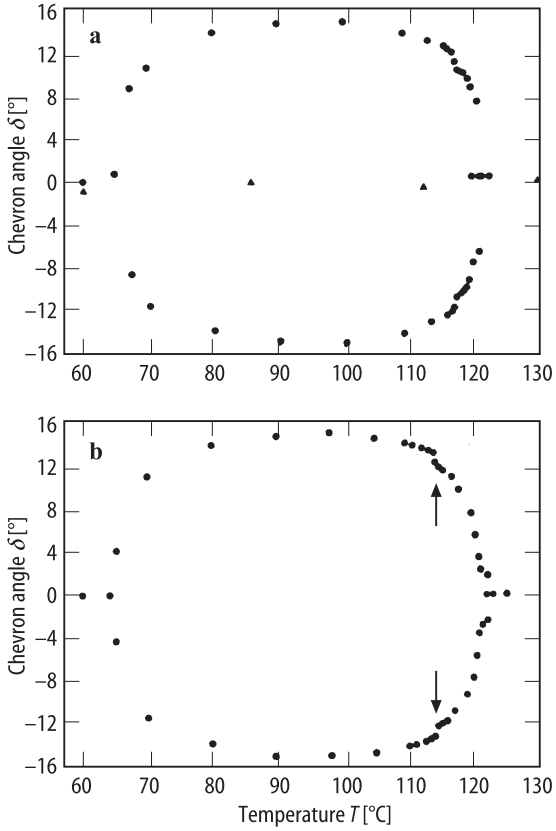

Fig. 71B-1-009. MHPOBC. δ vs. T [90Suz]. δ: chevron angle of smectic layer structure. (**a**) Pure sample. (**b**) Mixture of *R*- and *S*-MHPOBC with $R : S = 8 : 2$. Circle: cooling. Triangle: heating.

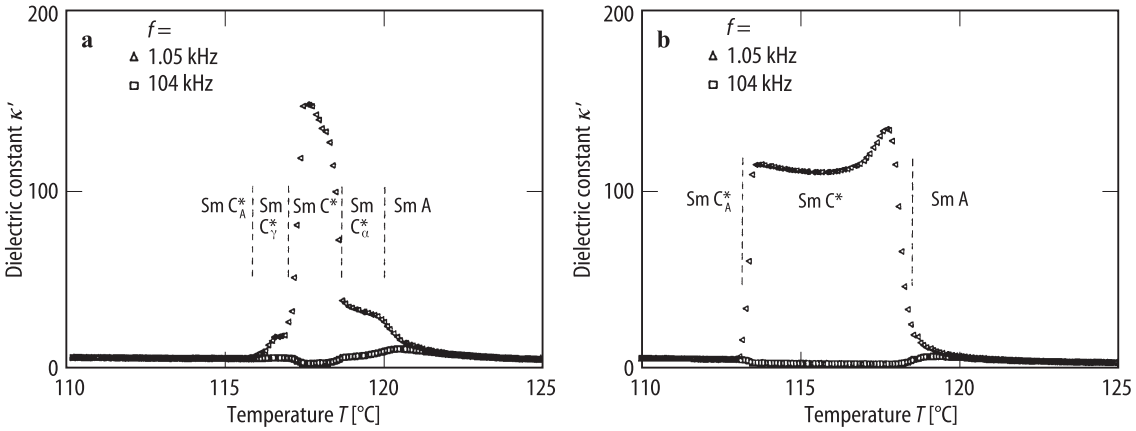

Fig. 71B-1-010. MHPOBC. κ' vs. T [90Hir1]. Parameter: *f*. (**a**) *R*-MHPOBC. (**b**) Mixture of *R*- and *S*-MHPOBC with $R : S = 8 : 2$.

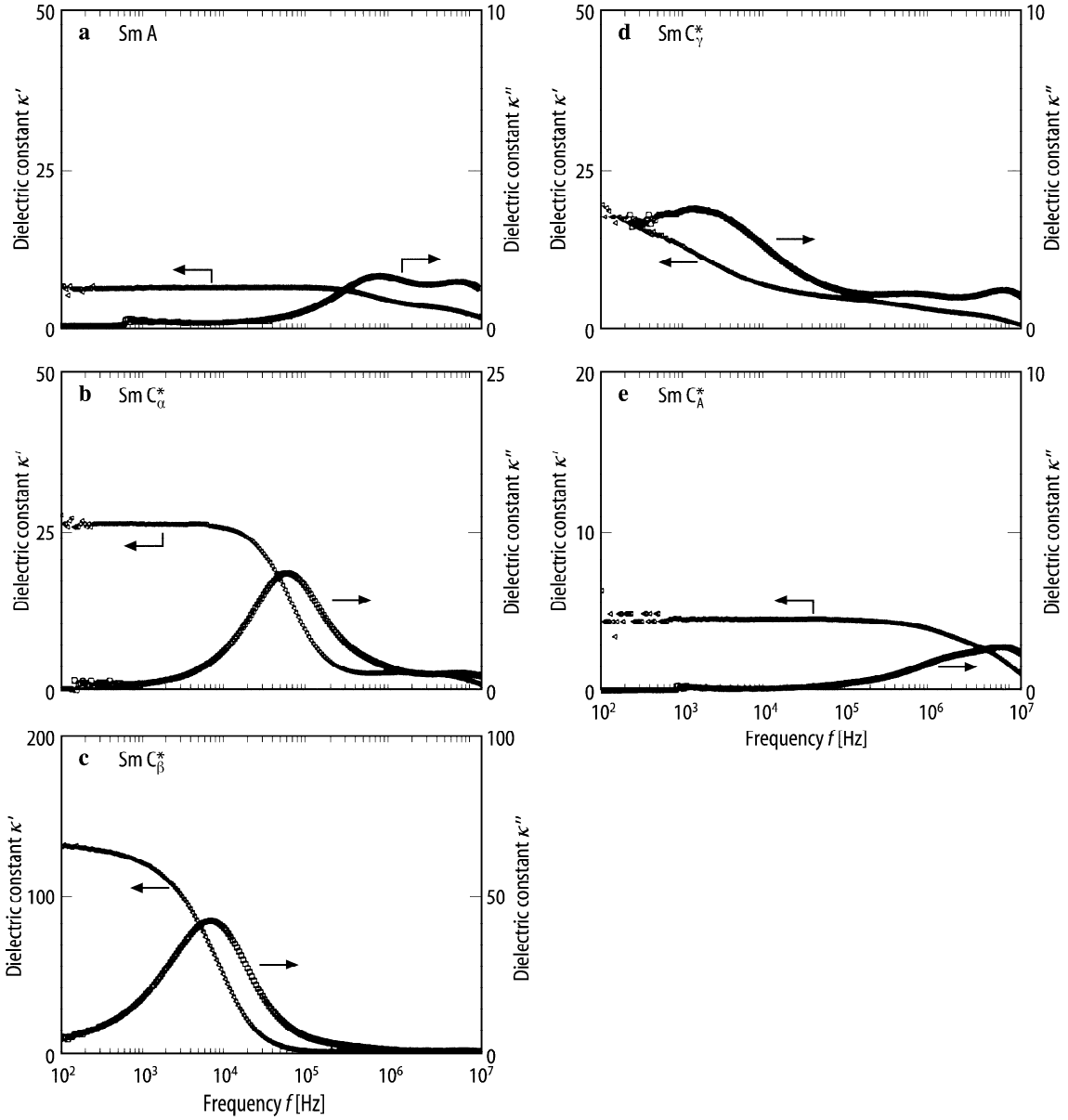

Fig. 71B-1-011. MHPOBC. κ', κ'' vs. f [90Hir1]. (**a**) Sm A phase. (**b**) Sm C^*_α phase. (**c**) Sm C^*_β phase. (**d**) Sm C^*_γ phase. (**e**) Sm C^*_A phase.

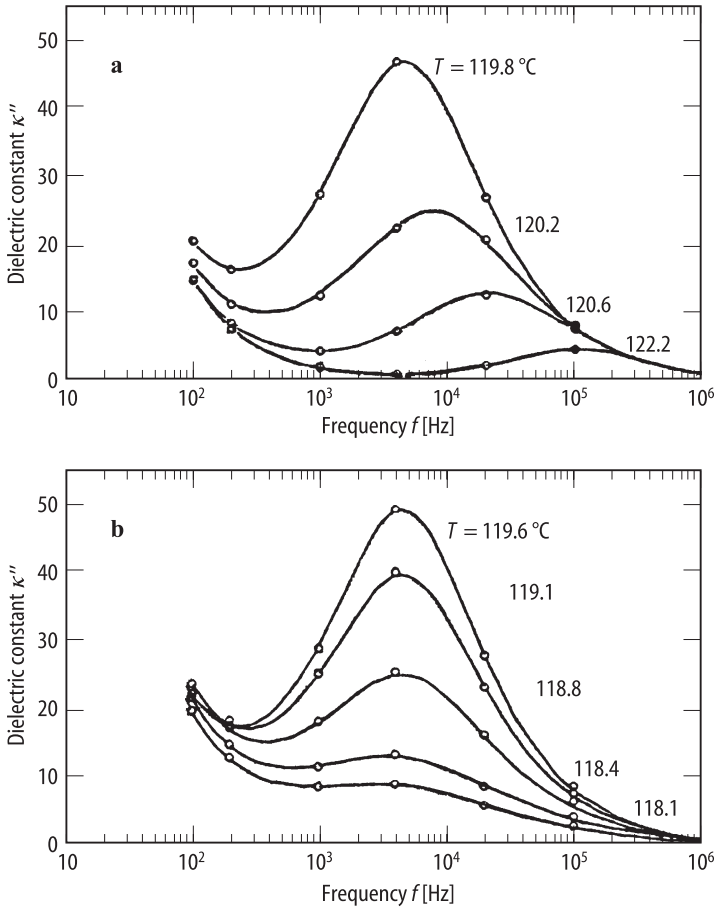

Fig. 71B-1-012. MHPOBC. κ'' vs. f [90Fuk]. Parameter: T. (**a**) Sm A phase. (**b**) From Sm C_A^* to Sm C^* phase.

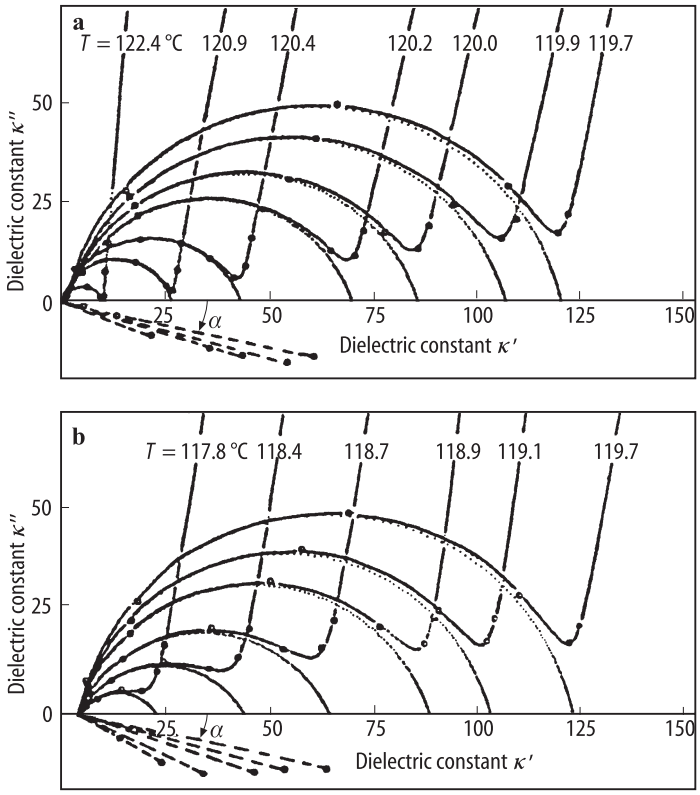

Fig. 71B-1-013. MHPOBC. κ' vs. κ'' (Cole-Cole plot) [90Fuk]. Parameter: T. (**a**) Sm A phase. (**b**) From Sm C_A^* to Sm C^* phase. Dotted lines: best fit to the Cole-Cole formula. Circles below the abscissa are the centers of the arcs.

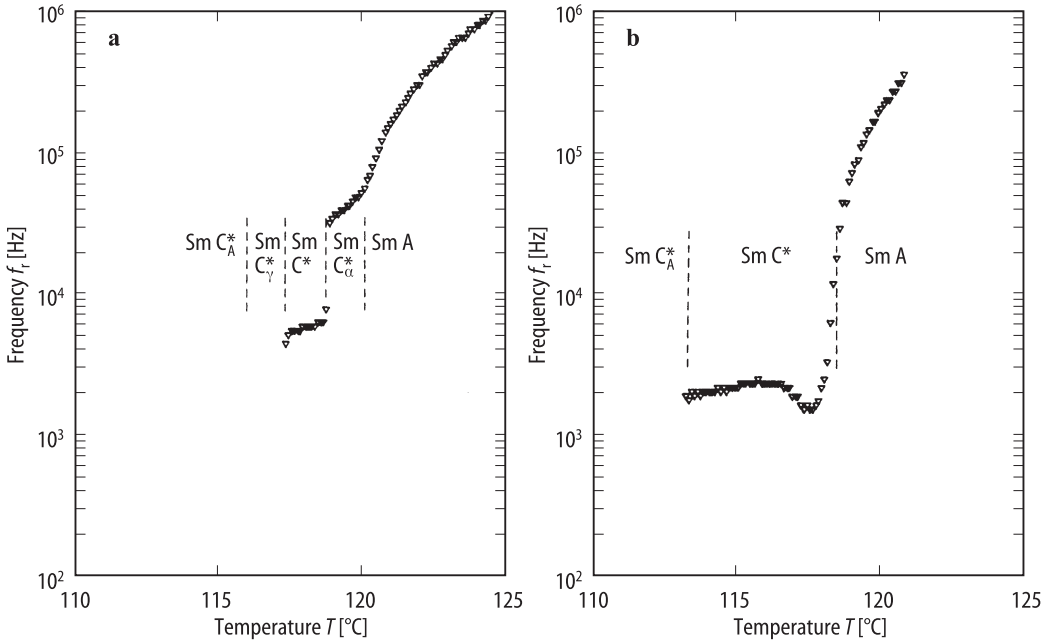

Fig. 71B-1-014. MHPOBC. f_r vs. T [90Hir1]. f_r: dielectric relaxation frequency. (**a**) Pure *R*-MHPOBC. (**b**) Mixture of *R*- and *S*-MHPOBC with $R : S = 8 : 2$.

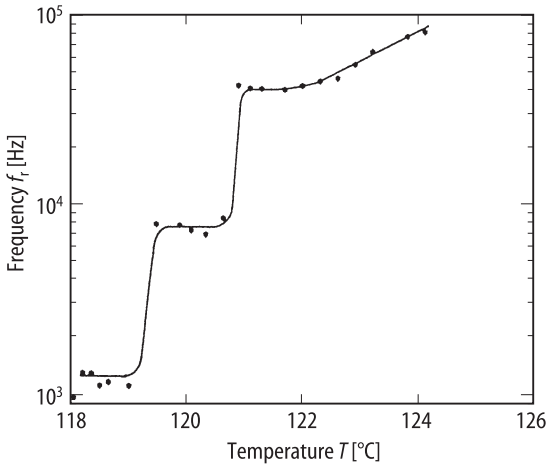

Fig. 71B-1-015. MHPOBC. f_r vs. T [93Glo]. f_r: dielectric relaxation frequency in Sm A, Sm C^*_γ and Sm C^* phases.

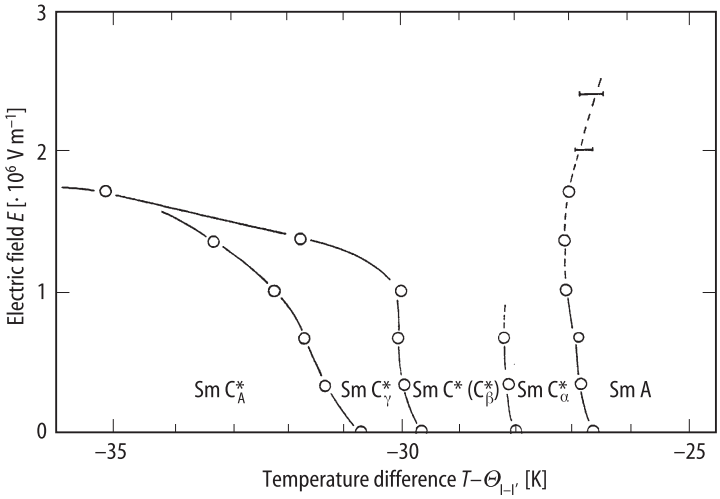

Fig. 71B-1-016. MHPOBC. E vs. $T - \Theta_{I-I'}$ obtained by dielectric measurements [90Hir2]. E: applied electric field.

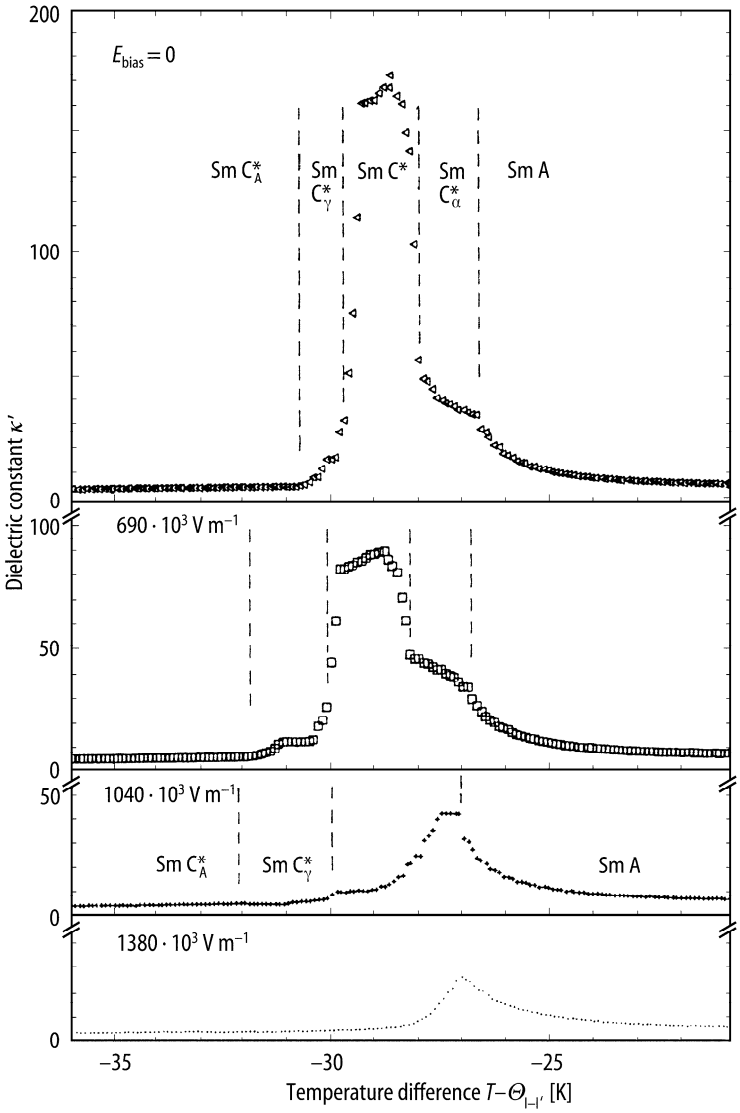

Fig. 71B-1-017. MHPOBC. κ' vs. $T - \Theta_{I-I'}$ [90Hir2]. Parameter: E_{bias}.

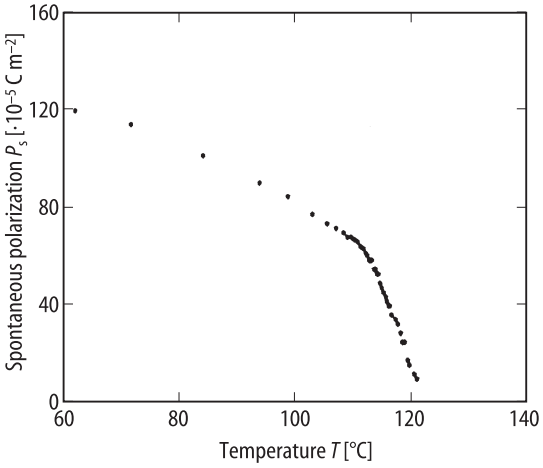

Fig. 71B-1-018. MHPOBC. P_s vs. T [93Glo].

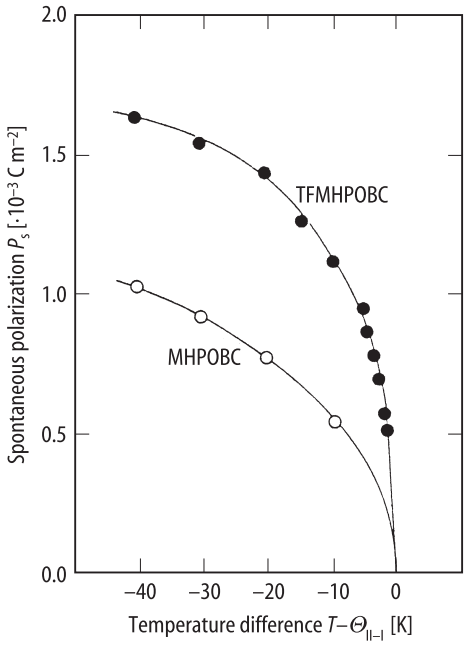

Fig. 71B-1-019. MHPOBC, TFMHPOBC. P_s vs. $T - \Theta_{II-I}$ [89Suz].

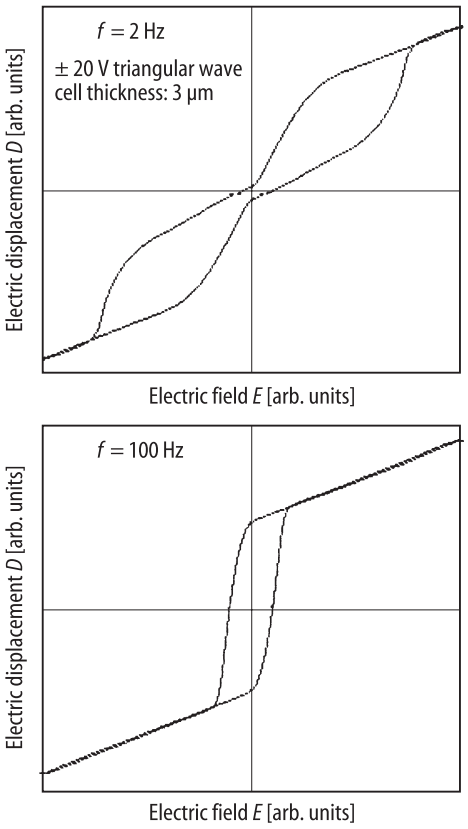

Fig. 71B-1-020. MHPOBC. $D - E$ hysteresis loop in Sm C_A^* phase [90Lee1]. Parameter: f.

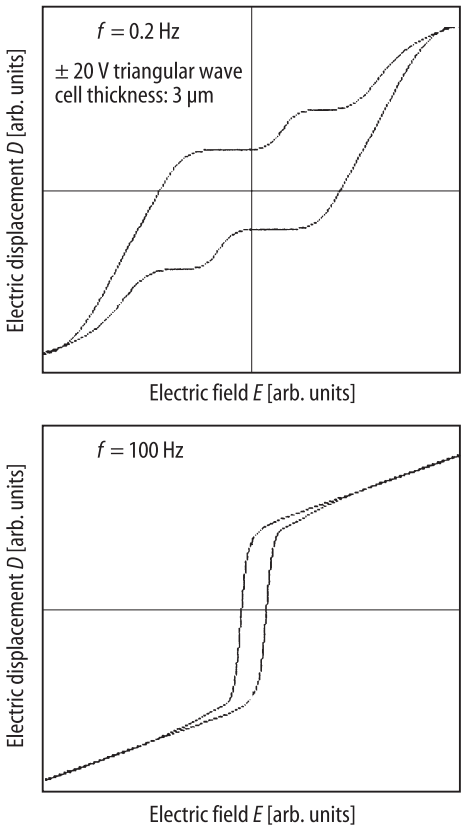

Fig. 71B-1-021. MHPOBC. $D - E$ hysteresis loop in Sm C^*_γ phase [90Lee1]. Parameter: *f*.

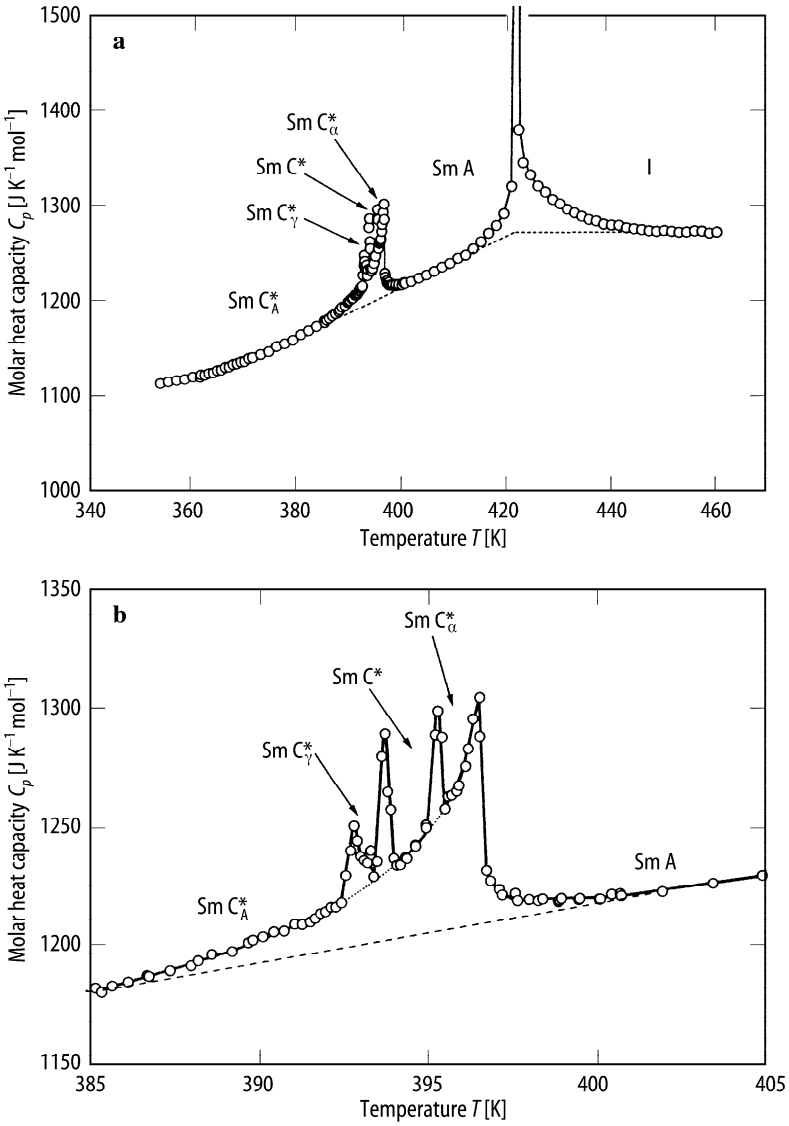

Fig. 71B-1-022. MHPOBC. C_p vs. T [97Asa]. C_p: molar heat capacity at constant pressure. (**a**) T = 350 K ... 460 K. (**b**) T = 385 K ... 405 K.

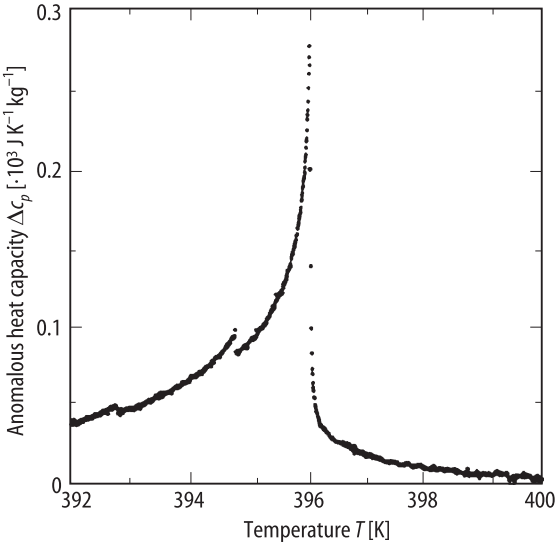

Fig. 71B-1-023. MHPOBC. Δc_p vs. T [96Ema1]. Δc_p: anomalous part of specific heat capacity at constant pressure.

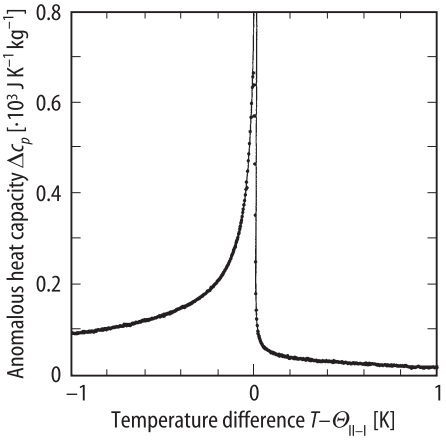

Fig. 71B-1-024. MHPOBC racemic mixture. Δc_p vs. $T - \Theta_{II-I}$ near Sm A – Sm C* phase transition [96Ema2]. Δc_p: anomalous part of specific heat capacity at constant pressure.

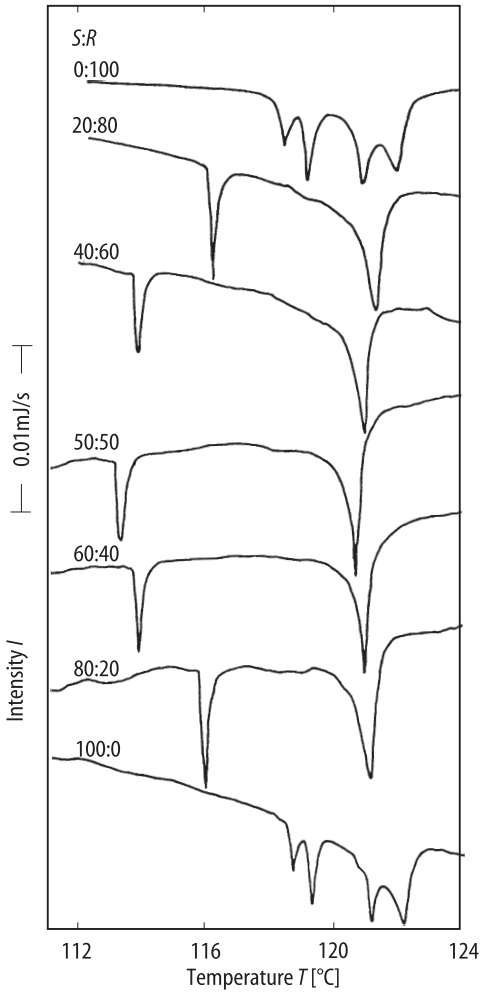

Fig. 71B-1-025. *R*-, *S*-MHPOBC. *I* vs. *T* [91Tak1]. *I*: intensity of DSC signal. Parameter: *S* : *R*.

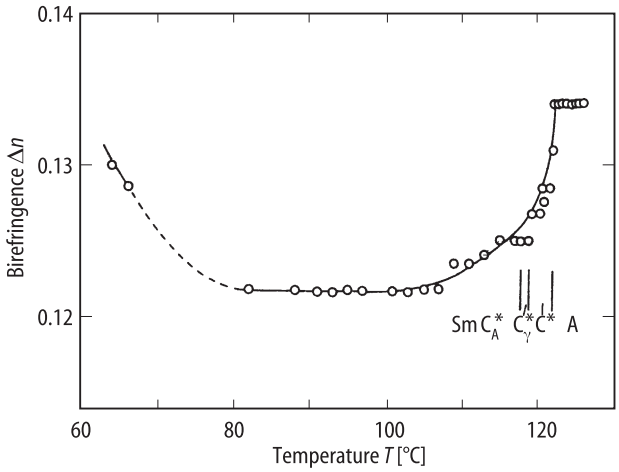

Fig. 71B-1-026. MHPOBC. Δ*n* vs. *T* [90Gor]. Δ*n*: birefringence obtained from conoscopic figure using He-Ne laser light.

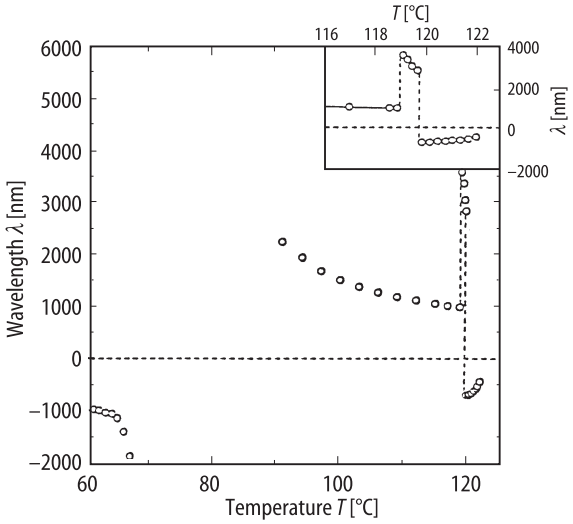

Fig. 71B-1-027. MHPOBC. λ vs. T [91Tak2]. λ: wavelength of a reflection mode. The sign distinguishes the sense of the helix.

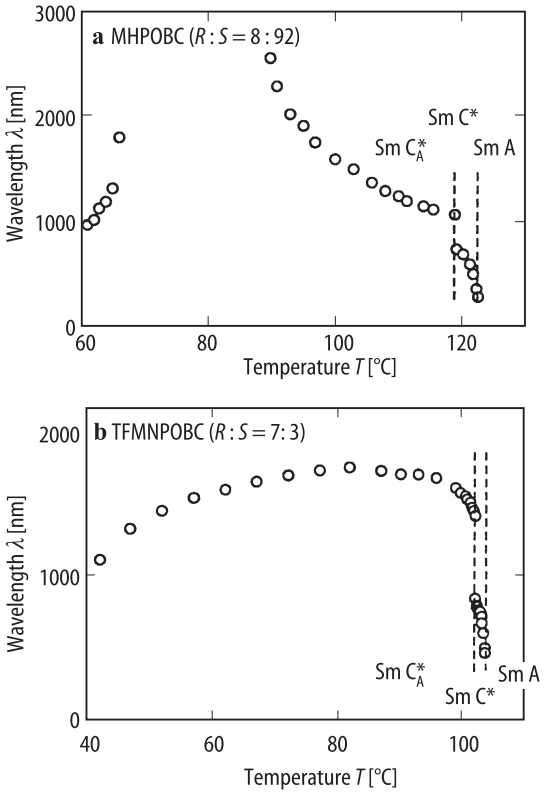

Fig. 71B-1-028 (continued).

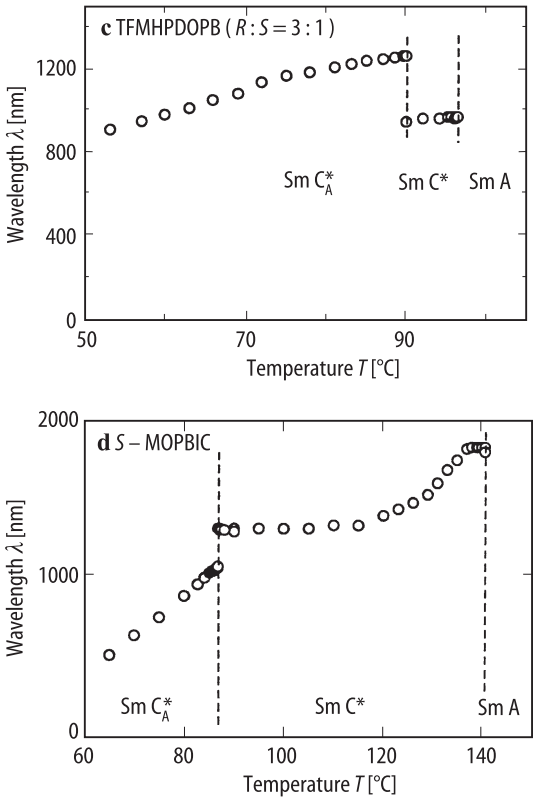

Fig. 71B-1-028. *R*-, *S*-MHPOBC, *R*-, *S*-TFMNPOBC, *R*-, *S*-TFMHPDOPB, *S*-MOPBIC. λ vs. T [91LiJ]. λ: wavelength of a reflection mode. (**a**) MHPOBC. (**b**) TFMNPOBC. (**c**) TFMHPDOPB. (**d**) MOPBIC.

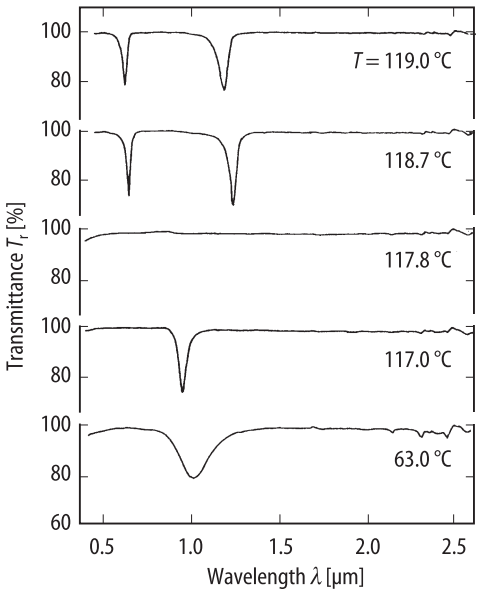

Fig. 71B-1-029. MHPOBC. T_r vs. λ [89Cha]. Parameter: T. T_r: transmittance for oblique incidence.

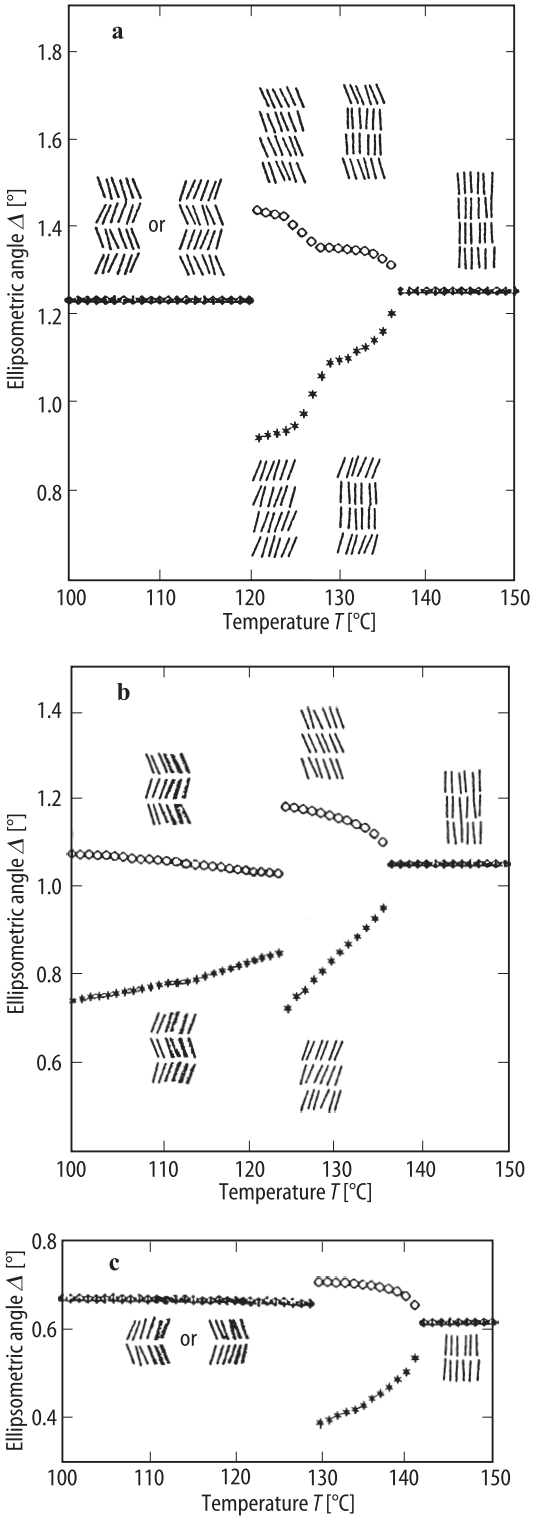

Fig. 71B-1-030. MHPOBC. Δ vs. T of N layer films [93Bah]. Δ: ellipsometric angle, the difference of the phase angle between *s*- and *p*-polarized components of the transmitted light. Smectic layer structures are schematically shown in the corresponding temperature regions. (**a**) $N = 4$. (**b**) $N = 3$. (**c**) $N = 2$. Asterisk and empty lozenge correspond to the two opposite tilt directions.

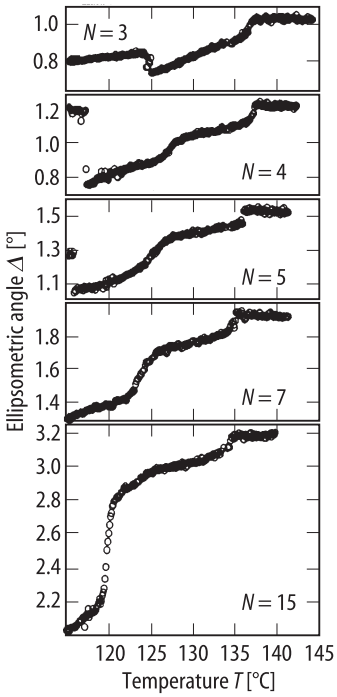

Fig. 71B-1-031. MHPOBC. Δ vs. T of N layer films [96Bah]. Parameter: N. Δ: ellipsometric angle, the difference of the phase angle between *s*- and *p*-polarized components of the transmitted light. $\lambda = 633$ nm.

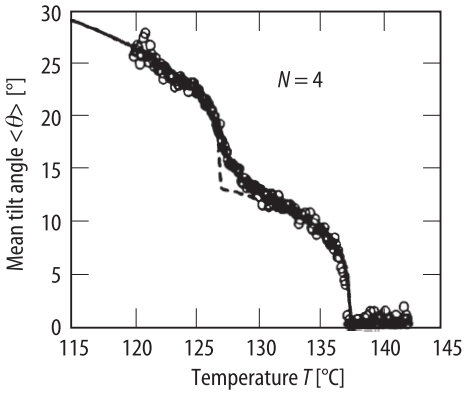

Fig. 71B-1-032. MHPOBC. $\langle\theta\rangle$ vs. T of 4 layer films [96Bah]. $\langle\theta\rangle$: mean tilt angle of optical axis. $\mu = 633$ nm.

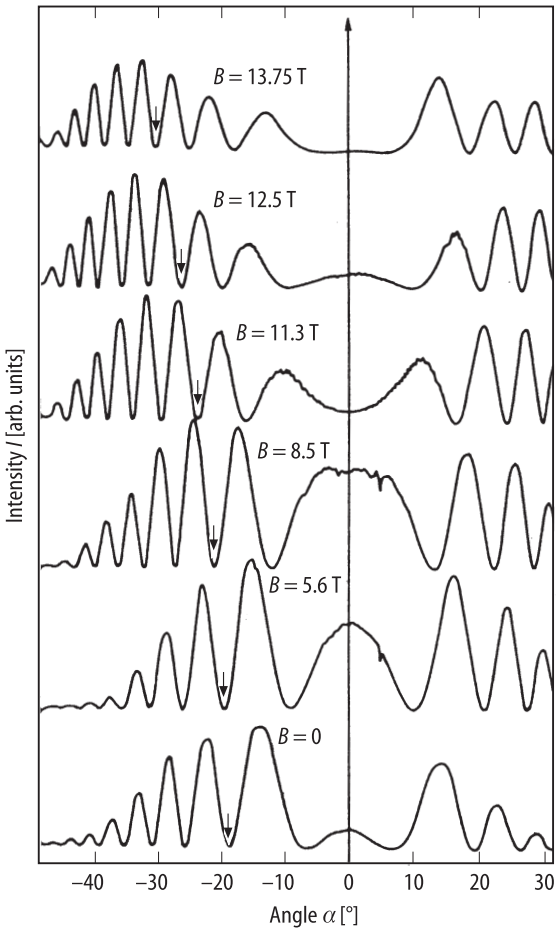

Fig. 71B-1-033. MHPOBC. I vs. α [93Mus]. Parameter: B, magnetic flux density applied along the y axis. I: intensity of the x-z cross-section of the conoscopic figure at the angle α. α: angle between the direction of wave propagation and the z axis.

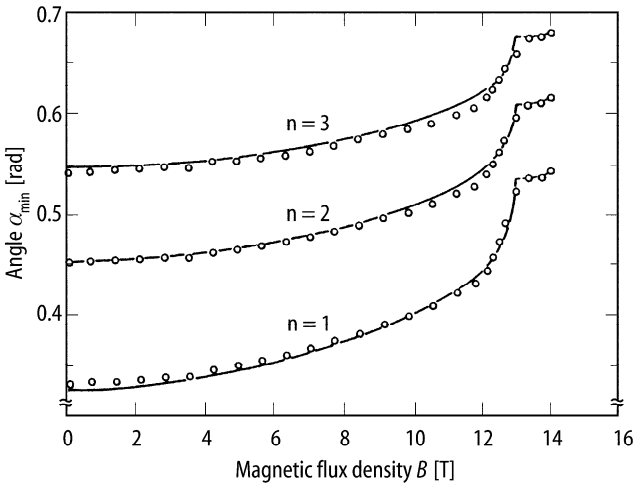

Fig. 71B-1-034. MHPOBC. α_{min} vs. B [93Mus]. α_{min}: angle of the intensity minima of x-z cross section of conoscopic figure. B: magnetic flux density applied along the y axis. α_{min} of n th (n = 1, 2, 3) minima are indicated.

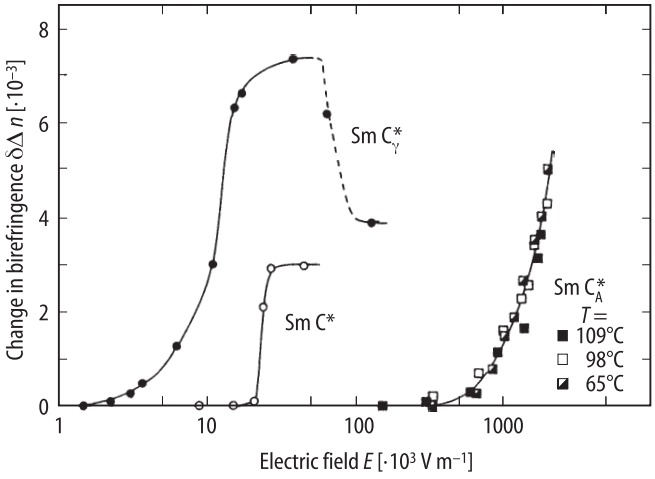

Fig. 71B-1-035. MHPOBC. δΔ*n* vs. *E* [90Gor]. δΔ*n:* change in birefringence by electric field. Parameter: *T* for the case of Sm C_A^*.

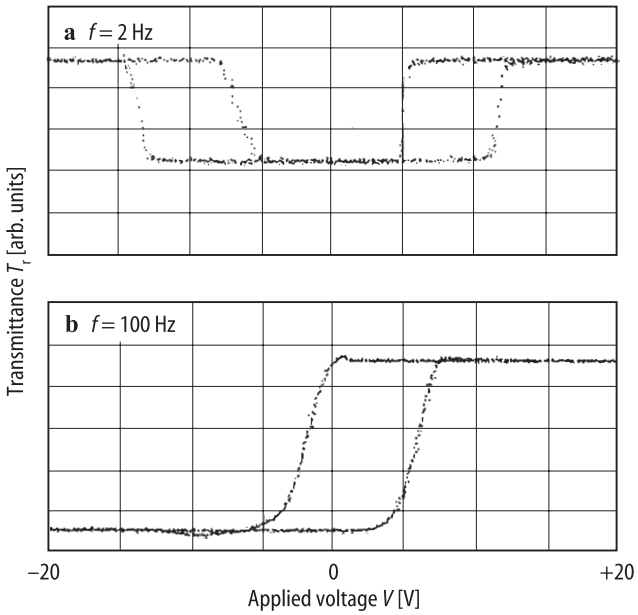

Fig. 71B-1-036. MHPOBC. T_r vs. *V* hysteresis loop in Sm C_A^* phase [90Lee1]. T_r: transmittance. *V*: applied voltage. Cell thickness: 3 μm. (**a**) *f* = 2 Hz, crossed polarizers were set for antiferroelectric state to be dark. (**b**) *f* = 100 Hz, set for one of the ferroelectric states to be dark.

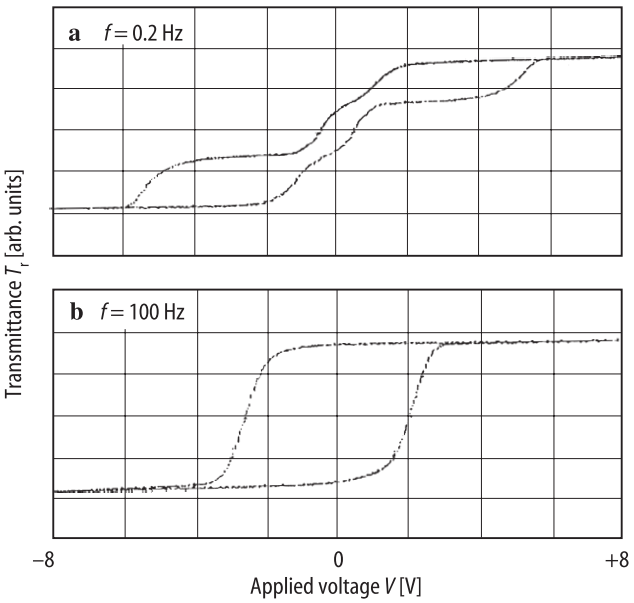

Fig. 71B-1-037. MHPOBC. T_r vs. V hysteresis loop in Sm C^*_γ phase [90Lee1]. T_r: transmittance. V: applied voltage. Cell thickness: 3 μm. (**a**) f = 0.2 Hz. (**b**) f = 100 Hz. The crossed polarizers were set for one of the ferroelectric states to be dark.

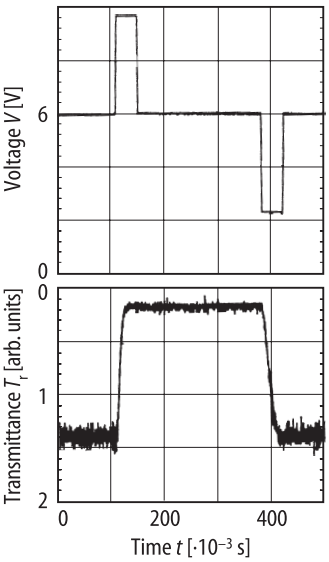

Fig. 71B-1-038. MHPOBC. V, T_r vs. t [88Cha]. V: applied voltage. T_r: transmittance. T = 107 °C. Cell thickness: 3 μm.

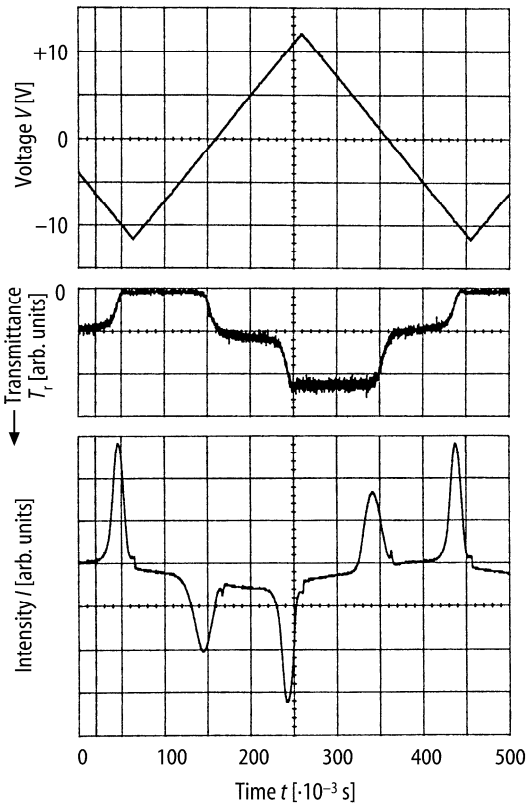

Fig. 71B-1-039. MHPOBC. V, T_r, I vs. t [88Cha]. V: applied voltage. T_r: transmittance. I: switching current. T = 107 °C. Cell thickness: 3 µm.

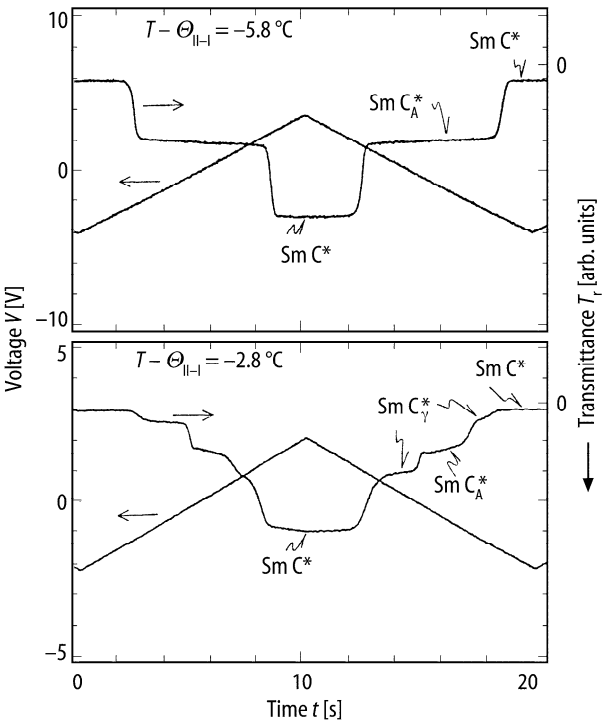

Fig. 71B-1-040. MHPOBC. V, T_r vs. t [90Hir2]. V: applied voltage. T_r: transmittance.

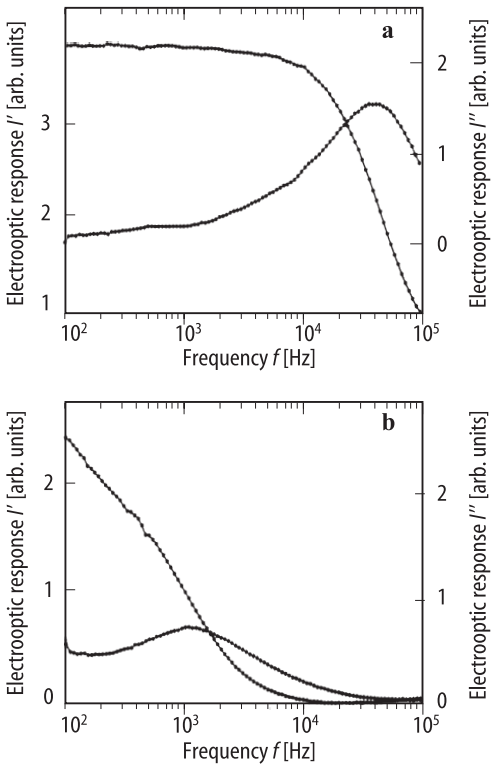

Fig. 71B-1-041. MHPOBC. I', I'' vs. f [93Glo]. I', I'': real and imaginary part of electrooptic response. f: frequency of applied electric field. (**a**) T = 122.5 °C (Sm A phase). (**b**) T = 118.5 °C (Sm C^*_γ phase).

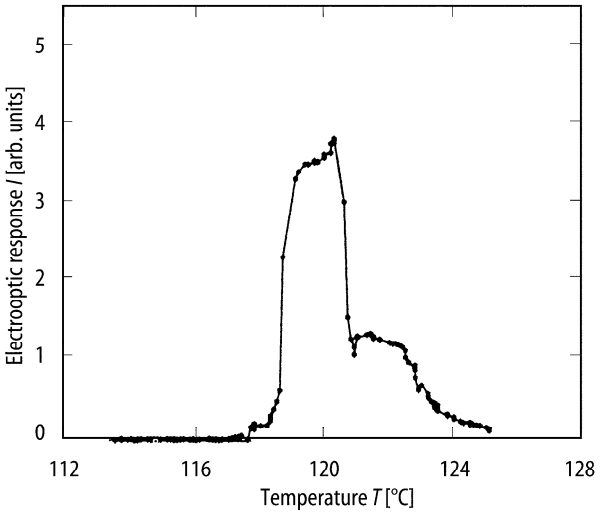

Fig. 71B-1-042. MHPOBC. I vs. T [93Glo]. I: electrooptic response at 1 kHz.

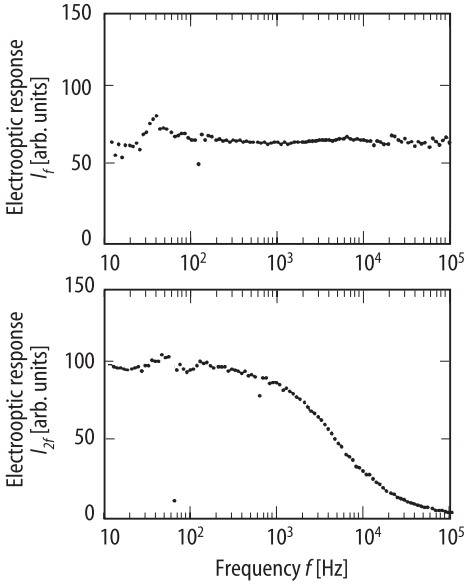

Fig. 71B-1-043. MHPOBC. I_f, I_{2f} vs. f [93Hir]. I_f, I_{2f}: electrooptic response of f and $2f$ components. f: frequency of applied electric field. T = 89 K.

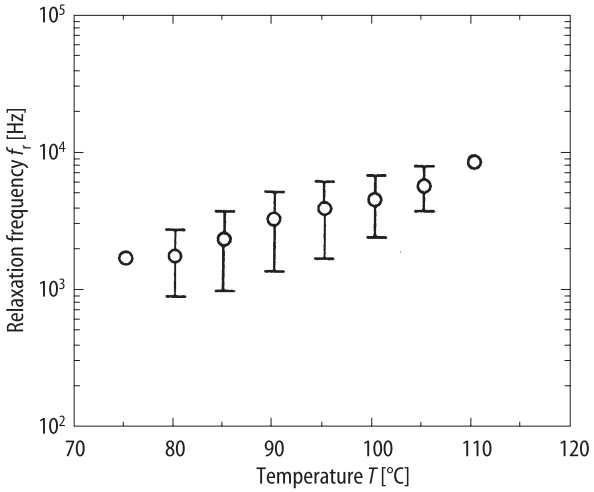

Fig. 71B-1-044. MHPOBC. f_r vs. T [93Hir]. f_r: relaxation frequency of electrooptic $2f$ response. See Fig. 71B-1-043.

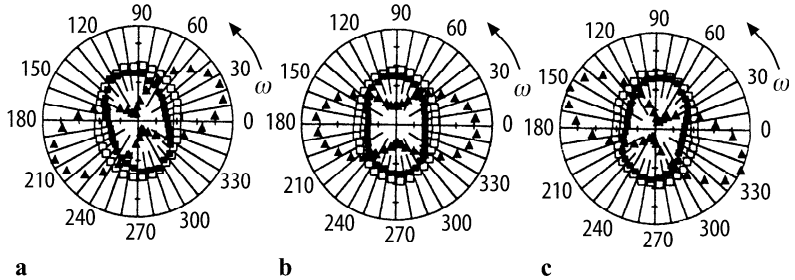

Fig. 71B-1-045. MHPOBC. Polar diagram of infrared absorbance of stretching peaks [95Kim]. ω: polarizer rotation angle. Full upside triangle: phenyl ring. Open square: core C=O. Full square: chiral C=O. T = 105 °C (Sm C_A^* phase). (**a**) $E = 5.7 \cdot 10^6$ V m^{-1}. (**b**) $E = 0$. (**c**) $E = -5.7 \cdot 10^6$ V m^{-1}.

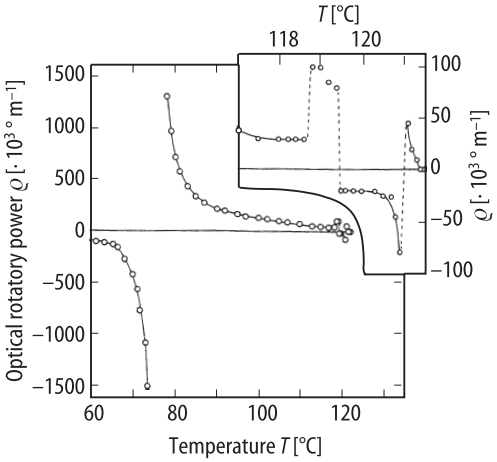

Fig. 71B-1-046. MHPOBC. ρ vs. T [89Cha]. ρ: optical rotatory power. λ = 514.5 nm.

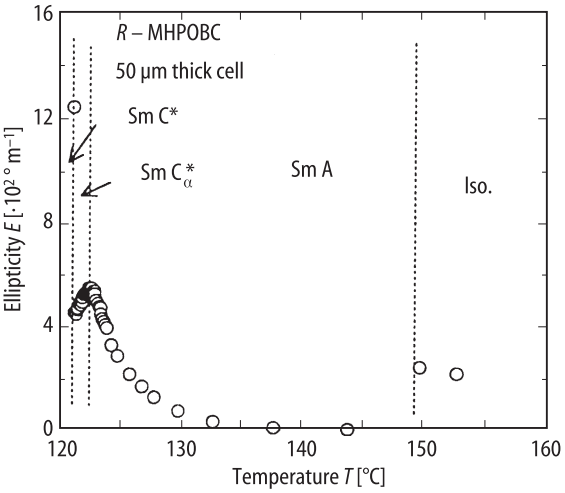

Fig. 71B-1-047. MHPOBC. E vs. T [95LiJ]. E: ellipticity of liquid crystal induced circular dichroism. λ = 360 nm. Iso.: isotropic.

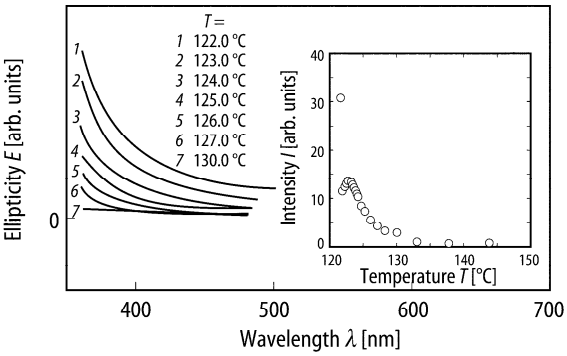

Fig. 71B-1-048. MHPOBC. E vs. λ [90Lee2]. Parameter: T. E: ellipticity. Insert: I vs. T at λ = 360 nm. I: intensity of circular dichroism signal.

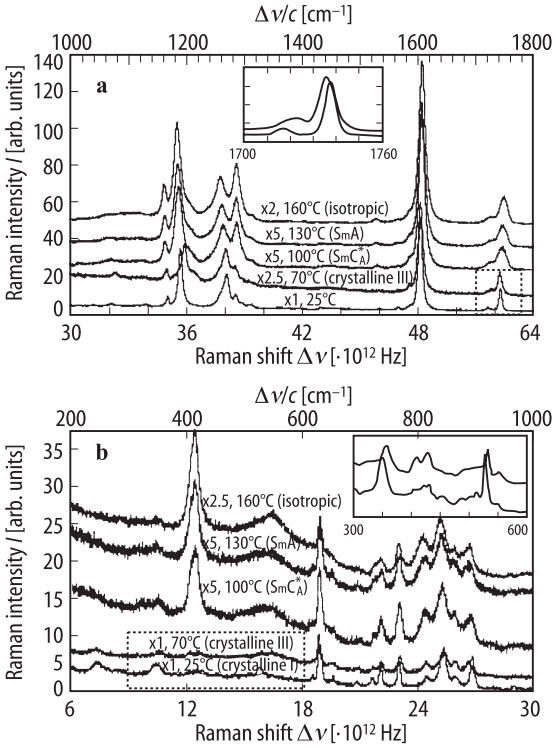

Fig. 71B-1-049. MHPOBC. I vs. $\Delta\nu$ [94Kim]. Parameter: T. I: intensity of Raman scattering. $\Delta\nu$: Raman shift. (**a**) $\Delta\nu/c$ = 1000 ... 1800 cm^{-1}, (**b**) $\Delta\nu/c$ = 200 ... 1000 cm^{-1}. Assignment of peaks [cm^{-1}]: 1736: C=O stretching in COO between two phenyl groups. 1713: C=O stretching in COO near chiral group. 1600: C–C stretching of benzene. 1285: C–C stretching in biphenyl link. 1270: asymmetric C–O stretching. 1190: Aromatic C–H in-plane deformation. 418: vibrational mode of twisted biphenyl. Insert: signals of two different crystalline phases, I and III, in enclosed areas. As to the crystalline I and III phases, see [93Hor].

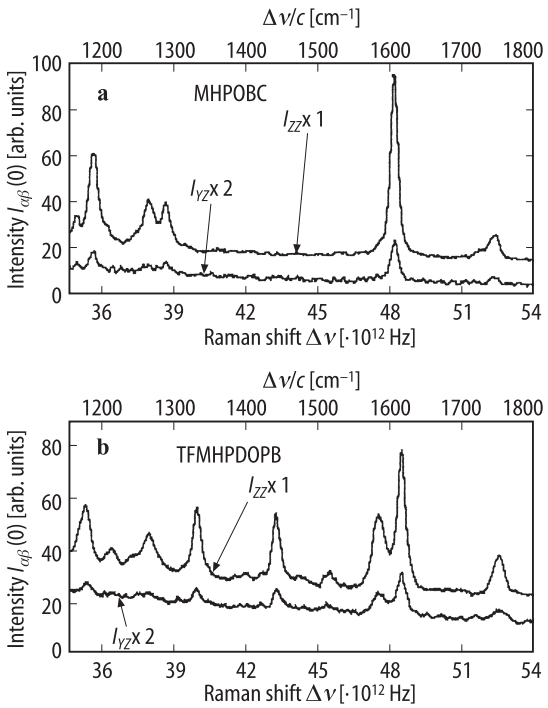

Fig. 71B-1-050. MHPOBC (**a**), TFMHPDOPB (**b**). $I_{ZZ}(0)$, $I_{YZ}(0)$ vs. $\Delta\nu$ [94Kim]. $I_{\alpha\beta}(\omega)$ (α, $\beta = X, Y, Z$): intensity of α polarized Raman scattering by β polarized excitation with layer normal inclined by ω from Z. $\Delta\nu$: Raman shift. (X, Y, Z): coordinates of fixed laboratory frame. X: propagation direction of incident beam. Z: polarization direction of incident beam.

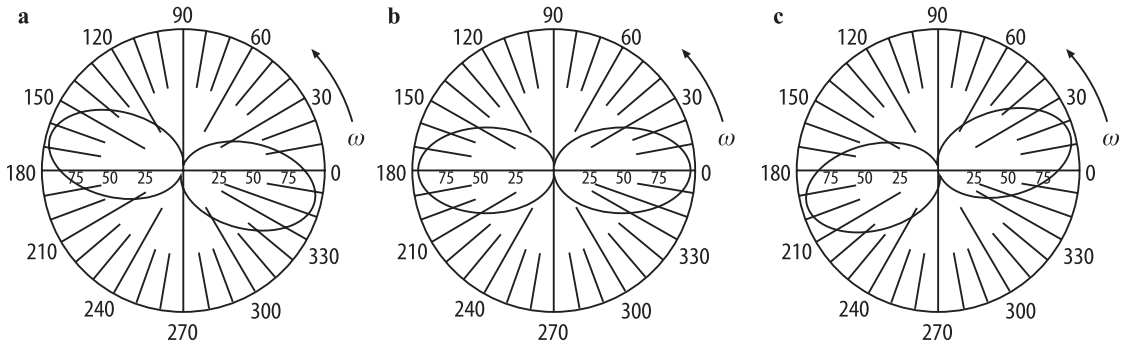

Fig. 71B-1-051. MHPOBC. Polar diagram of $I_{ZZ}(\omega)$ in Sm C* phase [94Kim]. $I_{ZZ}(\omega)$: intensity of Z polarized Raman scattering by Z polarized excitation with layer normal inclined by ω from Z. (**a**) $E = +0.5 \cdot 10^6$ V m^{-1}. (**b**) $E = 0$. (**c**) $E = -0.5 \cdot 10^6$ V m^{-1}.

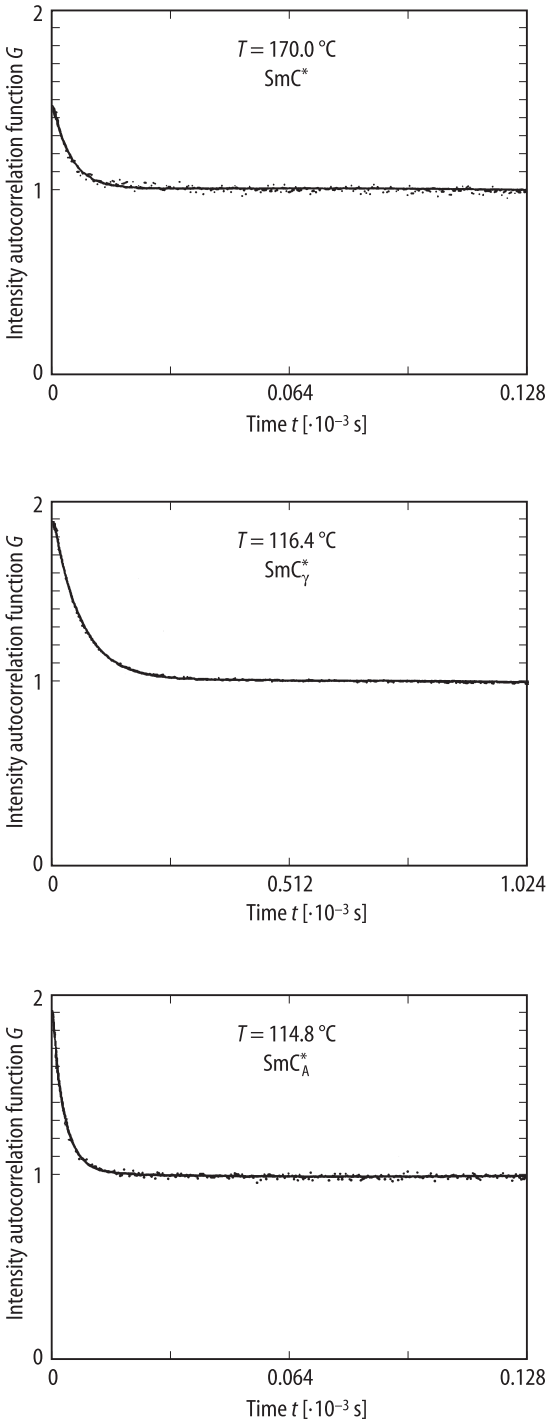

Fig. 71B-1-052. MHPOBC. G vs. t [91Sun]. Parameter: T. G: intensity autocorrelation function of scattering light. Scattering angle: $\alpha = 8°$.

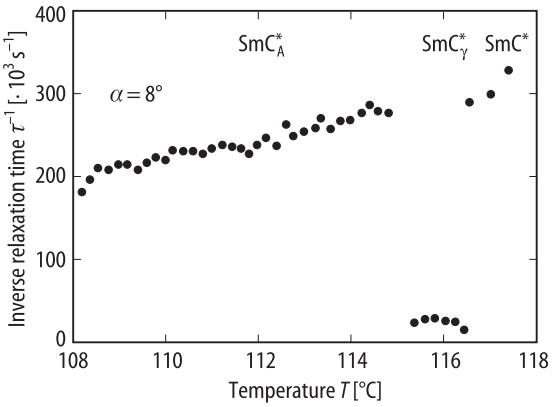

Fig. 71B-1-053. MHPOBC. τ^{-1} vs. T [91Sun]. τ: relaxation time of photon autocorrelation function. Scattering angle: $\alpha = 8°$.

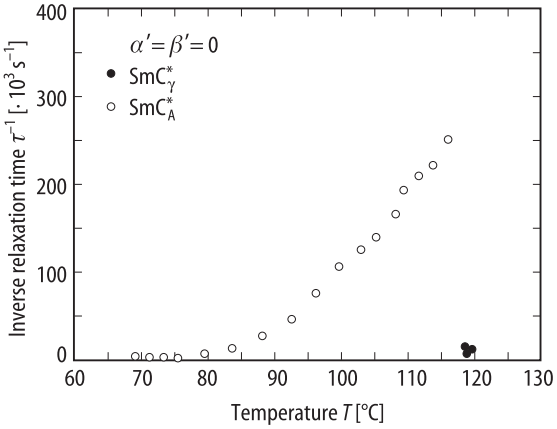

Fig. 71B-1-054. MHPOBC. τ^{-1} vs. T [93Sun]. τ: relaxation time of photon autocorrelation function. Scattering angle: $\alpha' = 0$. Azimuthal angle: $\beta' = 0$.

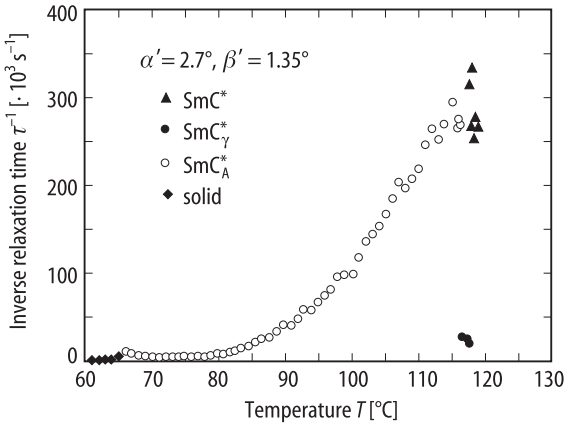

Fig. 71B-1-055. MHPOBC. τ^{-1} vs. T [93Sun]. τ: relaxation time of photon autocorrelation function. Scattering angle: $\alpha' = 2.7°$. Azimuthal angle: $\beta' = 1.35°$.

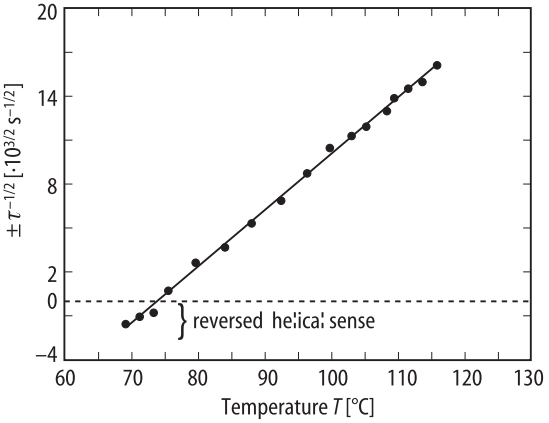

Fig. 71B-1-056. MHPOBC. $\tau^{-1/2}$ vs. T in Sm C^*_γ phase [93Sun]. τ: relaxation time of photon autocorrelation function. Data are replotted from Fig. 71B-1-054.

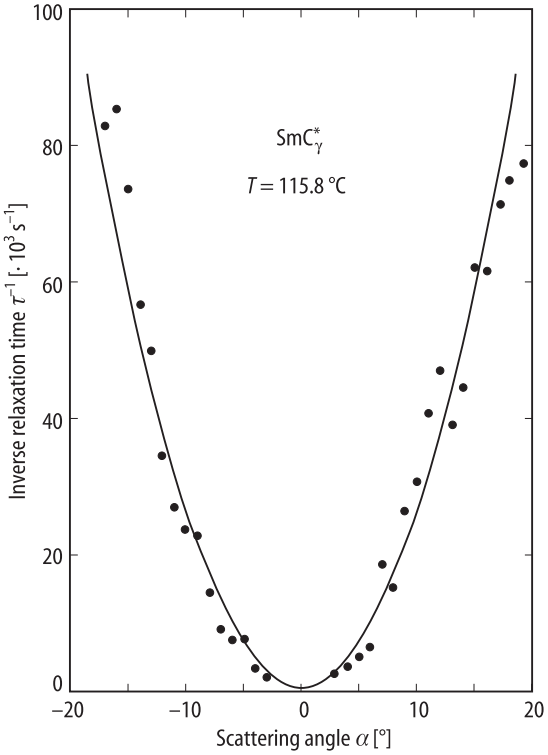

Fig. 71B-1-057. MHPOBC. τ^{-1} vs. α [91Sun]. τ: relaxation time of photon autocorrelation function. α: scattering angle. T = 115.8 °C (Sm C^*_γ).

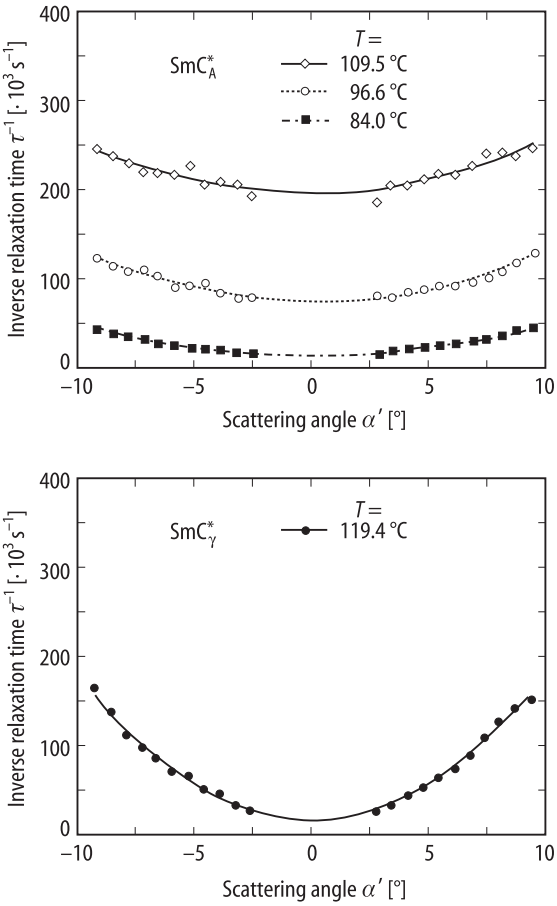

Fig. 71B-1-058. MHPOBC. τ^{-1} vs. α' [93Sun]. Parameter: T. τ: relaxation time of photon autocorrelation function. α': scattering angle. $\beta' = \alpha'/2$.

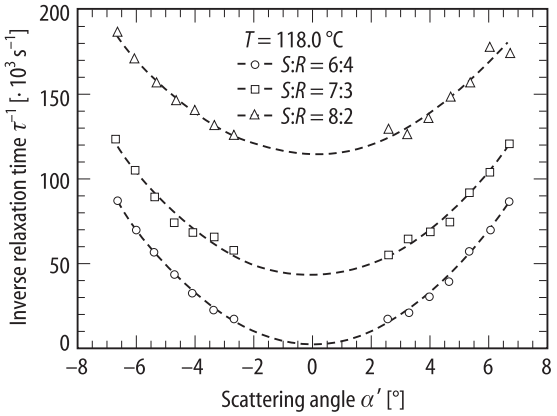

Fig. 71B-1-059. *S*-, *R*-MHPOBC. τ^{-1} vs. α' [93Ori]. Parameter: S : R. τ: relaxation time of photon autocorrelation function. T = 118.0 °C (Sm C* phase). α': scattering angle.

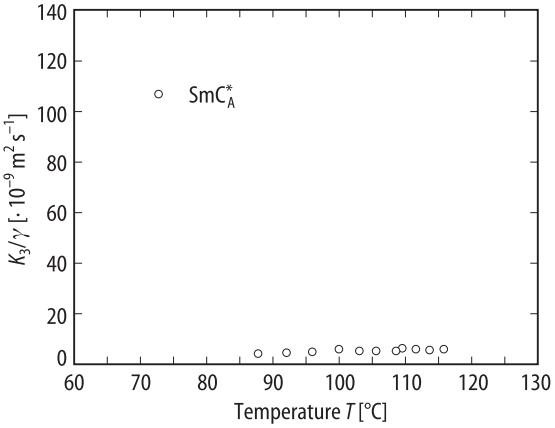

Fig. 71B-1-060. MHPOBC. K_3/γ vs. T [93Sun]. K_3: twist elastic constant. γ: viscosity coefficient. K_3/γ is obtained from the dispersion relation of relaxation frequency, $\tau^{-1} = (K_3/\gamma)(q_z - q_0)^2 + (K_+/\gamma)q_z^2$, where q_0 is the wave number of helix defined as $q_0 = 2\pi/P$ where P is the helical pitch of the helix, q_X and q_Z the scattering wave vector components along X and Z, respectively, and $K_+ = (K_1 + K_2)/2$, where K_1 and K_2 are splay and bend elastic constants, respectively.

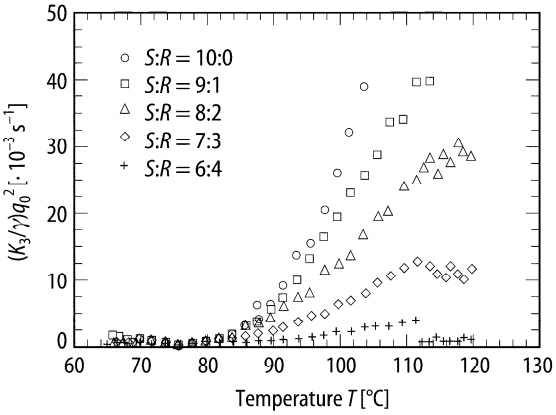

Fig. 71B-1-061. *S*-, *R*-MHPOBC. $(K_3/\gamma)q_0^2$ vs. T [93Ori]. Parameter: S : R. For K_3, γ and q_0, see the caption of Fig. 71B-1-060.

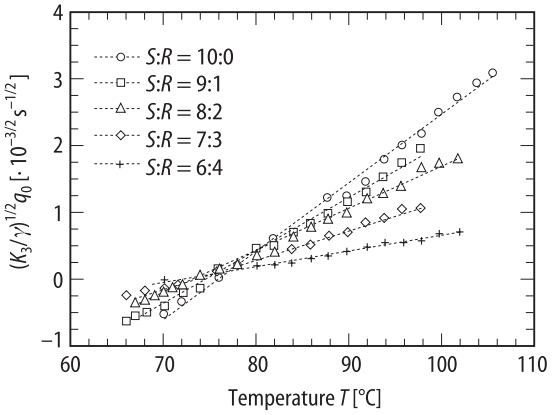

Fig. 71B-1-062. *S*-, *R*-MHPOBC. $(K_3/\gamma)^{1/2}q_0$ vs. T [93Ori]. Parameter: S : R. For K_3, γ and q_0, see the caption of Fig. 71B-1-060.

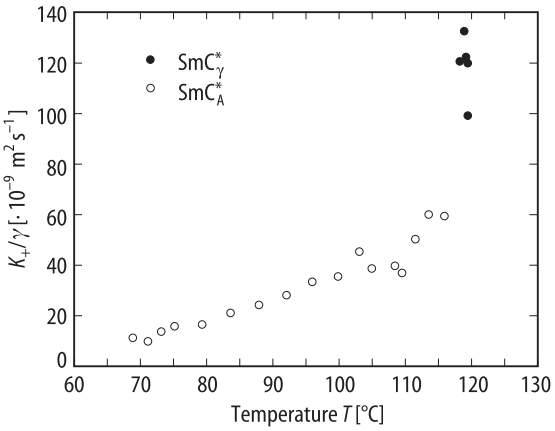

Fig. 71B-1-063. MHPOBC. K_+/γ vs. T [93Ori]. For K_+, γ see the caption of Fig. 71B-1-060.

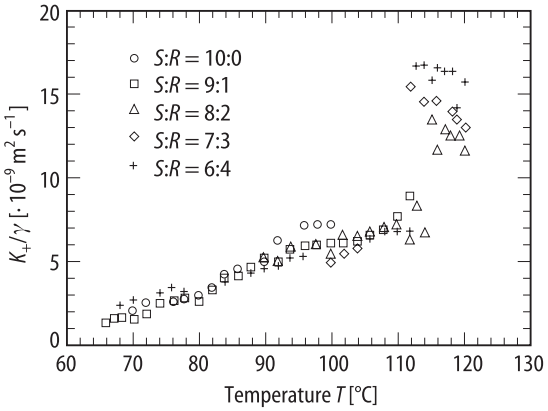

Fig. 71B-1-064. *S*-, *R*-MHPOBC. K_+/γ vs. T [93Ori]. Parameter: S : R. For K_+, γ see the caption of Fig. 71B-1-060.

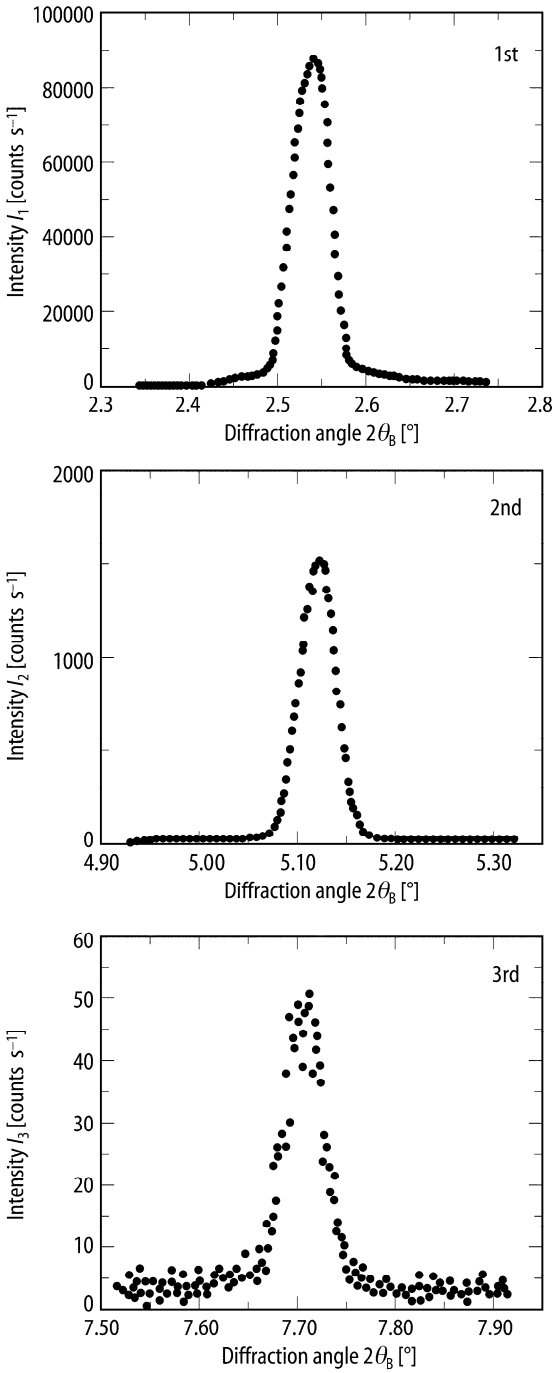

Fig. 71B-1-065. MHPOBC. I_n vs. $2\theta_B$ [95Tak]. I_n : intensity of nth order X-ray Bragg reflection corresponding to layer thickness. θ_B: Bragg angle. $T = 90$ °C (Sm C_A).

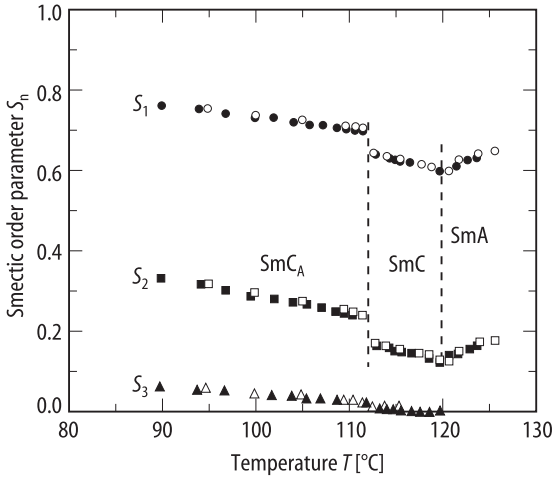

Fig. 71B-1-066. MHPOBC (racemic). S_n vs. T [95Tak]. S_n: n th smectic order parameter. Open symbol: heating. Full symbol: cooling.

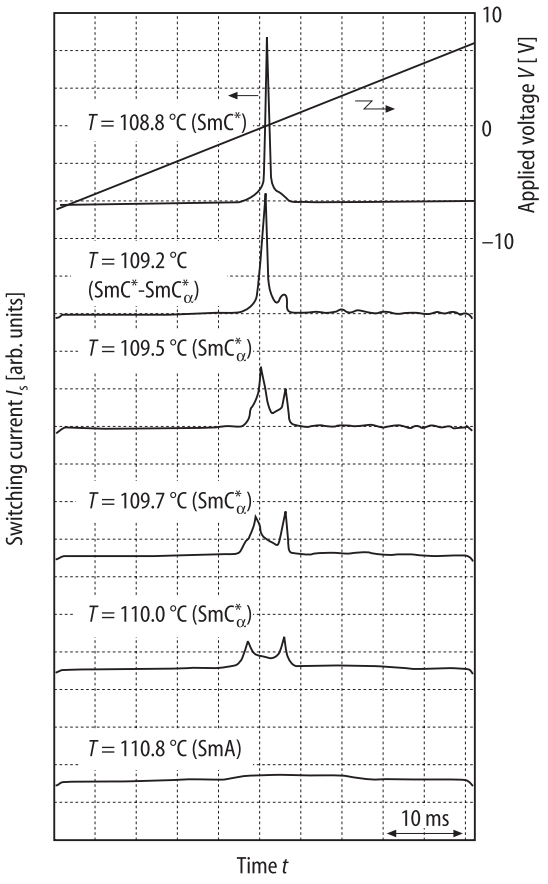

Fig. 71B-1-067. MHPOBC. I_s , V vs. t [91Tak3]. Parameter: T. I_s: switching current observed by applying triangular electric wave. V: applied voltage of the triangular wave. f = 10 Hz. Cell thickness: 2 µm.

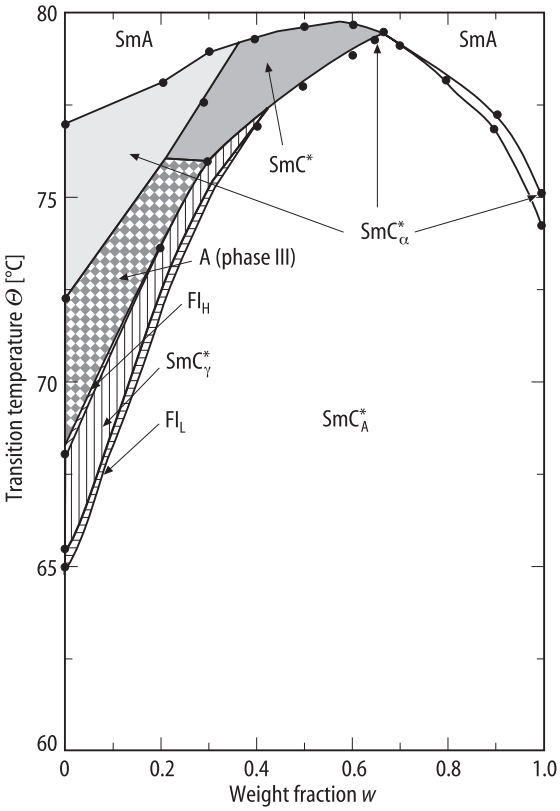

Fig. 71B-1-068. (*R*-MHPBC)–(*R*-TFMHPBC). Θ vs. *w* phase diagram [93Iso1]. *w*: weight fraction of *R*-TFMHPBC. FI_H and FI_L: ferrielectric phases. TFMHPBC: L–⬡–⬡–COO–⬡–R; L: C_8H_{17}, R: $COOCH(CF_3)C_6H_{13}$.

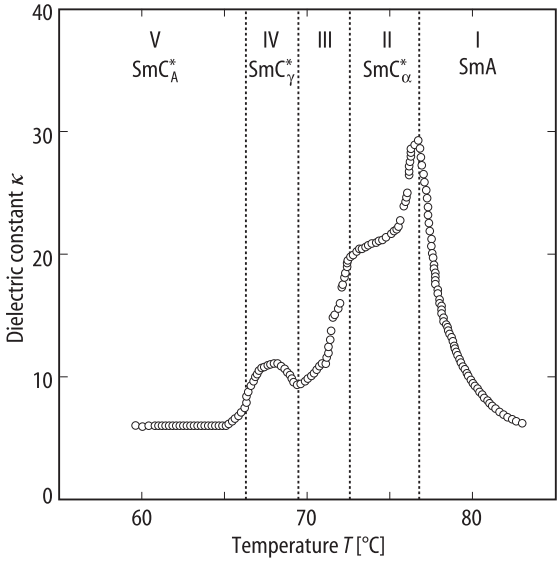

Fig. 71B-1-069. MHPBC. κ vs. *T* [92Oka]. *f* = 100 Hz.

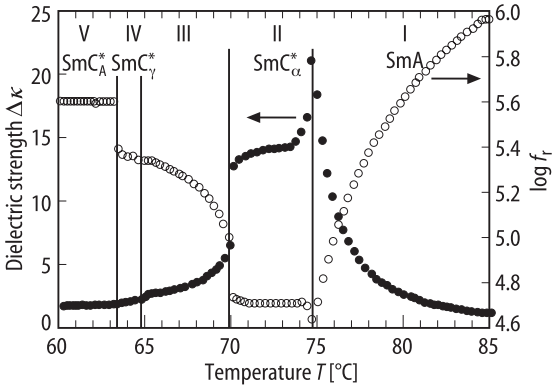

Fig. 71B-1-070. MHPBC. $\Delta\kappa$, $\log f_r$ vs. T [95Cep]. $\Delta\kappa$: dielectric strength. f_r: relaxation frequency [Hz].

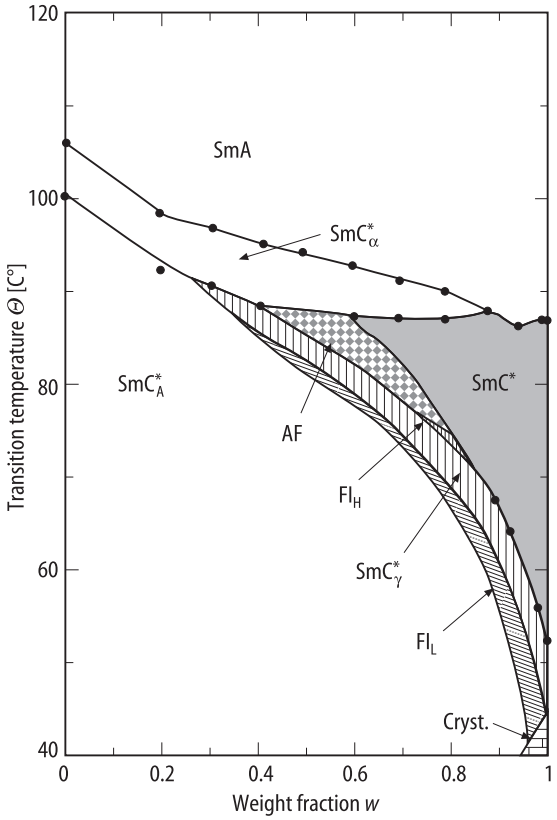

Fig. 71B-1-071. (MHPOCBC)–(MHPOOCBC). Θ vs. w phase diagram [93Iso2]. w: weight fraction of MHPOOCBC. FI_H and FI_L: ferrielectric phases which are adjacent to Sm C^*_γ

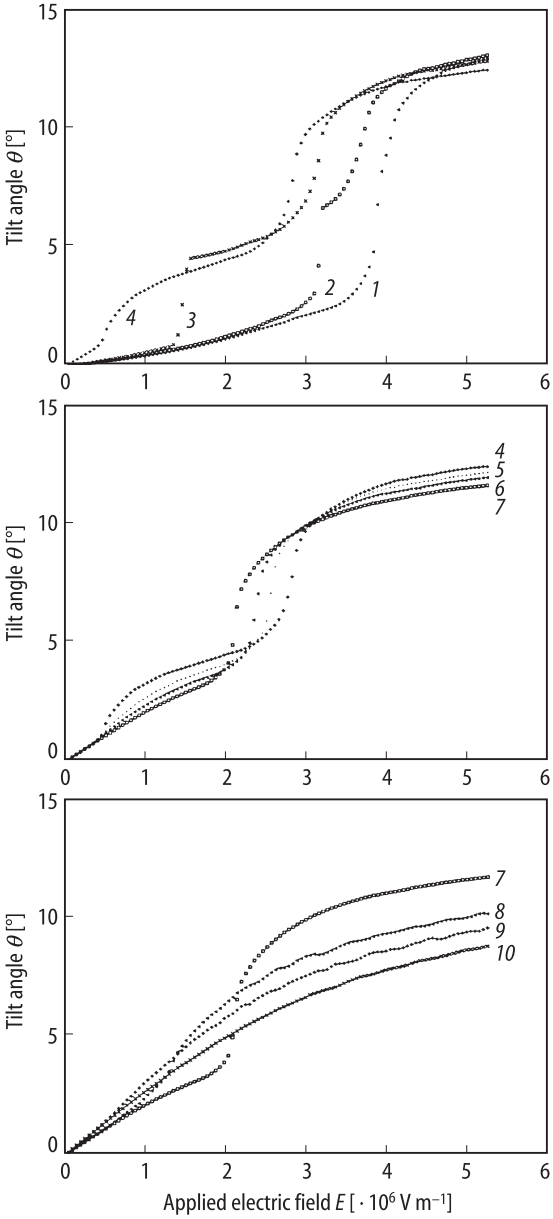

Fig. 71B-1-072. MHPOCBC. θ vs. E [92Hir]. Parameter: T. θ: tilt angle. E: applied electric field. *1*: 90 °C. *2*: 92.5 °C. *3*: 95.6 °C. *4*: 96.8 °C. *5*: 97.7 °C. *6*: 98.3 °C. *7*: 99 °C. *8*: 100.9 °C. *9*: 101.4 °C. *10*: 102 °C. *1...3*: Sm C^*_A phase. *4...9*: Sm C^*_α phase. *10*: Sm A phase.

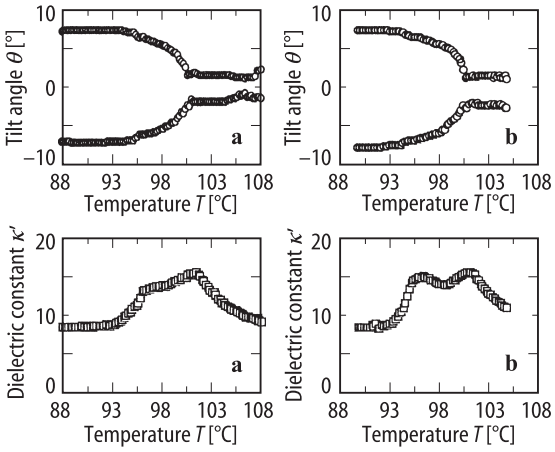

Fig. 71B-1-073. MHPOCBC. θ, κ' vs. T [92Iso]. θ: tilt angle. (**a**) heating. (**b**) cooling. f = 10 kHz for κ'.

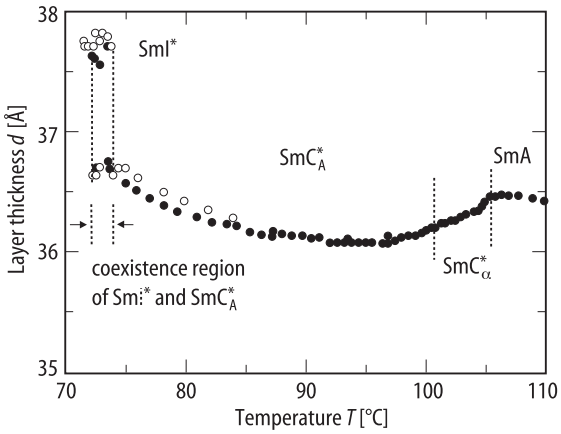

Fig. 71B-1-074. MHPOCBC. d vs. T [93Tak]. d: layer thickness. Open and full circles: independent measurement to each other.

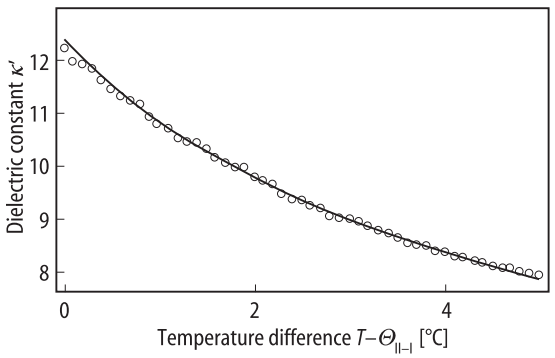

Fig. 71B-1-075. MHPOCBC. κ' vs. $T - \Theta_{II-I}$ [96Sak]. f = 120 Hz.

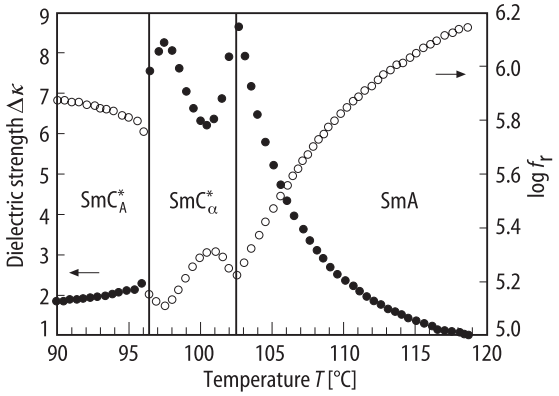

Fig. 71B-1-076. MHPOCBC. $\Delta\kappa$; $\log f_r$ vs. T [95Cep]. $\Delta\kappa$: dielectric strength. f_r: relaxation frequency [Hz].

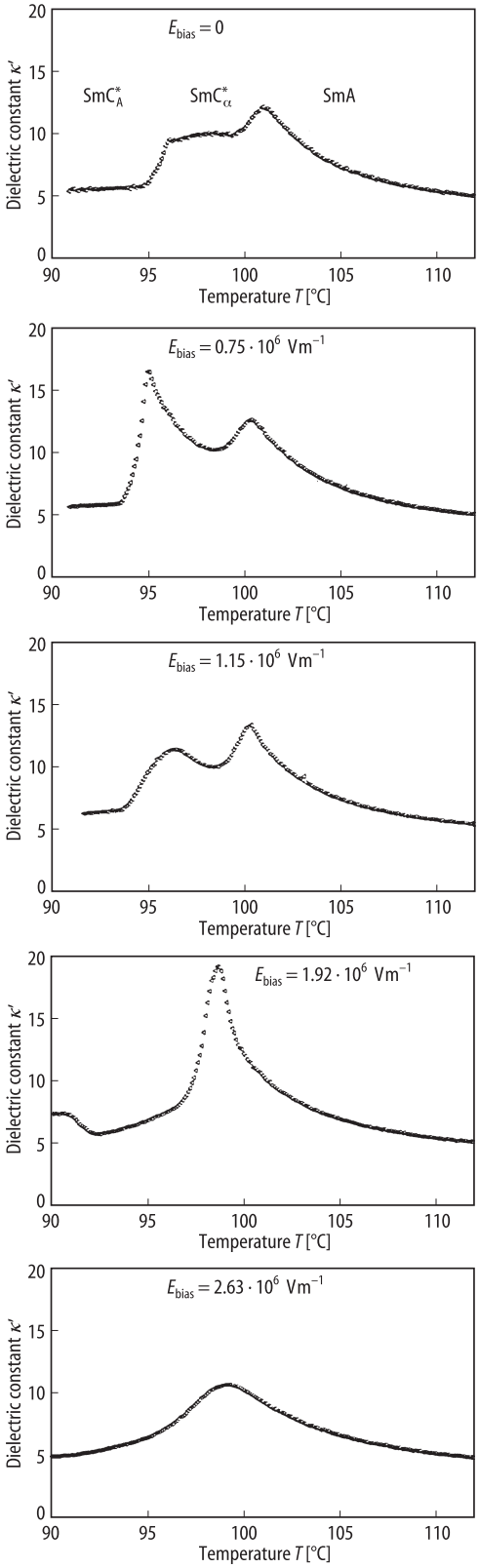

Fig. 71B-1-077. MHPOCBC. κ' vs. T [92Hir]. Parameter: E_{bias}. f = 1.05 kHz.

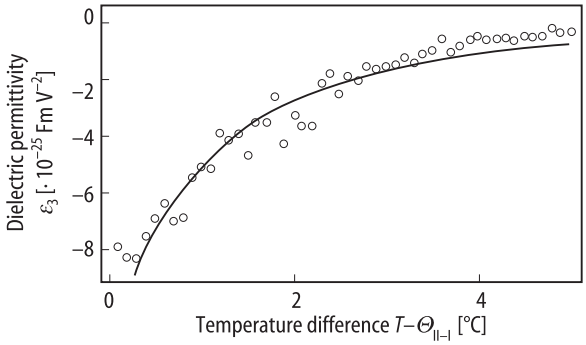

Fig. 71B-1-078. MHPOCBC. ε_3 vs. $T - \Theta_{II-I}$ [96Sak]. ε_3: third order dielectric permittivity.

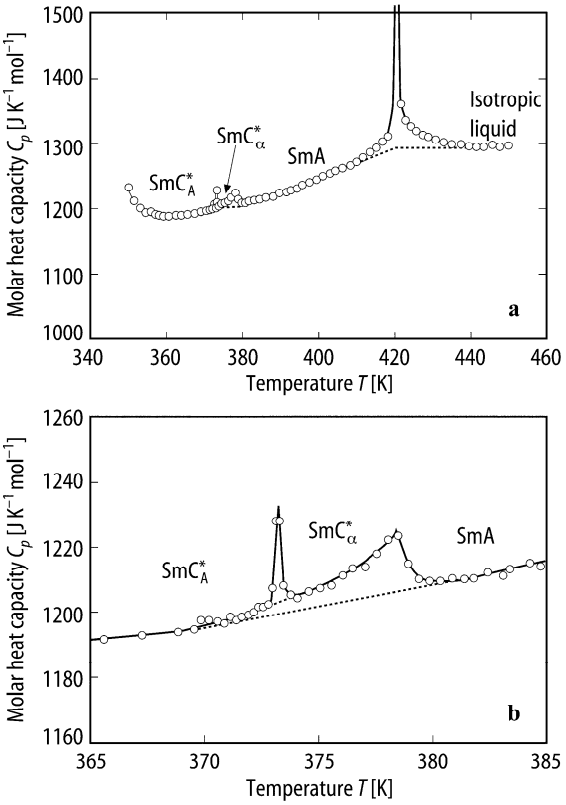

Fig. 71B-1-079. MHPOCBC. C_p vs. T [97Asa]. C_p: molar heat capacity at constant pressure. (**a**) T = 350 K ... 450 K. (**b**) T = 365 K ... 385 K.

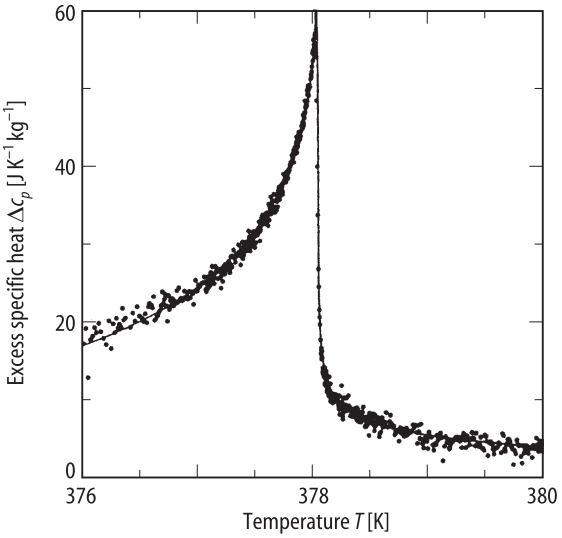

Fig. 71B-1-080. MHPOCBC. Δc_p vs. T [96Ema3]. Δc_p: excess specific heat at constant pressure.

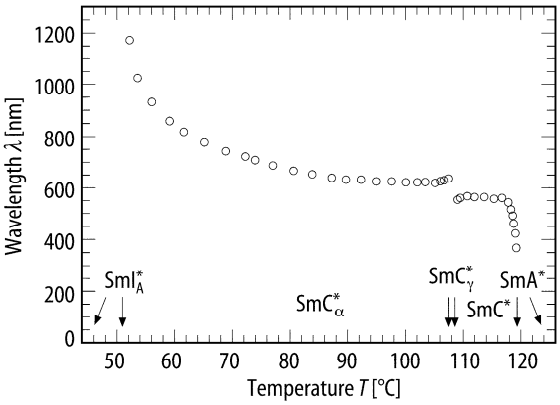

Fig. 71B-1-081. LC1. λ vs. T [96Gou]. λ: wavelength of selective reflection band (helical pitch multiplied by average refractive index).

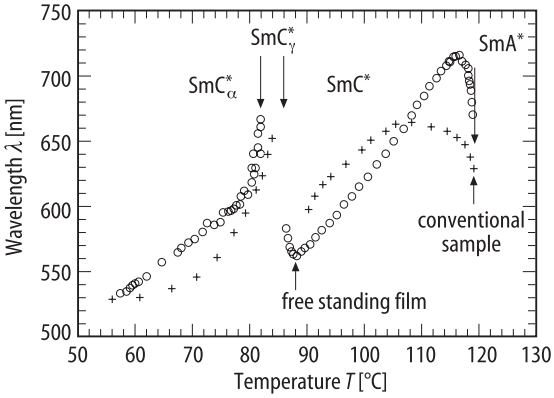

Fig. 71B-1-082. LC2. λ vs. T [96Gou]. λ: wavelength of selective reflection band (helical pitch multiplied by average refractive index).

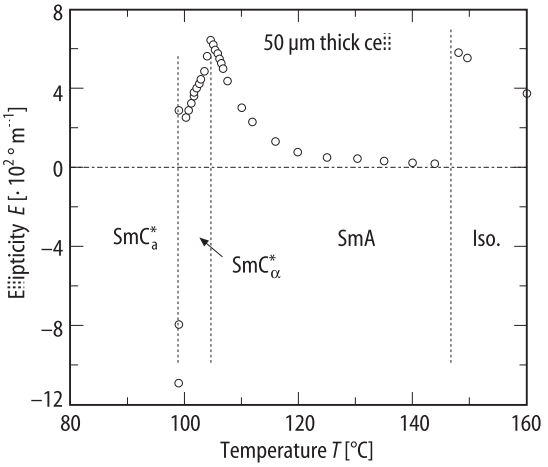

Fig. 71B-1-083. *R*-MHPOCBC. *E* vs. *T* [95LiJ]. *E*: ellipticity of liquid crystal induced circular dichroism. λ = 360 nm. Iso.: isotropic.

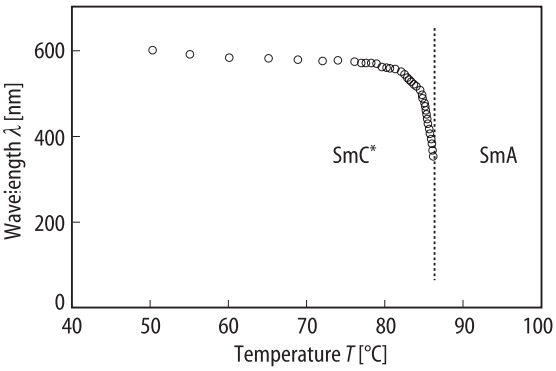

Fig. 71B-1-084. *R*-MHPOOCBC. λ vs. *T* [91Tak4]. λ: wavelength of selective reflection band (helical pitch multiplied by average refractive index).

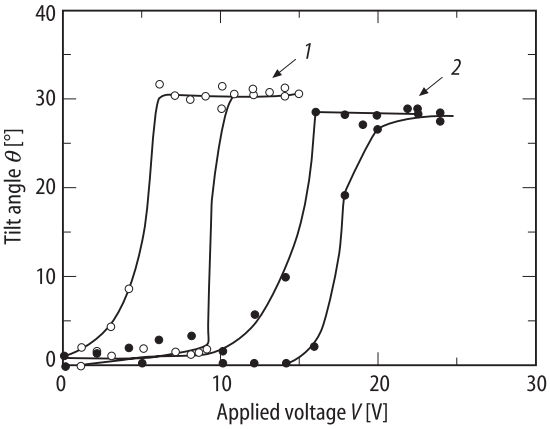

Fig. 71B-1-085. MOPBIC (*1*), $C_8H_{17}O$–⟨⬡⟩–COO–⟨⬡⟩–⟨⬡⟩–$COCH(CH_3)C_6H_{13}$ (*2*). θ vs. *V* [89Nis]. θ: tilt angle. *V*: applied voltage. Sm C^*_A phase. Cell thickness: 5 µm.

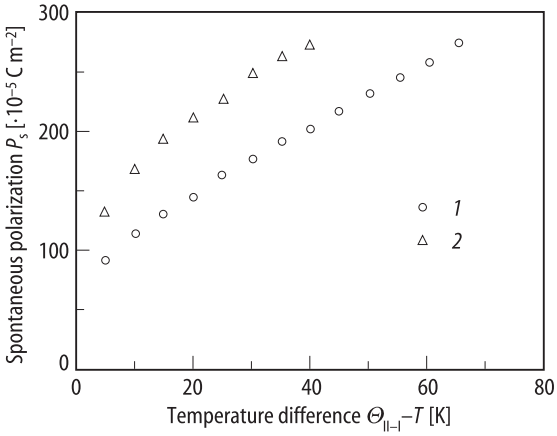

Fig. 71B-1-086. MOPBIC (*1*), $C_8H_{17}O$–⬡–COO–⬡–⬡–$COCH(CH_3)C_6H_{13}$ (*2*). P_s vs. $\Theta_{II-I} - T$ [89Nis]. Cell thickness: 2.6 μm.

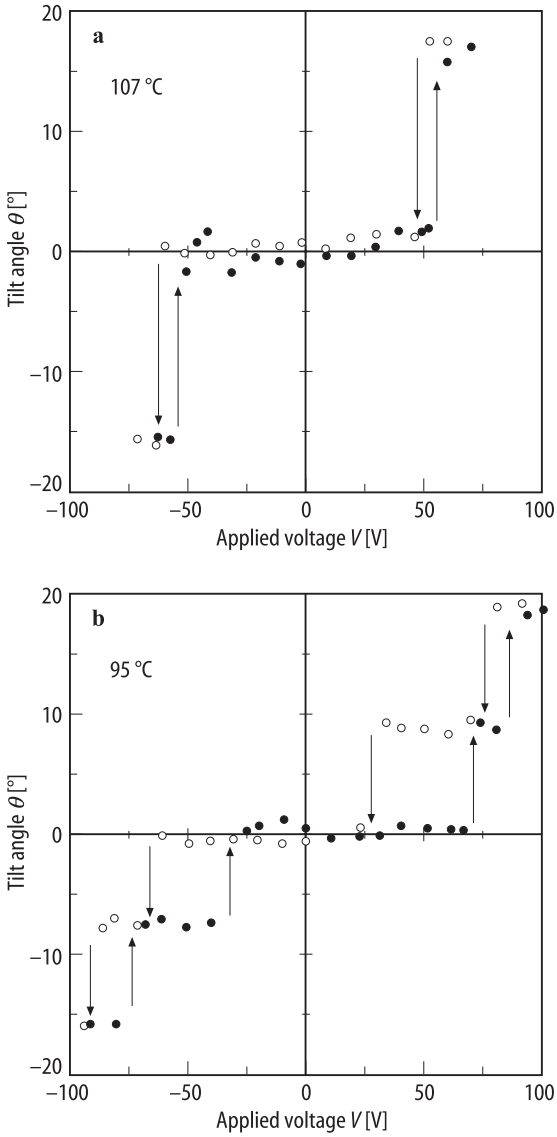

Fig. 71B-1-087. 3MC2PCPOPB. θ vs. V [92Mor]. Parameter: T. θ: tilt angle. V: applied voltage. Full circle: increasing applied field, open circle: decreasing applied field. (**a**) 107 °C. (**b**) 95 °C. Cell thickness: 6 µm.

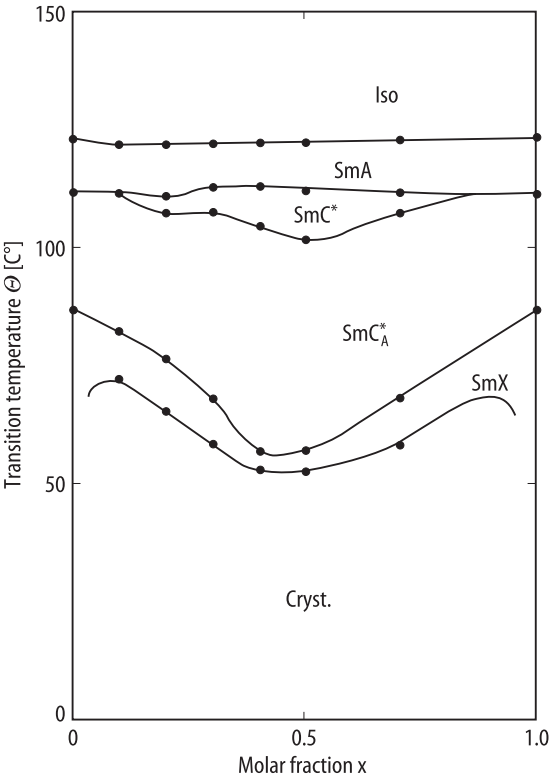

Fig. 71B-1-088. $(S\text{-TFMHPOBC})_{1-x}(R\text{-TFMHPOBC})_x$. Θ vs. x [89Yam].

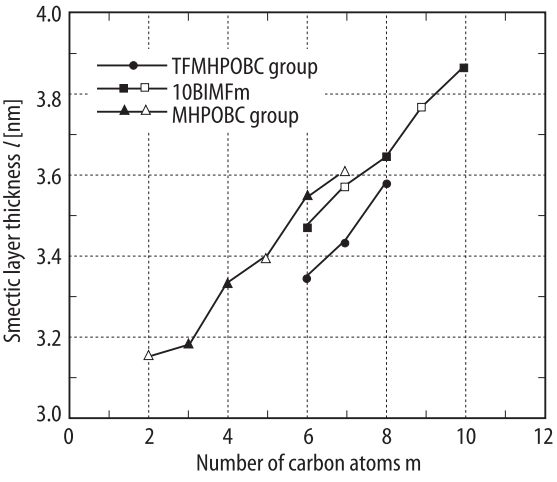

Fig. 71B-1-089. L– 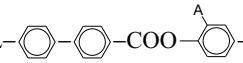 –R (L = $C_nH_{7n+1}O$); n = 8, A = H, R = $COOCH(CF_3)C_mH_{2m+1}$ (TFMHPOBC group). n = 10, A = F, R = $COOCH(CF_3)C_mH_{2m+1}$ (10BIMFm). n = 8, A = H, R = $COOCH(CH_3)C_mH_{2m+1}$ (MHPOBC group). *l* vs. m [93Ike]. *l*: smectic layer thickness. $T = \Theta_{I-I} + 3.5$ °C.

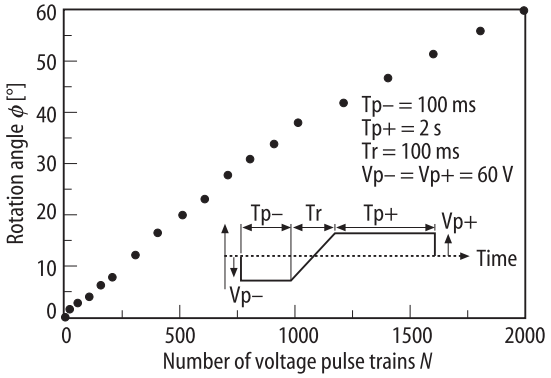

Fig. 71B-1-090. TFMHPOBC. ϕ vs. N [95Mor]. ϕ: rotation angle of smectic layer. N: number of voltage pulse trains. Waveform of the pulse is indicated.

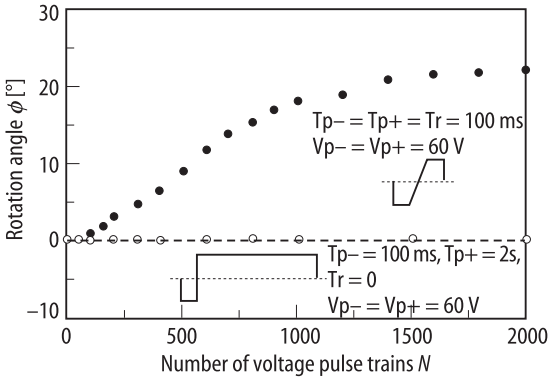

Fig. 71B-1-091. TFMHPOBC. ϕ vs. N [95Mor]. ϕ: rotation angle of smectic layer. N: number of voltage pulse trains. Two different waveforms of the pulse trains corresponding to different symbols (full circle: upper wave form, open circle: lower wave form) are indicated. For symbols see Fig. 71B-1-090.

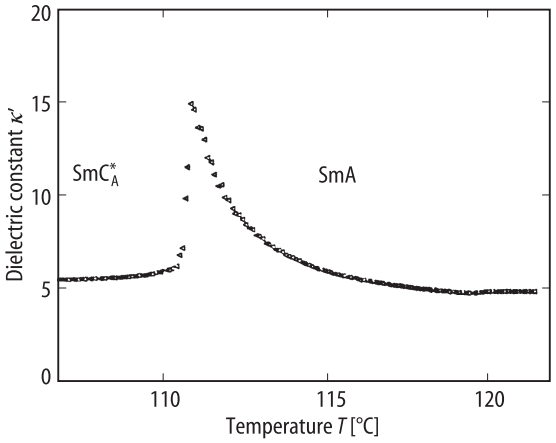

Fig. 71B-1-092. TFMHPOBC. κ' vs. T [91Hir2]. f = 10.6 kHz.

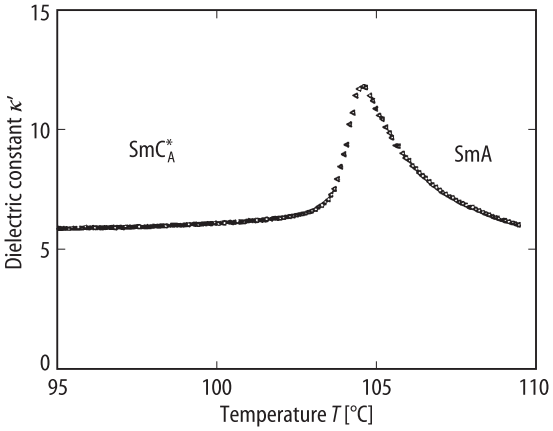

Fig. 71B-1-093. TFMNPOBC. κ' vs. T [91Hir2]. f = 10.6 kHz.

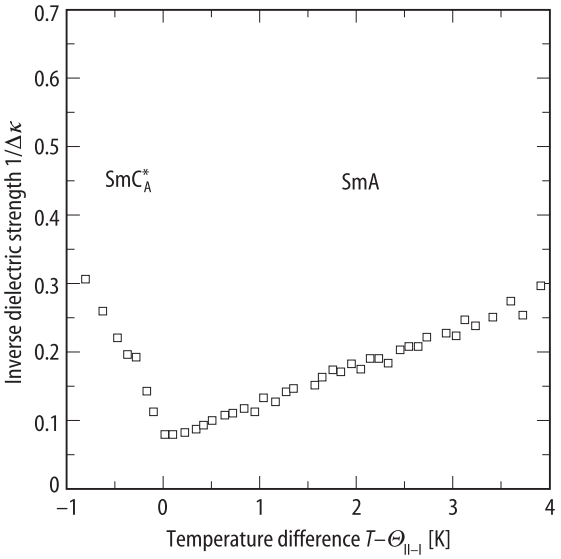

Fig. 71B-1-094. TFMHPOBC. $1/\Delta\kappa$ vs. $T - \Theta_{II-I}$ [91Hir2]. $\Delta\kappa$: dielectric strength.

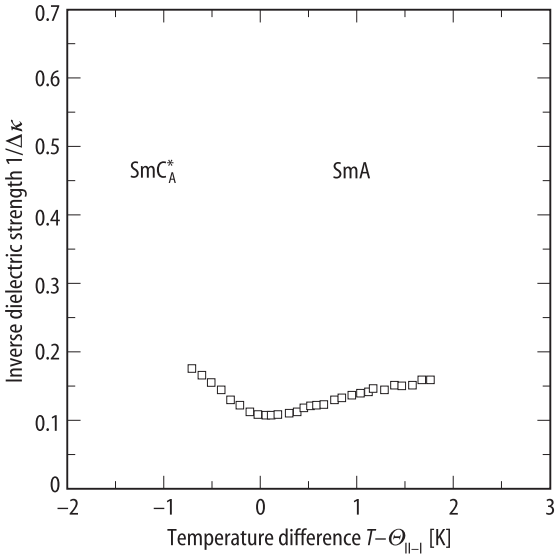

Fig. 71B-1-095. TFMNPOBC. $1/\Delta\kappa$ vs. $T - \Theta_{II-I}$ [91Hir2]. $\Delta\kappa$: dielectric strength.

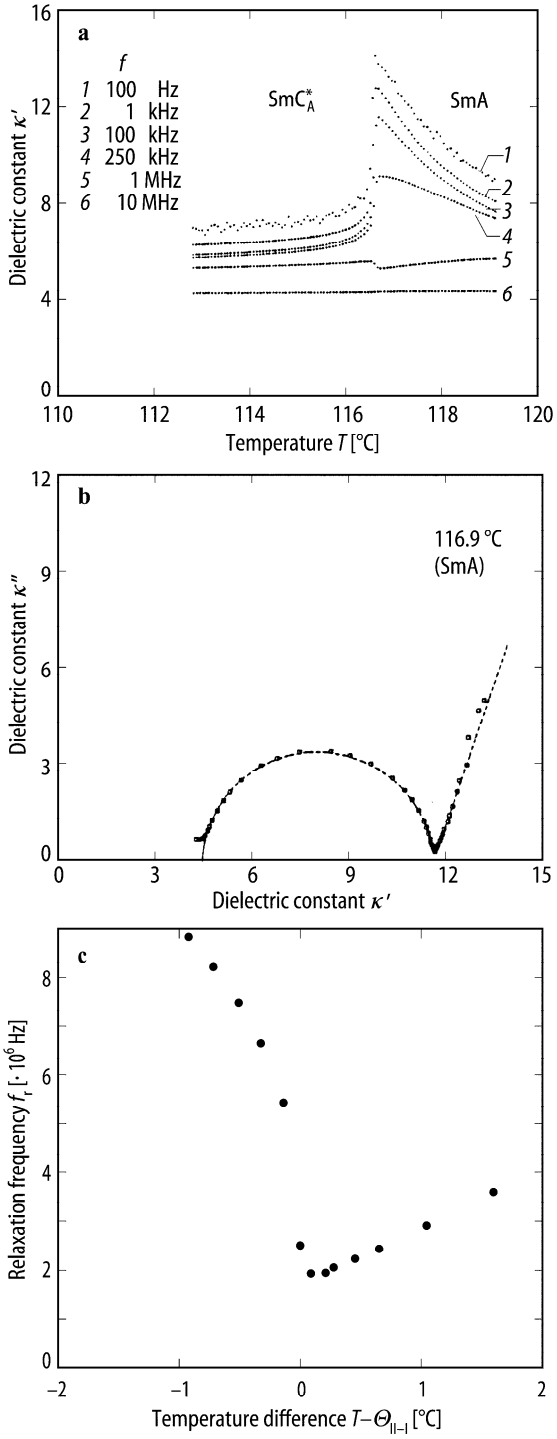

Fig. 71B-1-096. *R*-TFMHPOBC. (**a**) κ' vs. *T*. Parameter: *f*. (**b**) κ' vs. κ'' (Cole-Cole plot). T = 116.9 °C. (**c**) f_r vs. $T - \Theta_{II–I}$ [91Fuj]. f_r: relaxation frequency.

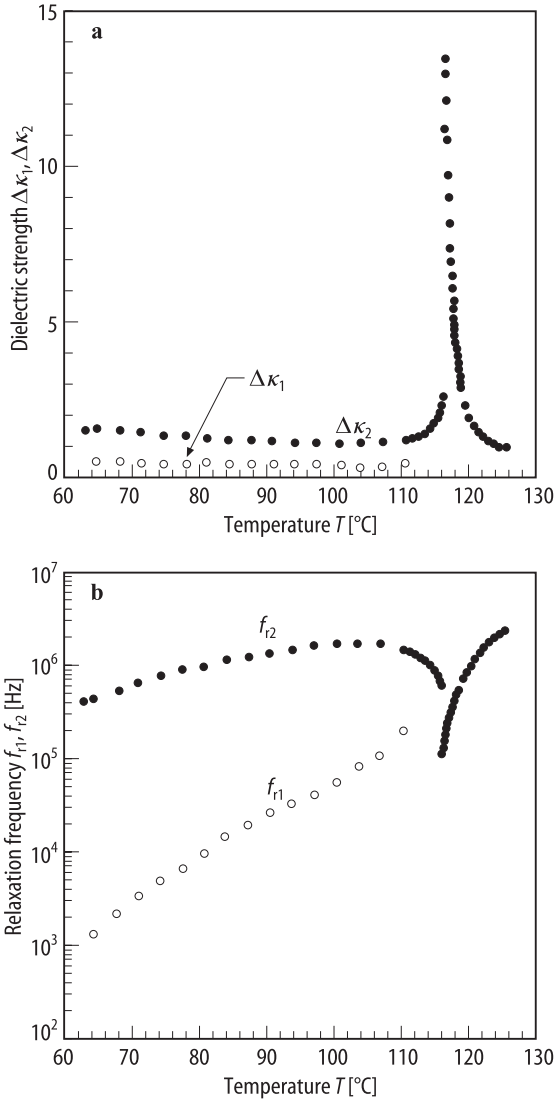

Fig. 71B-1-097. TFMHPOBC. (**a**) $\Delta\kappa_1$, $\Delta\kappa_2$ vs. T. (**b**) f_{r1}, f_{r2} vs. T [93Mor2]. $\Delta\kappa_i$: dielectric strength. f_{ri}: relaxation frequency; i = 1: low frequency dispersion, i = 2: high frequency dispersion.

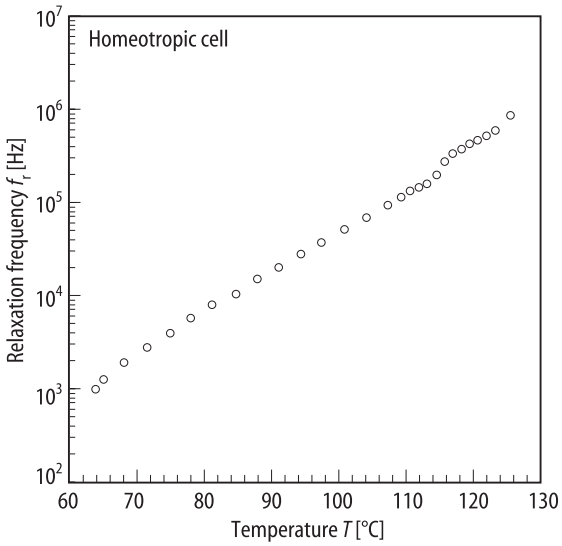

Fig. 71B-1-098. TFMHPOBC. f_r vs. T [93Mor2]. f_r: relaxation frequency. Homeotropically aligned cell.

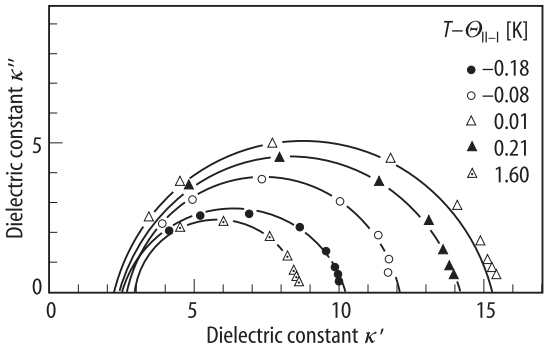

Fig. 71B-1-099. TFMHPOBC. κ' vs. κ'' (Cole-Cole plot) [91Hir2]. Parameter: $T - \Theta_{II-I}$.

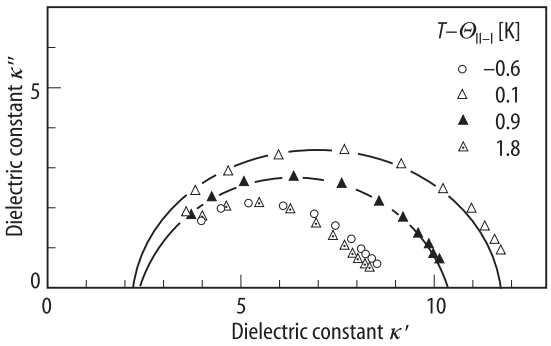

Fig. 71B-1-100. TFMNPOBC. κ' vs. κ'' (Cole-Cole plot) [91Hir2]. Parameter: $T - \Theta_{II-I}$.

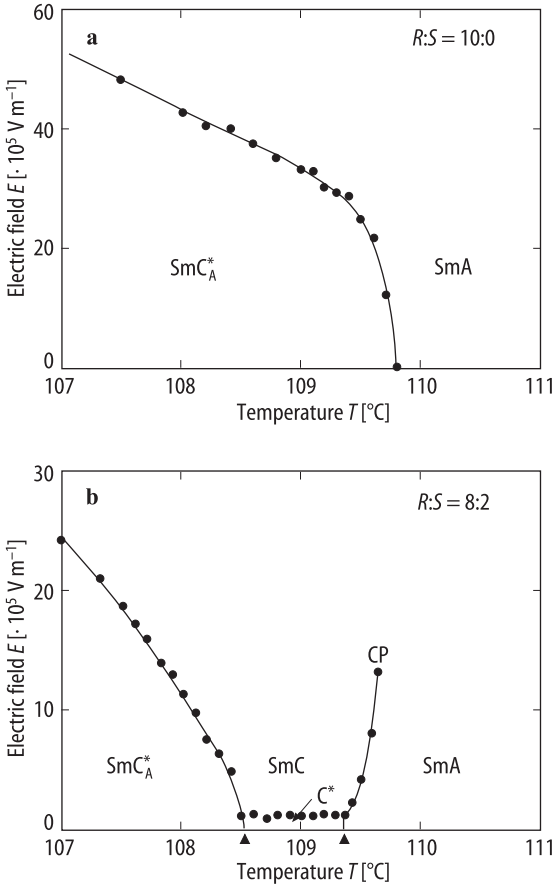

Fig. 71B-1-101. (*R*-TFMHPOBC) · (*S*-TFMHPOBC). *E*–*T* phase diagram [91Fuj]. (**a**) *R* : *S* = 10 : 0. (**b**) *R* : *S* = 8 : 2. CP: critical point.

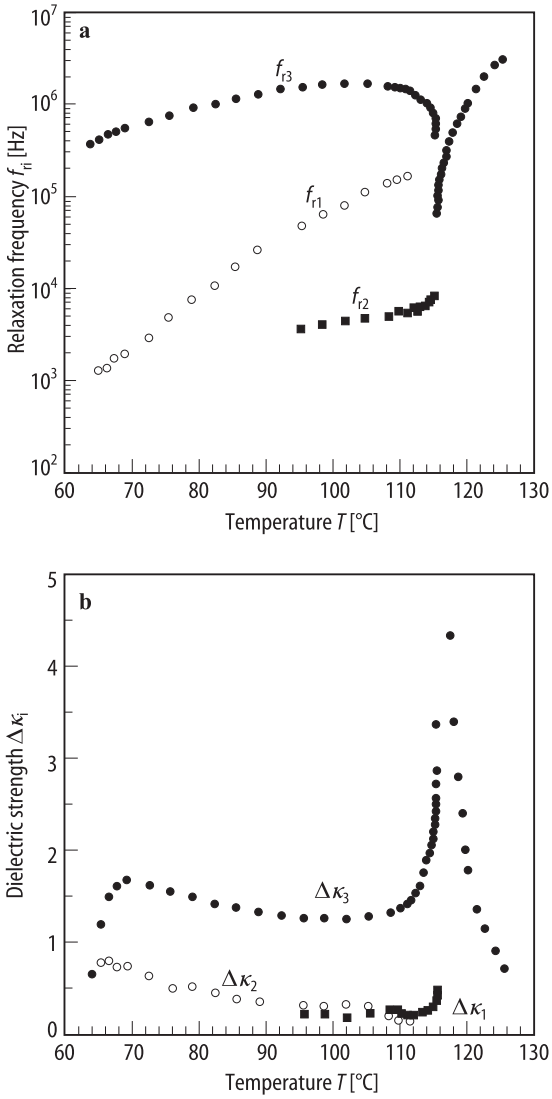

Fig. 71B-1-102. TFMHPOBC. (**a**) f_{r1}, f_{r2}, f_{r3} vs. T. (**b**) $\Delta\kappa_1$, $\Delta\kappa_2$, $\Delta\kappa_3$ vs. T [93Mor2]. $E_{bias} = 1 \cdot 10^6$ V m^{-1}. $\Delta\kappa_i$: dielectric strength. f_{ri}: relaxation frequency. i = 1: low frequency dispersion, i = 2: medium frequency dispersion, i = 3: high frequency dispersion.

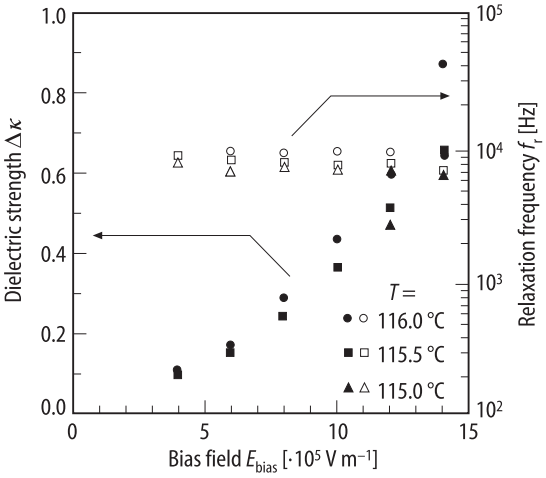

Fig. 71B-1-103. TFMHPOBC. $\Delta\kappa$; f_r vs. E_{bias} [93Mor2]. Parameter: T. $\Delta\kappa$: dielectric strength (full symbols). f_r: relaxation frequency (open symbols).

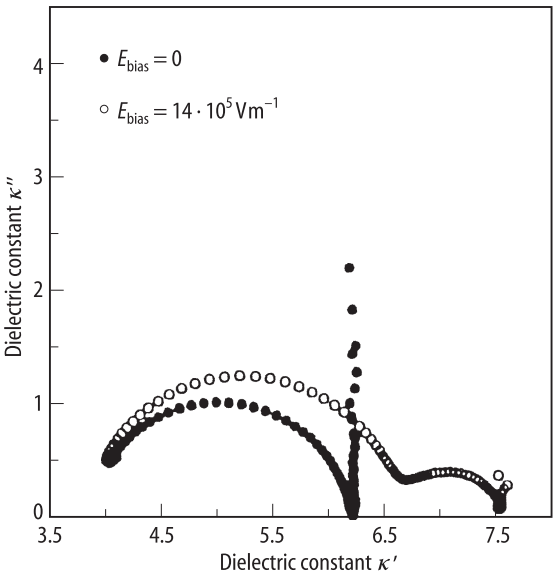

Fig. 71B-1-104. TFMHPOBC. κ' vs. κ'' (Cole-Cole plot) [93Mor2]. Parameter: E_{bias}. T = 116.0 °C.

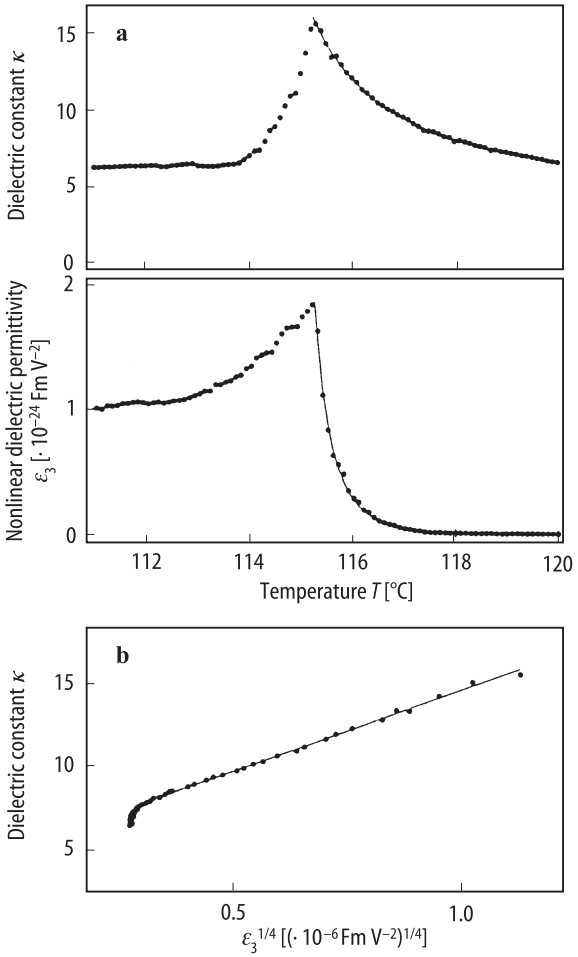

Fig. 71B-1-105. TFMHPOBC. (**a**) ε_3, κ vs. T. (**b**) κ vs. $\varepsilon_3^{1/4}$ in $Sm\,C_A^*$ phase [96Kim]. ε_3: third order nonlinear dielectric permittivity. f = 5 kHz.

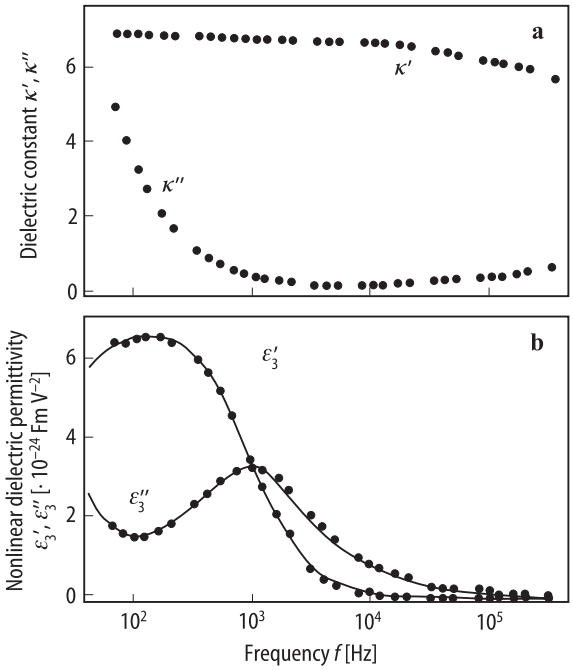

Fig. 71B-1-106. TFMHPOBC. (**a**) κ', κ'' vs. *f*. (**b**) ε_3', ε_3'' vs. *f* [96Kim]. ε_3', ε_3'' : real and imaginary parts of third order nonlinear dielectric permittivity. T = 85 °C.

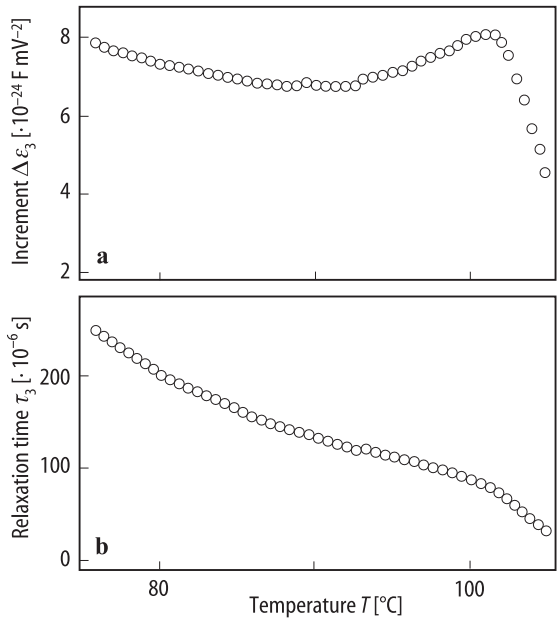

Fig. 71B-1-107. TFMHPOBC. (**a**) $\Delta\varepsilon_3$ vs. *T*. (**b**) τ_3 vs. *T* [96Kim]. $\Delta\varepsilon_3$: increment of third order nonlinear dielectric permittivity in Sm C_A^* . τ_3: relaxation time of the third order dielectric constant.

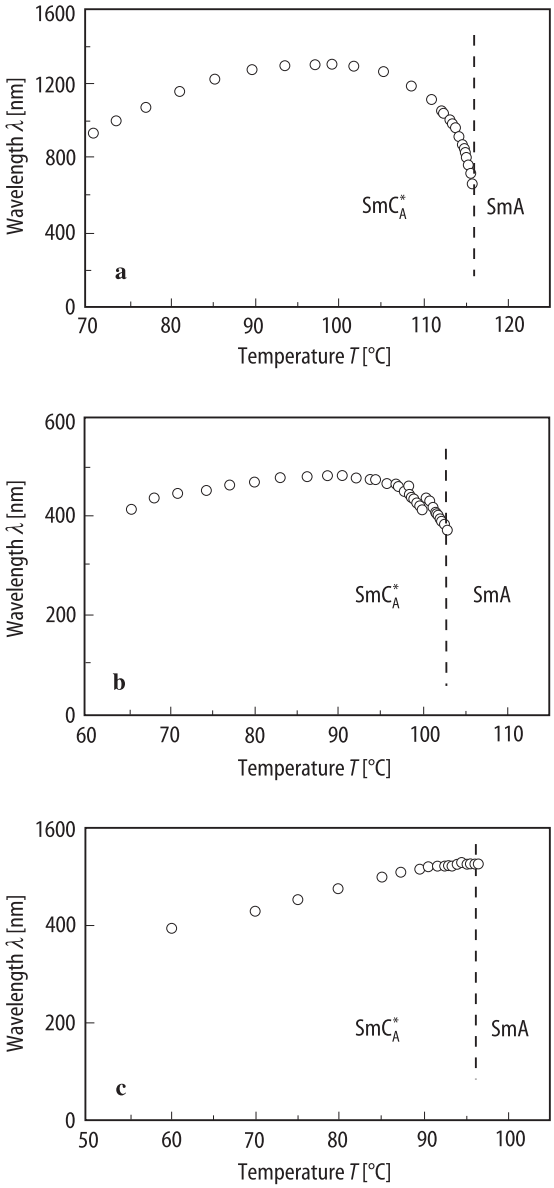

Fig. 71B-1-108. *R*-TFMHPOBC (**a**), *R*-TFMNPOBC (**b**), *R*-TFMHPDOPB (**c**). λ vs. T [91LiJ]. λ: wavelength of a selective reflection band (helical pitch multiplied by average refractive index).

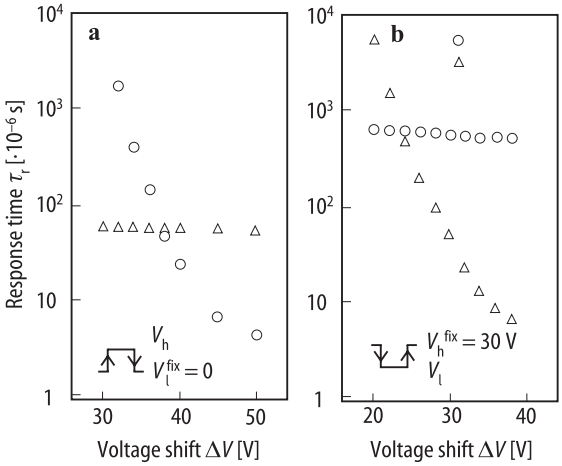

Fig. 71B-1-109. TFMNPOBC. τ_r vs. ΔV [90Joh]. τ_r: response time representing the transmittance change from 10 % to 90 %. $\Delta V = |V_h - V_l|$. V_h, V_l: high and low voltages of applied voltage square waves (see inserts). Circle: Sm C_A^* → Sm C^*. Triangle: Sm C^* → Sm C_A^*. (**a**) $V_l = 0$. (**b**) $V_h = 30$ V.

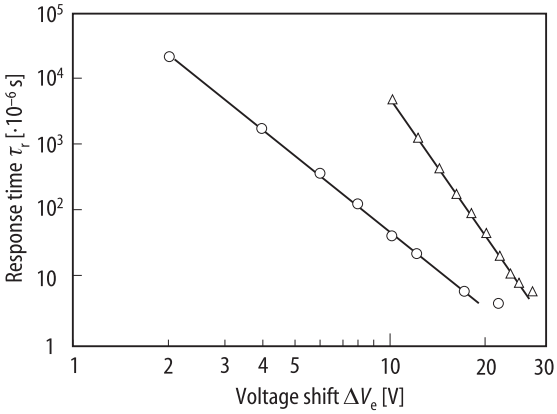

Fig. 71B-1-110. TFMNPOBC. τ_r vs. ΔV_e [90Joh]. τ_r: response time representing the transmittance change from 10 % to 90 %. $\Delta V_e = V_h - V_{th,h}$ for Sm C_A^* → Sm C^* (circle) and $\Delta V_e = V_{th,l} - V_l$ for Sm C^* → Sm C_A^* (triangle). V_h, V_l: high and low voltages of applied voltage square waves. $V_{th,h}$, $V_{th,l}$: upper and lower threshold voltages.

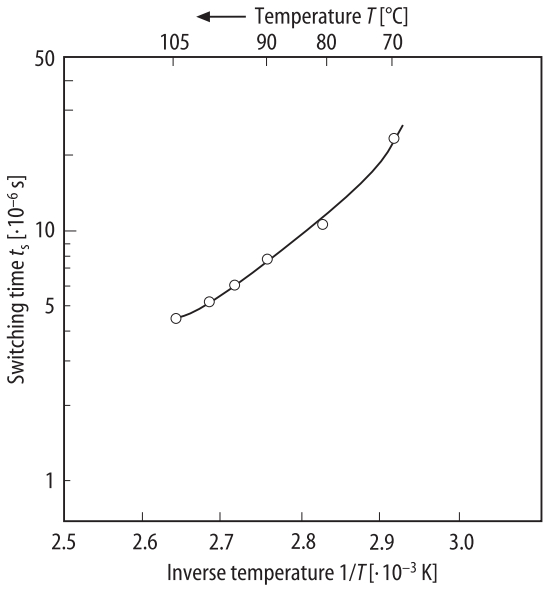

Fig. 71B-1-111. TFMHPOBC. t_s vs. $1/T$ [89Suz]. t_s: switching time from one uniform state to the other obtained from the transmittance change by reversing applied voltage from +30 V to –30 V.

References

88Cha Chadani, A.D.L., Hagiwara, T., Suzuki, Y., Ouchi, Y., Takezoe, H., Fukuda, K.: Jpn. J. Appl. Phys. **27** (1988) L729.

89Cha Chadani, A.D.L., Ouchi, Y., Takezoe, H., Fukuda, K., Terashima, K., Furukawa, K., Kishi, A.: Jpn. J. Appl. Phys. **28** (1989) L1265.

89Nis Nishiyama, I., Yoshizawa, A., Fukumasa, M., Hirai, T.: Jpn. J. Appl. Phys. **28** (1989) L2248.

89Suz Suzuki, Y., Hagiwara, T., Kawamura, T., Okamura, N., Kitazume, T., Kakimoto, M.: Liq. Cryst. **6** (1989) 167.

89Yam Yamada, Y., Mori, K., Yamamoto, N., Hayashi, H., Nakamura, K., Yamawaki, M., Orihara, H., Ishibashi, Y.: Jpn. J. Appl. Phys. **28** (1989) L1606.

90Fuk Fukui, M., Orihara, H., Suzuki, S., Ishibashi, Y., Yamada, Y., Yamamoto, N., Mori, K., Nakamura, K., Suzuki, Y., Kawamura, I.: Jpn. J. Appl. Phys. **29** (1990) L329.

90Gor Gorecka, E., Chadani, A.D.L., Ouchi, Y., Takezoe, H., Fukuda, A.: Jpn. J. Appl. Phys. **29** (1990) 131.

90Hir1 Hiraoka, K., Taguchi, A., Ouchi, Y., Takezoe, H., Fukuda, A.: Jpn. J. Appl. Phys. **29** (1990) L103.

90Hir2 Hiraoka, K., Chadani, A.D.L., Gorecka, E., Ouchi, Y., Takezoe, H., Fukuda, A.: Jpn. J. Appl. Phys. **29** (1990) L1473.

90Joh Johno, M., Itoh, K., Lee, J., Ouchi, Y., Takezoe, H., Fukuda, A., Kitazume, T.: Jpn. J. Appl. Phys. **29** (1990) L107.

90Lee1 Lee, J., Chadani, A.D.L., Itoh, K., Ouchi, Y., Takezoe, H., Fukuda, A.: Jpn. J. Appl. Phys. **29** (1990) 1122.

90Lee2 Lee, J., Ouchi, Y., Takezoe, H., Fukuda, A., Watanabe, J.: J. Phys. Condens. Matter **2** (1990) SA271.

90Suz Suzuki, A., Orihara, H., Ishibashi, Y., Yamada, Y., Yamamoto, N., Mori, K., Nakamura, Y., Suzuki, Y., Hagiwara, T., Kawamura, K., Fukui, M.: Jpn. J. Appl. Phys. **29** (1990) L336.

91Fuj Fujikawa, T., Orihara, H., Ishibashi, Y., Yamada, Y., Yamamoto, N., Mori, K., Nakamura, K., Suzuki, Y., Hagiwara, T., Kawamura, I.: Jpn. J. Appl. Phys. **30** (1991) 2826.

91Hir1 Hiraoka, K., Tanishi, Y., Skarp, K., Takezoe, H., Fukuda, A.: Jpn. J. Appl. Phys. **30** (1991) L1819.

91Hir2 Hiraoka, K., Ouchi, Y., Takezoe, H., Fukuda, A., Inui, S., Kawano, S., Saito, M., Iwane, H., Itoh, K.: Mol. Cryst. Liq. Cryst. **199** (1991) 197.

91Iso Isozaki, T., Suzuki, Y., Kawamura, I., Mori, K., Yamamoto, N., Yamada, Y., Orihara, H., Ishibashi, Y.: Jpn. J. Appl. Phys. **30** (1991) L1573.

91LiJ Li, J., Takezoe, H., Fukuda, A.: Jpn. J. Appl. Phys. **30** (1991) 532.

91Sun Sun, H., Orihara, H., Ishibashi, Y.: J. Phys. Soc. Jpn. **60** (1991) 4175.

91Tak1 Takezoe, H., Lee, J., Chadani, A.D.L., Gorecka, E., Ouchi, Y., Fukuda, A., Terashima, K.: Ferroelectrics **114** (1991) 187.

91Tak2 Takezoe, H., Lee, J., Ouchi, Y., Fukuda, A.: Mol. Cryst. Liq. Cryst. **85** (1991) 202.

91Tak3 Takanishi, Y., Hiraoka, K., Agrawal, V.K., Takezoe, H., Fukuda, A., Matsushita, M.: Jpn. J. Appl. Phys. **30** (1991) 2023.

91Tak4 Takezoe, H., Fukuda, A.: Jpn. J. Appl. Phys. **30** (1991) 532.

91Yam Yamamoto, N., Yamada, Y., Mori, K., Nakamura, K., Orihara, H., Ishibashi, Y., Suzuki, Y., Negi,Y.S., Kawamura, I.: Jpn. J. Appl. Phys. **30** (1991) 2380.

92Hir Hiraoka, K., Takanishi, Y., Takezoe, H., Fukuda, A., Isozaki, T., Suzuki, Y., Kawamura, I.: Jpn. J. Appl. Phys. **31** (1992) 3394.

92Iso Isozaki, T., Hiraoka, K., Takanishi, Y., Takezoe, H., Fukuda, A., Suzuki, Y., Kawamura, I.: Liq. Cryst. **12** (1992) 59.

92Mor Moritake, H., Shigeno, N., Ozaki, M., Yoshino, K.: Jpn. J. Appl. Phys. **31** (1992) 3193.

92Oka Okabe, N., Suzuki, Y., Kawamura, I., Isozaki, T., Takezoe, H., Fukuda, A.: Jpn. J. Appl. Phys. **31** (1992) L793.

93Bah Bah, Ch., Fliegner, D.: Ferroelectrics **147** (1993) 1.

93Glo Glogarova, M., Sverenyak, H., Fukuda, A., Takezoe, H.: Liq. Cryst. **14** (1993) 463.

93Hir Hiraoka, K., Takezoe, H., Fukuda, A.: Ferroelectrics **147** (1993) 13.
93Hor Hori, K., Endo, K.: Bull. Chem. Soc. Jpn. **66** (1993) 46.
93Ike Ikeda, A., Takanishi, Y., Takezoe, H., Fukuda, A.: Jpn. J. Appl. Phys. **32** (1993) L97.
93Iso1 Isozaki, T., Ishikawa, K., Takezoe, H., Fukuda, A.: Ferroelectrics **147** (1993) 121.
93Iso2 Isozaki, T., Fujikawa, K., Takezoe, H., Fukuda, A.: Phys. Rev. B **48** (1993) 13439.
93Mor1 Moritake, H., Uchiyama, Y., Myojin, K., Ozaki, M., Yoshino, K.: Ferroelectrics **147** (1993) 53.
93Mor2 Moritake, H., Ozaki, M., Yoshino, K.: Jpn. J. Appl. Phys. **32** (1993) L1432.
93Mus Muševic, I., Žekš, B., Blinc, R., Rasing, Th.: Phys. Rev. E **47** (1993) 1094.
93Ori Orihara, H., Igasaki, Y., Ishibashi, Y.: Ferroelectrics **147** (1993) 67.
93Sun Sun, H., Orihara, H., Ishibashi, Y.: J. Phys. Soc. Jpn. **62** (1993) 2066.
93Tak Takanishi, Y., Takezoe, H., Fukuda, A.: Ferroelectrics **147** (1993) 135.
94Kim Kim, K.-H., Miyachi, K., Ishikawa, K., Takezoe, H., Fukuda, A.: Jpn. J. Appl. Phys. **33** (1994) 5850.
95Cep Cepic, M., Heppke, G., Hollidt, J.-M., Lötzsch, D., Moro, D., Žekš, B.: Mol. Cryst. Liq. Cryst. **263** (1995) 207.
95Kim Kim, K.-H., Ishikawa, K., Takezoe, H., Fukuda, A.: Phys. Rev. E **51** (1995) 2166.
95LiJ Li, J., Takezoe, H., Fukuda, A., Watanabe, J.: Liq. Cryst. **18** (1995) 239.
95Mor Moritake, H., Nakayama, K., Ozaki, M., Yoshino, K.: Mol. Cryst. Liq. Cryst. **263** (1995) 13.
95Tak Takanishi, Y., Ikeda, A., Takezoe, H., Fukuda, A.: Phys. Rev. E **51** (1995) 400.
96Bah Bahr, Ch., Booth, C.J., Fliegner, D., Goodby, J.W.: Ferroelectrics **178** (1996) 229.
96Ema1 Ema, K., Ogawa, M., Takagi, A., Yao, H.: Phys. Rev. E **54** (1996) R25.
96Ema2 Ema, K., Takagi, A., Yao, H.: Phys. Rev. E **53** (1996) R3036.
96Ema3 Ema, K., Yao, H., Fukuda, A., Takanishi, Y., Takezoe, H.: Phys. Rev. E **54** (1996) 4450.
96Gou Gouda, F., Dahlgren, A., Lagerwall, S.T., Stebler, B., Bömelburg, J., Heppke, G.: Ferroelectrics **178** (1996) 187.
96Kim Kimura, Y., Hayakawa, R., Okabe, N., Suzuki, Y.: Phys. Rev. E **53** (1996) 6080.
96Sak Sako, T., Kimura, Y., Hayakawa, R., Okabe, N., Suzuki, Y.: Jpn. J. Appl. Phys. **35** (1996) 679.
97Asa Asahina, J., Sorai, M., Fukuda, A., Takezoe, H., Furukawa, K., Terashima, K., Suzuki, Y., Kawamura, I.: Liq. Cryst. **23** (1997) 339.

No. 71B-2 10B1M7 and analogues

L–⬡–COO–⬡–⬡–R

(A) L: $C_nH_{2n+1}O$, R: $COOCH(CH_3)C_mH_{2m+1}$
1-methylalkyl 4′-(4″-*n*-alkoxybenzoyloxy) biphenyl-4-carboxylate

n = 10, m = 4:	**I(10, 4, 1):**	**1-methylpentyl 4′-(4″-*n*-decyloxybenzoyloxy) biphenyl-4-carboxylate**
n = 8, m = 6:	**I(8, 6, 1):**	**1-methylheptyl 4′-(4″-*n*-octyloxybenzoyloxy) biphenyl-4-carboxylate**
n = 9, m = 6:	**I(9, 6, 1):**	**1-methylheptyl 4′-(4″-*n*-nonyloxybenzoyloxy) biphenyl-4-carboxylate**
n = 10, m = 6:	**10B1M7 (I(10, 6, 1)):**	**1-methylheptyl 4′-(4″-*n*-decyloxybenzoyloxy) biphenyl-4-carboxylate**
n = 11, m = 6:	**I(11, 6, 1):**	**1-methylheptyl 4′-(4″-*n*-undecyloxybenzoyloxy) biphenyl-4-carboxylate**

1b n = 10 (*R*) 92Goo

phase		V	IV	III	II	I	I′
		crystalline solid	smectic C^*_A ($Sm\,C^*_A$)	smectic C^*_γ ($Sm\,C^*_\gamma$)	smectic C^* ($Sm\,C^*$)	smectic A (Sm A)	isotropic liquid
state			A	(F′)	F	P	
Θ [°C]	m = 4	66	74	85	107	134	
	m = 6	66	72	78	105	125	

Phase sequence of m = 6, n = 8...18 and n = 10, m = 2...6; see also Phase diagram for mixture of racemate with *R* isomer: Fig. 71B-2-001. 92Goo

3a Tilt angle: Fig. 71B-2-002, Fig. 71B-2-003, Fig. 71B-2-004.

6a Transition heat ΔH (n = 10): 92Goo

	m	$\Theta_{V–IV}$	$\Theta_{II–I}$	$\Theta_{I–I'}$
ΔH [kJ mol^{-1}]	4	31.7	0.05	4.9
ΔH [kJ mol^{-1}]	6	36.8	0.09	5.8

(B) L: $CH_2CHCOOC_{11}H_{22}O$, R: $COOCH(CH_3)C_mH_{2m+1}$
1-methylalkyl 4′-[4-(ω-acryloyloxyundecyloxy)benzoyloxy] biphenyl-4-carboxylate
m = 6: II(11, 6, 1): 1-methylheptyl 4′-[4-(ω-acryloyloxyundecyloxy)benzoyloxy] biphenyl-4- carboxylate
m = 8: II(11, 8, 1): 1-methylnonyl 4′-[4-(ω-acryloyloxyundecyloxy)benzoyloxy] biphenyl-4-carboxylate

1b	phase	IV	III	II	I	I′	93Nis
		smectic C_A^* (Sm C_A^*)	smectic C_γ^* (Sm C_γ^*)	smectic C^* (Sm C^*)	smectic A (Sm A)	isotropic liquid	
	state	(A)	(F′)	(F)	P		
	Θ [°C] m = 6	38.5	45.2	73.5	85.7		
	m = 8	27.4	39.9	72.0	82.9		
	Phase sequense of other II(11, m, 1): see						93Nis
3b	Tilt angle: Fig. 71B-2-005.						
6a	Transition heat at $\Theta_{I–I'}$: ΔH [kJ mol^{-1}] = 2.1 for m = 6 and 2.9 for m = 8.						93Nis

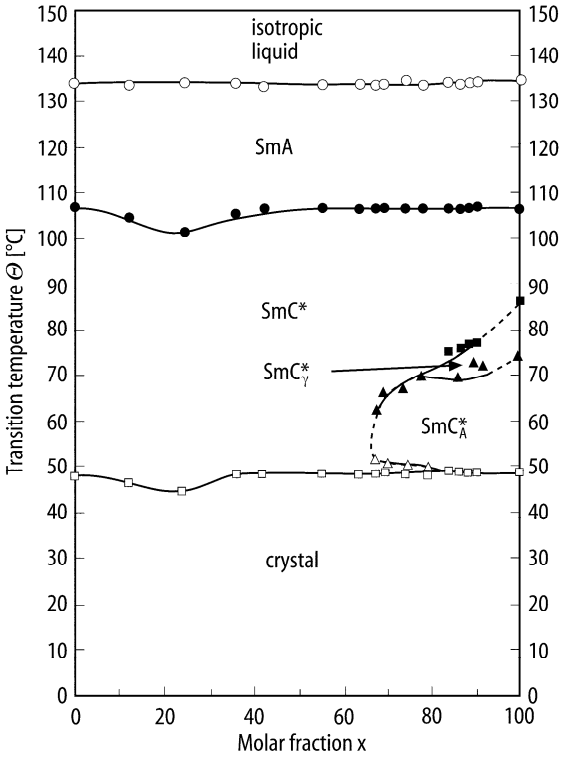

Fig. 71B-2-001. Mixture of racemate and *R* isomer of I(10, 4, 1). Θ vs. x [92Goo]. x: molar fraction of *R* isomer.

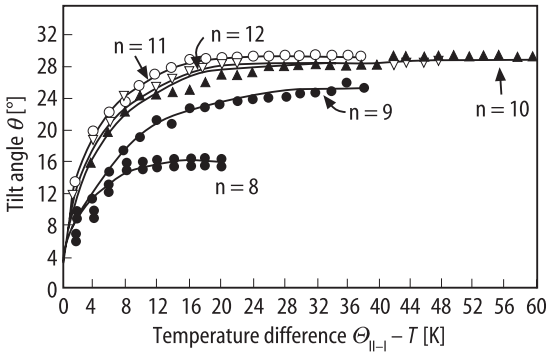

Fig. 71B-2-002. I(n, 6, 1). θ vs. $\Theta_{II-I} - T$ [92Goo]. Parameter: n. θ: tilt angle.

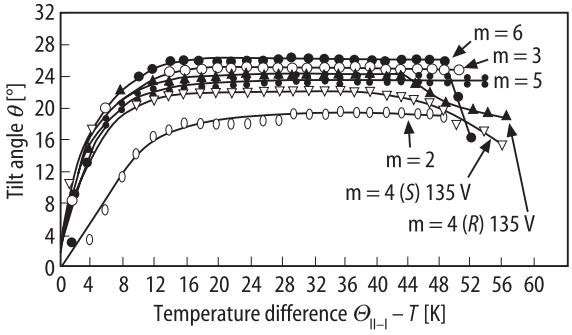

Fig. 71B-2-003. I(10, m, 1). θ vs. $\Theta_{II-I} - T$ [92Goo]. Parameter: m. θ: tilt angle. For m = 4, dc voltage of $V = 135$ V was applied.

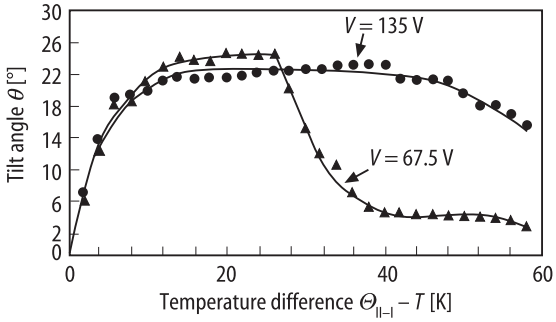

Fig. 71B-2-004. I(10, 4, 1). θ vs. $\Theta_{II-I} - T$ [92Goo]. Parameter: applied dc voltage V. θ: tilt angle.

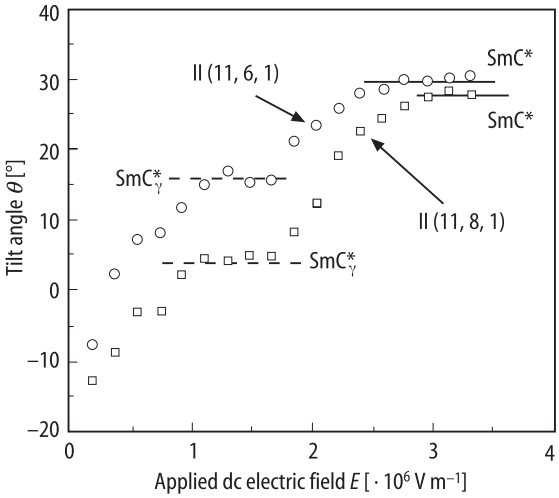

Fig. 71B-2-005. II(11, 6, 1), II(11, 8, 1). θ vs. E [93Nis]. θ: tilt angle. E: applied dc electric field. $T = 44$ °C in II(11, 6, 1). $T = 35$ °C in II(11, 8, 1).

References

92Goo Goodby, J.W., Patel, J.S., Chin. E.: J. Mater. Chem. **2** (1992) 197.
93Nis Nishiyama, I., Goodby, J.W.: J. Mater. Chem. **3** (1993) 169.

No. 71B-3 MHFPDBC group

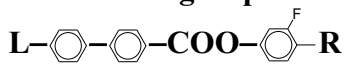

L: C_nH_{2n+1}, R: $COOCH(CH_3)C_6H_{13}$

4-(1-methylheptyloxycarbonyl) 3-flurophenyl 4′-alkoxybiphenyl-4-carboxylate

n = 7: MHFPHBC (4-(1-methylheptyloxycarbonyl) 3-flurophenyl 4′-heptyl-biphenyl-4-carboxylate)

n = 11: MHFPUBC (4-(1-methylheptyloxycarbonyl) 3-flurophenyl 4′-undecyl-biphenyl-4-carboxylate)

n = 12: MHFPDBC (4-(1-methylheptyloxycarbonyl) 3-flurophenyl 4′-dodecyl-biphenyl-4-carboxylate)

1b	Phase sequences: see Fig. 71B-3-001 for MHFPHBC, Fig. 71B-3-004 for MHFPUBC, Fig. 71B-3-005 for MHFPDBC.
5a	Dielectric dispersion: Fig. 71B-3-001, Fig. 71B-3-002, Fig. 71B-3-003, Fig. 71B-3-004, Fig. 71B-3-005, Fig. 71B-3-006, Fig. 71B-3-007, Fig. 71B-3-008.

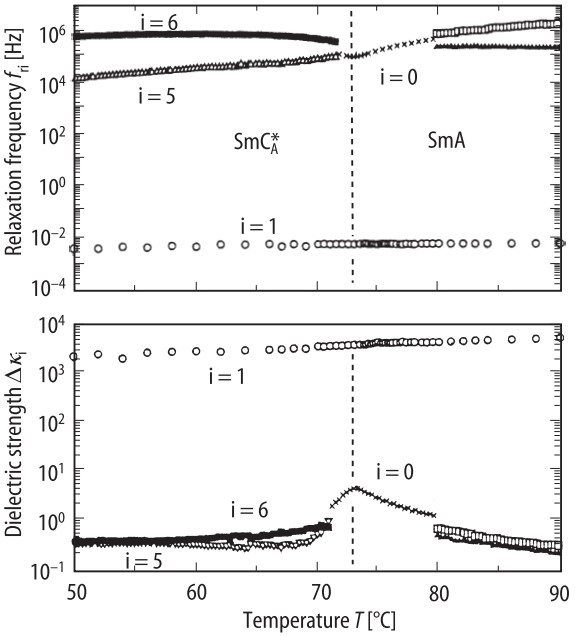

Fig. 71B-3-001. MHFPHBC. $\Delta\kappa_i$, f_{ri} vs. T [95Ueh]. $\Delta\kappa_i$: dielectric strength. f_{ri}: relaxation frequency. The data are analyzed with a generalized Cole-Cole formula, $\kappa = \kappa_\infty + \Sigma_i \Delta\kappa_i / [1 + (jf / f_{ri})^{\beta i}]$.

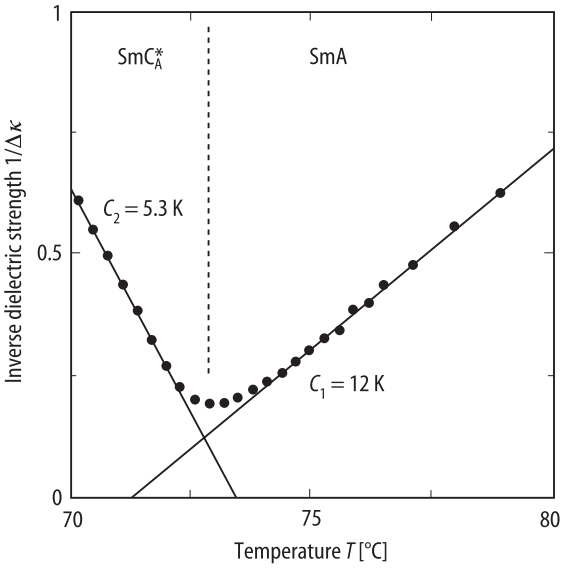

Fig. 71B-3-002. MHFPHBC. $1/\Delta\kappa$ vs. T [95Ueh]. $\Delta\kappa$: dielectric strength. C_1, C_2: Curie-Weiss constants of Sm A and Sm C^*_A phases, respectively.

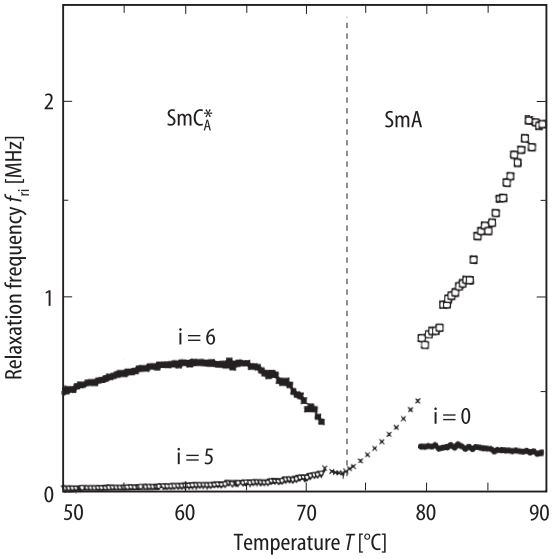

Fig. 71B-3-003. MHFPHBC. f_{ri} vs. T [95Ueh]. f_{ri}: relaxation frequency. As to i, see the caption of Fig. 71B-3-001.

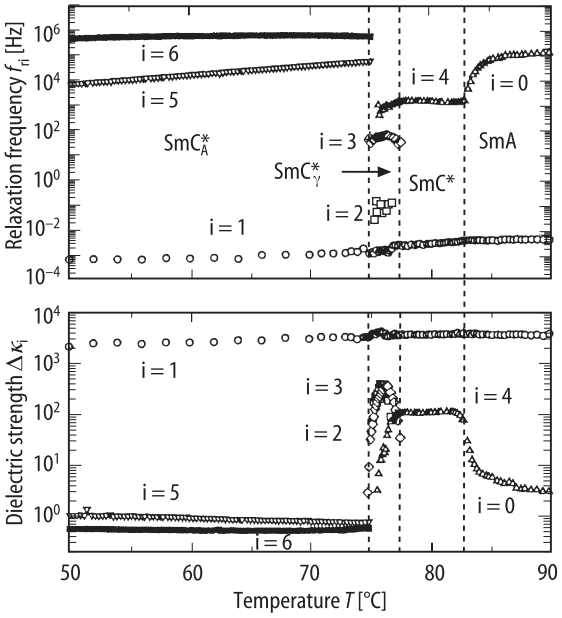

Fig. 71B-3-004. MHFPUBC. $\Delta\kappa_i$, f_{ri} vs. T [95Ueh]. $\Delta\kappa_i$: dielectric strength. f_{ri}: relaxation frequency. The data are analyzed with a generalized Cole-Cole formula, $\kappa = \kappa_\infty + \Sigma_i \Delta\kappa_i / [1 + (jf / f_{ri})^{\beta_i}]$.

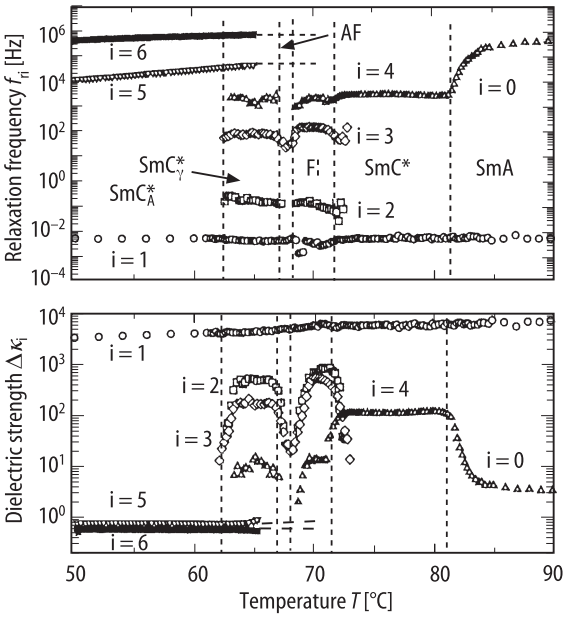

Fig. 71B-3-005. MHFPDBC. $\Delta\kappa_i$, f_{ri} vs. T [95Ueh]. $\Delta\kappa_i$: dielectric strength. f_{ri}: relaxation frequency. The data are analyzed with a generalized Cole-Cole formula, $\kappa = \kappa_\infty + \Sigma_i \Delta\kappa_i / [1 + (jf / f_{ri})^{\beta i}]$.

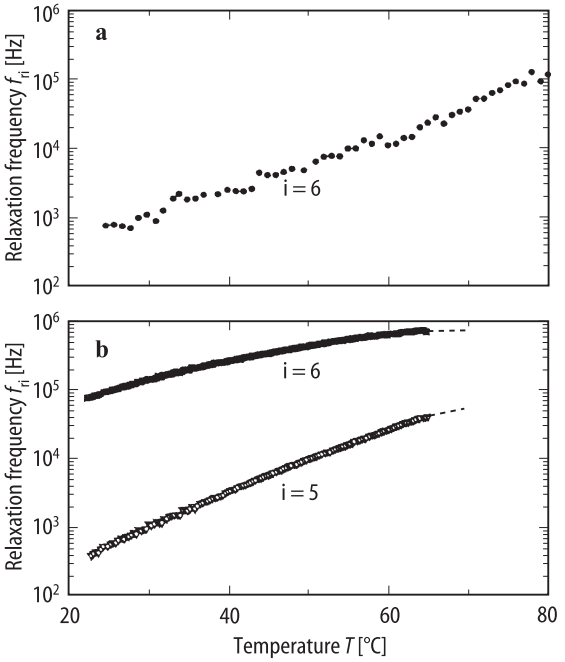

Fig. 71B-3-006. MHFPDBC. f_{ri} vs. T [95Ueh]. f_{ri}: relaxation frequency. As to i, see the caption of Fig. 71B-3-005. (**a**) homeotropically aligned cell. (**b**) homogeneously aligned cell.

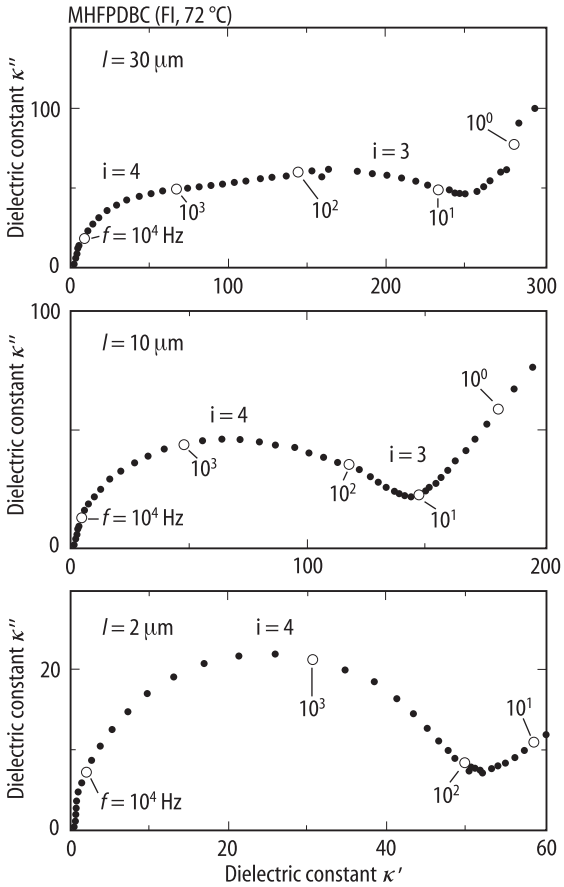

Fig. 71B-3-007. MHFPDBC. κ' vs. κ'' (Cole-Cole diagram) [95Ueh]. Parameter: l, cell thickness. $T = 72$ °C. As to i, see the caption of Fig. 71B-3-005.

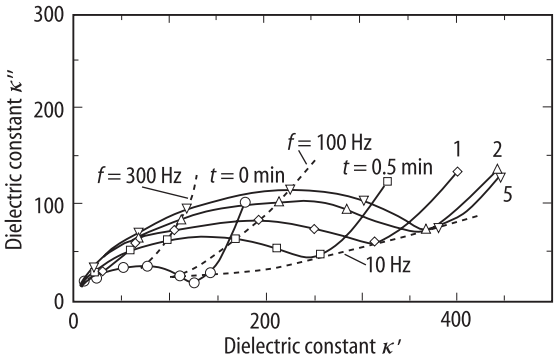

Fig. 71B-3-008. MHFPDBC. κ' vs. κ'' (Cole-Cole diagram) [95Ueh]. Parameter: t, time after removal of the bias field of $1.3 \cdot 10^5$ V m^{-1}. $T = 71$ °C.

Reference

95Ueh Uehara, H., Hanakai, Y., Hatano, J., Saito, S., Murashiro, K.: Jpn. J. Appl. Phys. **34** (1995) 5424.

No. 71B-4 12F1M7 and analogues

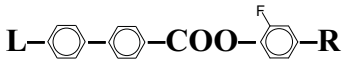

(A) L: $C_{12}H_{25}O$, R: $COOCH(CH_3)C_6H_{13}$
12F1M7: (4-(1-methylheptyloxycarbonyl)2-fluorophenyl 4′-dodecyloxybiphenyl-4-carboxylate)

1b Phase diagram of free standing films: Fig. 71B-4-001.

9a Ellipsometric parameters of transmitted light: Fig. 71B-4-002, Fig. 71B-4-003.

(B) L: $C_nH_{2n+1}O$, R: $COOCH(CF_3)C_mH_{2m+1}$
nBIMFm: (4-(1-trifluoromethylalkyloxycarbonyl)2-fluorophenyl 4′-alkoxybiphenyl-4-carboxylate)

1b n = 10: 95Tak

phase		IV	III	II	I	I′
		crystalline solid	smectic C_A^* (Sm C_A^*)	smectic C^* (Sm C^*)	smectic A (Sm A)	isotropic liquid
state			(A)	(F)	P	
Θ [°C]	m = 6	30	76.9		95.0	
	m = 7	30		70.2	88.3	

3b Layer thickness: Fig. 71B-4-004, Fig. 71B-4-005; see also Fig. 71B-1-089 in No. 71B-1.

14a Integrated intensity of X-ray reflection: see Fig. 71B-4-005.
Smectic layer order parameter: Fig. 71B-4-006.

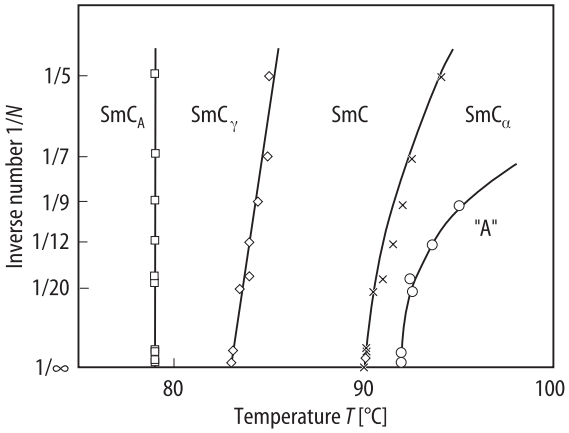

Fig. 71B-4-001. 12F1M7. $1/N$ vs. T [94Bah]. N: number of layers of free-standing films. "A": Sm A phase with tilted surface layers.

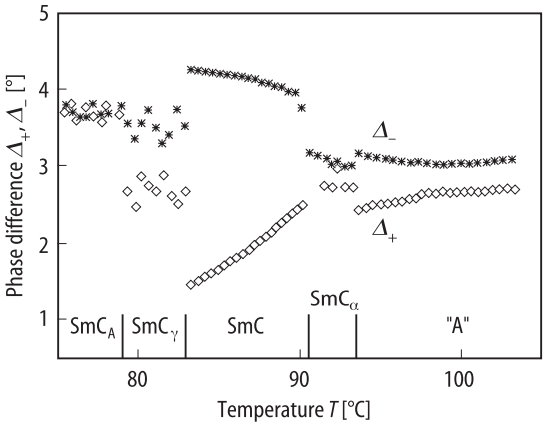

Fig. 71B-4-002. 12F1M7. Δ_+, Δ_- vs. T [94Bah]. Δ: phase difference between the *s*- and *p*-polarized components of the transmitted light. + and – correspond to the polarities of the orientating electric field. 20 layer film. Incident angle: 45°. $\lambda = 633$ nm. "A": Sm A phase with tilted surface layers.

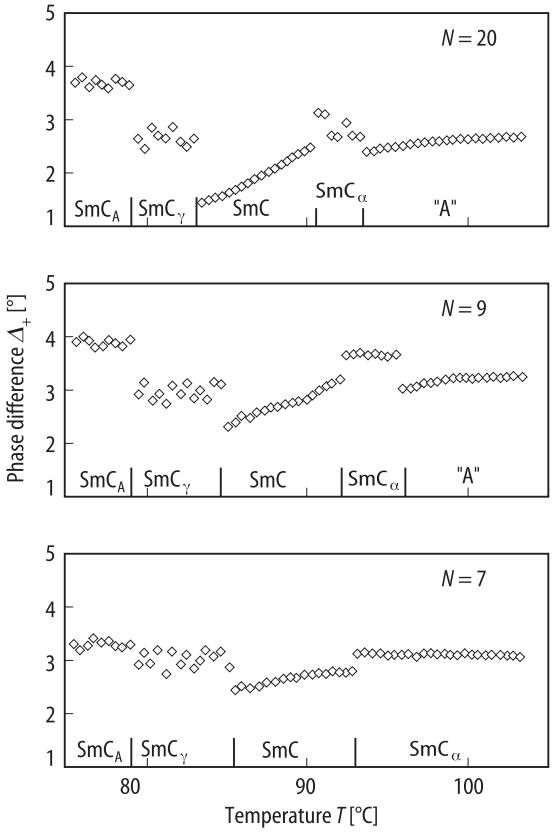

Fig. 71B-4-003. 12F1M7. Δ_+ vs. T [94Bah]. See the caption of Fig. 71B-4-002. N: number of layers in the film. "A": Sm A phase with tilted surface layers.

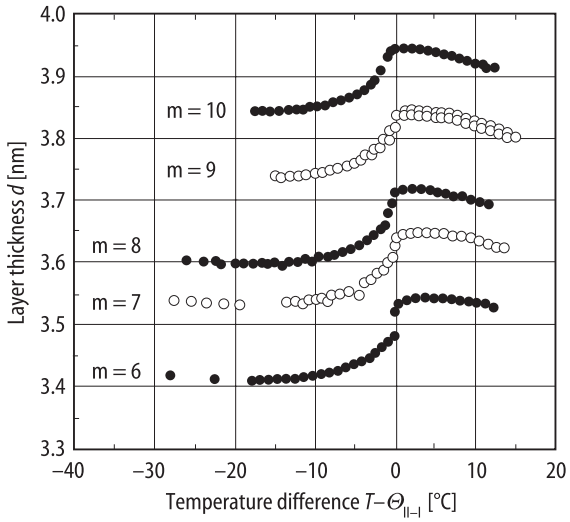

Fig. 71B-4-004. 10BIMFm (m = 6...10). d vs. $T - \Theta_{II-I}$ [93Ike]. d: layer thickness. Parameter: m.

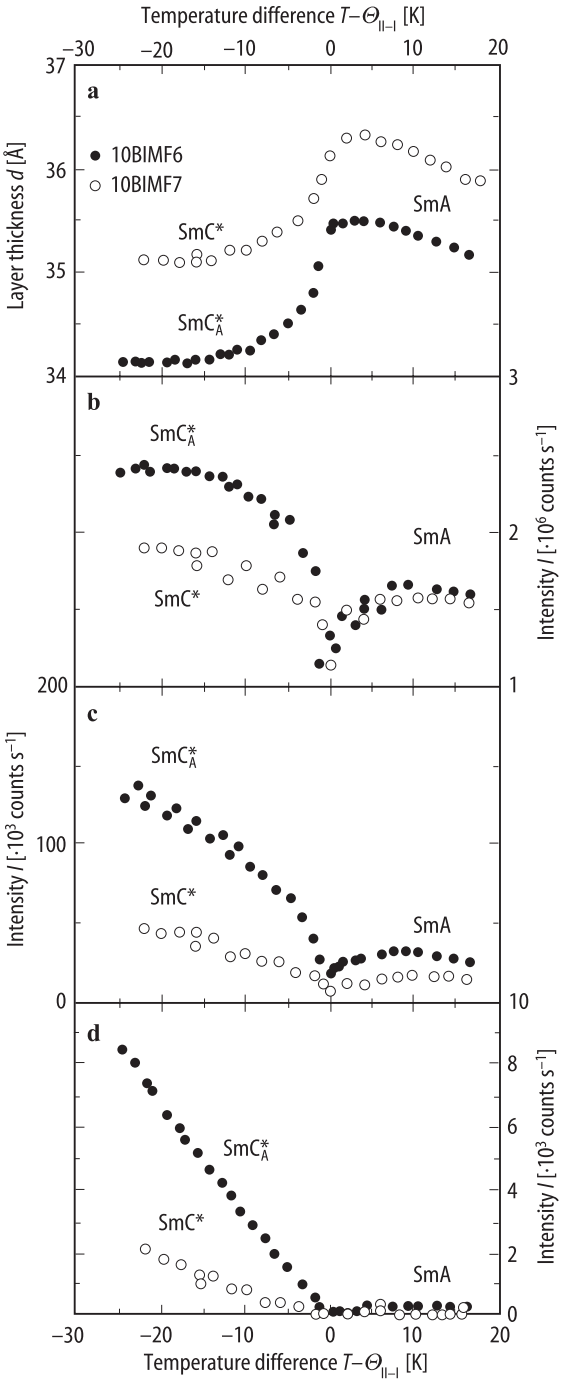

Fig. 71B-4-005. 10BIMFm (m = 6, 7). *d*, *I* vs. $T - \Theta_{II-I}$ [95Tak]. *d*: layer thickness. *I*: X-ray integrated intensity of the layer reflections. (**a**) Layer thickness. (**b**) The first reflection. (**c**) The second reflection. (**d**) The third reflection. Full circle: 10BIMF6. Open circle: 10BIMF7.

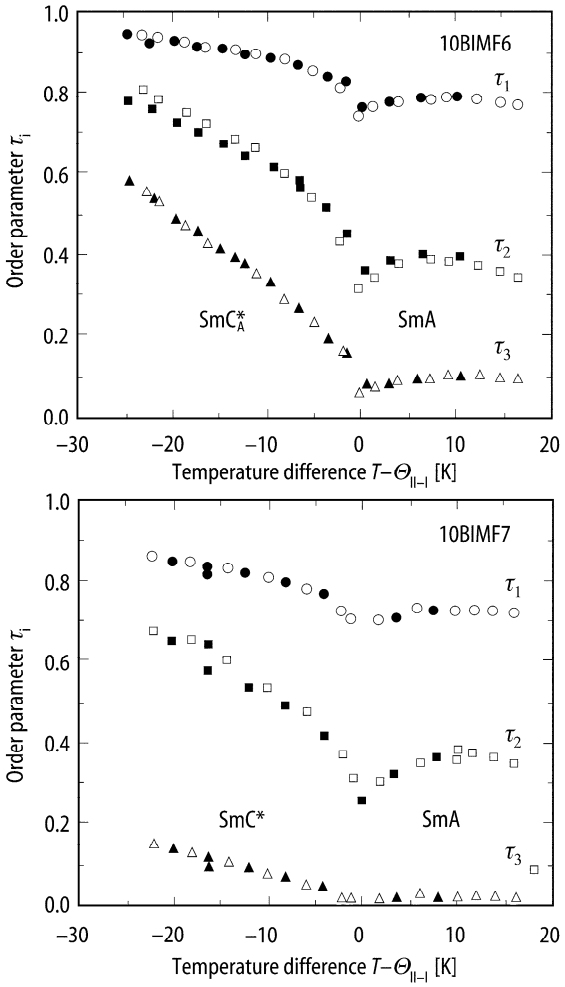

Fig. 71B-4-006. 10BIMFm (m = 6, 7). τ_i vs. $T - \Theta_{II-I}$ [95Tak]. τ_i: ith smectic-layer order parameter. Open symbol: heating. Full symbol: cooling.

References

93Ike Ikeda, A., Takanishi, Y., Takezoe, H., Fukuda, A.: Jpn. J. Appl. Phys. **32** (1993) L97.

94Bah Bahr, Ch., Fliegner, D., Booth, C.J., Goodby, J.W.: Europhys. Lett. **26** (1994) 539.

95Tak Takanishi, Y., Ikeda, A., Takezoe, H., Fukuda, A.: Phys. Rev. E **51** (1995) 400.

No. 71B-5 TFMHPDOPB

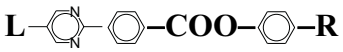

L: $C_{12}H_{25}O$, R: $COOCH(CF_3)C_6H_{13}$
4-(1-trifluromethylheptyloxycarbonyl) phenyl 4-(5-dodecyloxypyrimidin-2-yl)benzoate

1b	phase	III	II	I	I′	90Inu
		crystalline solid	smectic C_A^* (Sm C_A^*)	smectic A (Sm A)	isotropic liquid	
	state		A	P		
	Θ [°C] (heating)	58	98	105		
	(cooling)	32	97	104		
	Phase diagram of racemic mixture: Fig. 71B-5-001.					
3b	Layer thickness: Fig. 71B-5-002. Hysteresis loop of tilt angle: Fig. 71B-5-003.					
5a	Dielectric constant: Fig. 71B-5-004, Fig. 71B-5-005, Fig. 71B-5-006.					
6a	Differential scanning calorimetry: Fig. 71B-5-007.					
9a	Reflection band: see Fig. 71B-1-028, Fig. 71B-1-108 in No. 71B-1.					
d	Liquid crystal induced circular dichroism: see					95LiJ
10a	Raman scattering: see Fig. 71B-1-050 in No. 71B-1.					

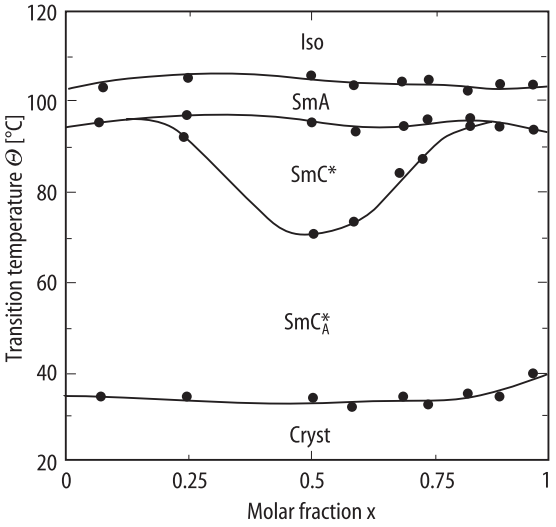

Fig. 71B-5-001. $(S\text{-TFMHPDOPB})_{1-x}(R\text{-TFMHPDOPB})_x$. Θ vs. x [91Ike]. Cooling process.

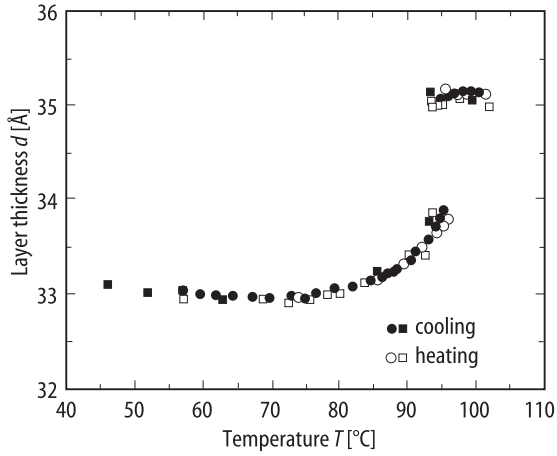

Fig. 71B-5-002. TFMHPDOPB. *d* vs. *T* [91Ike]. *d*: layer thickness. Full circle, open circle: *R*-TFMHPDOB. Full square, open square: *S*-TFMHPODB. Open symbol: heating. Full symbol: cooling.

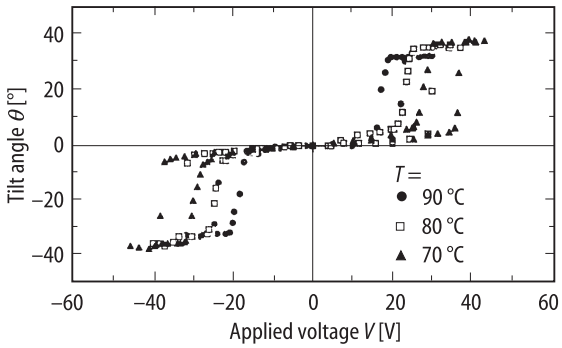

Fig. 71B-5-003. TFMHPDOPB. θ vs. *V* [90Inu]. Parameter: *T*. θ: tilt angle. *V*: applied voltage.

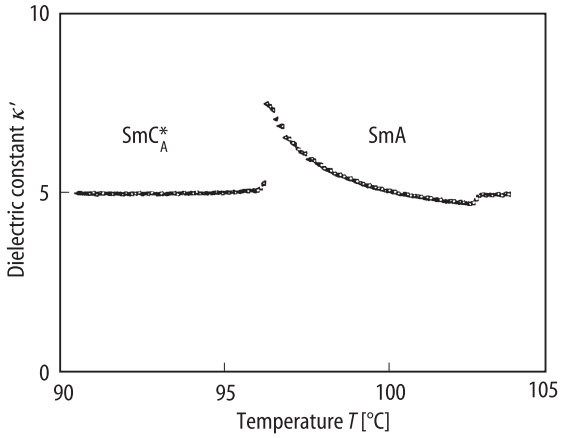

Fig. 71B-5-004. TFMHPDOPB. κ' vs. T [91Hir]. f = 10.6 kHz.

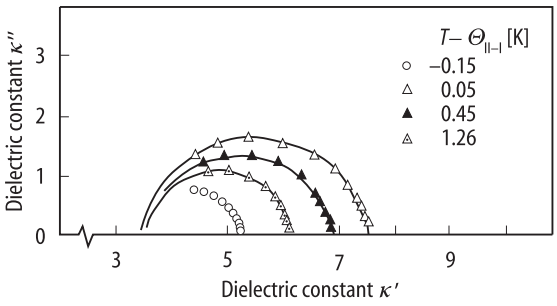

Fig. 71B-5-005. TFMHPDOPB. κ' vs. κ'' (Cole-Cole diagram) [91Hir]. Parameter: $T - \Theta_{II-I}$.

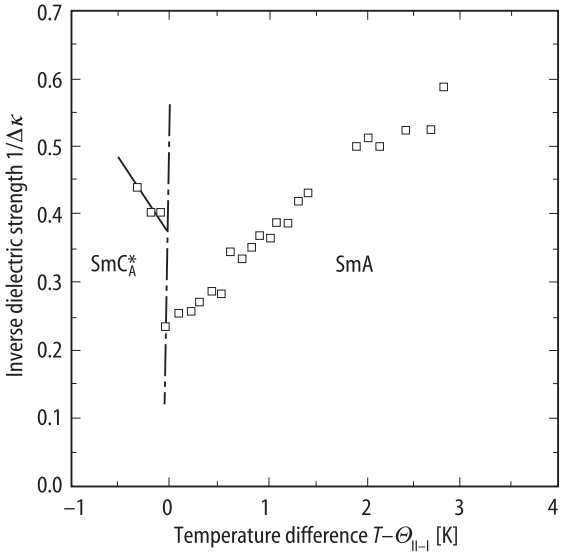

Fig. 71B-5-006. TFMHPDOPB. $1/\Delta\kappa$ vs. $T - \Theta_{II-I}$ [91Hir]. $\Delta\kappa$: dielectric strength.

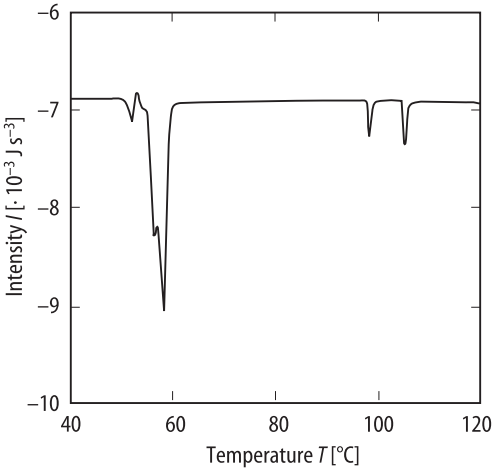

Fig. 71B-5-007. TFMHPDOPB. *I* vs. *T* [90Inu]. *I*: DSC signal intensity. Heating process. Rate: 5 °C/min.

References

90Inu Inui, S., Kawano, S., Saito, M., Iwane, H., Takanishi, Y., Hiraoka, K., Ouchi, Y., Takezoe, H., Fukuda, A.: Jpn. J. Appl. Phys. **29** (1990) L987.

91Hir Hiraoka, K., Ouchi, Y., Takezoe, H., Fukuda, A.: Mol. Cryst. Liq. Cryst. **199** (1991) 197.

91Ike Ikeda, A., Takanishi, Y., Takezoe, H., Fukuda, A., Inui, S., Kawano, S., Saito, M., Iwane, H.: Jpn. J. Appl. Phys. **30** (1991) L1032.

95LiJ Li, J., Takezoe, H., Fukuda, A., Watanabe, J.: Liq. Cryst. **18** (1995) 239.

No. 71B-6 TFMHPODB

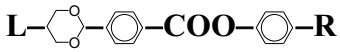

L: $C_8H_{17}O$, R: $COOCH(CF_3)C_6H_{13}$
4-(1-trifluromethylheptyloxycarbonyl) phenyl 4-(5-octyloxydioxane)benzoate

1b	phase	III	II	I	I′	95Kim
		crystalline solid	smectic C_A^* ($Sm\,C_A^*$)	smectic A (Sm A)	isotropic liquid	
	state		A	P		
	Θ [°C]	10	65	80		
9a	Infrared spectra: Fig. 71B-6-001.					

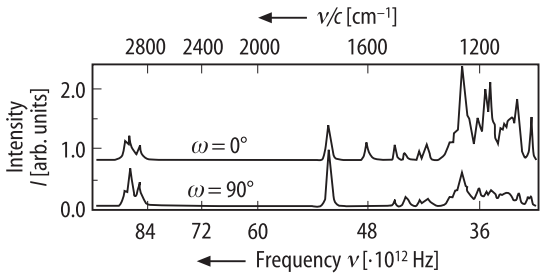

Fig. 71B-6-001. TFMHPODB. I vs. ν [95Kim]. I: intensity of infrared spectra. ω: angle between the polarization direction of IR ray and the smectic layer normal.

Reference

95Kim Kim, K.-H., Ishikawa, K., Takezoe, H., Fukuda, A.: Phys. Rev. E **51** (1995) 2166.

No. 71B-7 Thiobenzoate compound

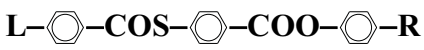

L: $C_{12}H_{25}O$, R: $COOCH(CH_3)C_6H_{13}$
4-(1-methylheptyloxycarbonyl)phenyloxycarbonyl 4′-*n*-dodecyloxyphenyl thiobenzoate

1b	phase	VI	V	IV	III	II	I	I′	93Glo
		crystalline solid	smectic C_A^* (Sm C_A^*)	smectic C_γ^* (Sm C_γ^*)	smectic C^* (Sm C^*)	smectic C_α^* (Sm C_α^*)	smectic A (Sm A)	isotropic liquid	
	state		(A)	(F′)	F	P	P		
	Θ[°C]	98		111	115	128.5	129	145	
3b	Spontaneous tilt angle: Fig. 71B-7-001.								
5a	Dielectric constant: Fig. 71B-7-002.								
c	Spontaneous polarization: Fig. 71B-7-003.								

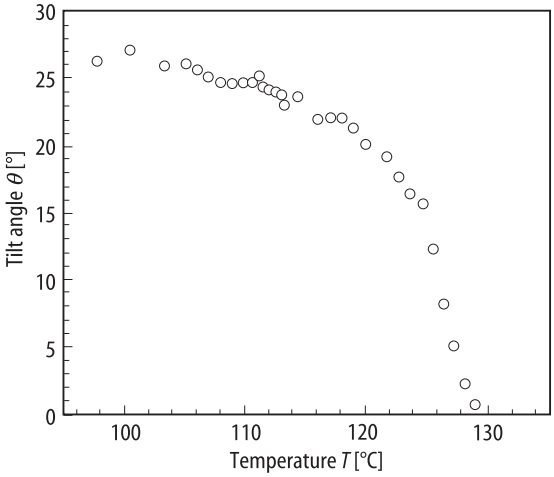

Fig. 71B-7-001. $C_{12}H_{25}O$–⬡–COS–⬡–COO–⬡–$COOCH(CH_3)C_6H_{13}$. θ vs. T [93Glo]. θ: spontaneous tilt angle.

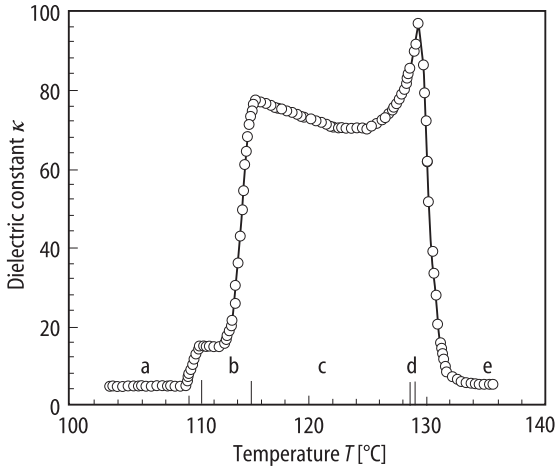

Fig. 71B-7-002. $C_{12}H_{25}O$–⬡–COS–⬡–COO–⬡–$COOCH(CH_3)C_6H_{13}$. κ vs. T [93Glo]. f = 120 Hz. Cooling rate: 0.1 K min^{-1}. a: Sm C^*_A . b: Sm C^*_γ . c: Sm C^*. d: Sm C^*_α . e: Sm A.

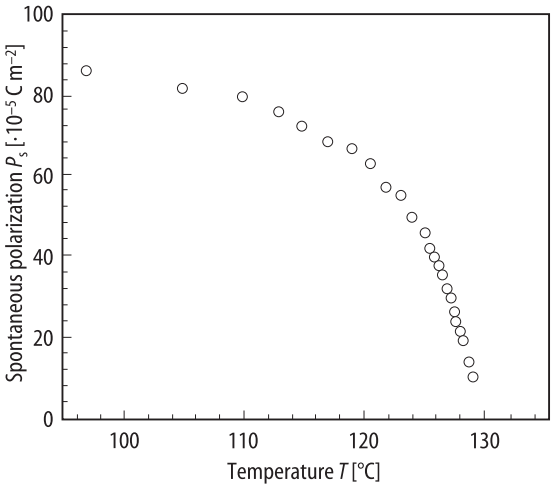

Fig. 71B-7-003. $C_{12}H_{25}O$–⬡–COS–⬡–COO–⬡–$COOCH(CH_3)C_6H_{13}$. P_s vs. T [93Glo].

Reference

93Glo Glogarova, M., Sverenyák, H., Nguyen, H.T., Destrade, Ch.: Ferroelectrics **147** (1993) 43.

No. 71B-8 Tolan group

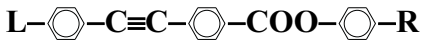

L: $C_nH_{2n+1}O$, R: $COOCH(CH_3)C_6H_{13}$
n = 8: tolan C8
n = 10: tolan C10

1b phase	VIII	VII	VI	V	IV	III	II	I	I′	93Gis
	crys-talline solid	smectic I^*_A (Sm I^*_A)	smectic C^*_A (Sm C^*_A)	smectic $C^*_{\gamma 1}$ (Sm $C^*_{\gamma 1}$)	smectic $C^*_{\gamma 2}$ (Sm $C^*_{\gamma 2}$)	smectic C^*_β (Sm C^*_β)	smectic C^*_α (Sm C^*_α)	smectic A (Sm A)	iso-tropic liquid	
state			A	(F′)	(F′)	F	(A)	P		
Θ[°C] n = 8	67.6	71.6	95.1	96	97	104	105.5	135.5		
10	58.2		94.6		96.1		111.2	128.6		

5a Dielectric constant: Fig. 71B-8-001, Fig. 71B-8-002, Fig. 71B-8-003.
Dielectric relaxation frequency: Fig. 71B-8-004.

9a Electrooptic effect: Fig. 71B-8-005.

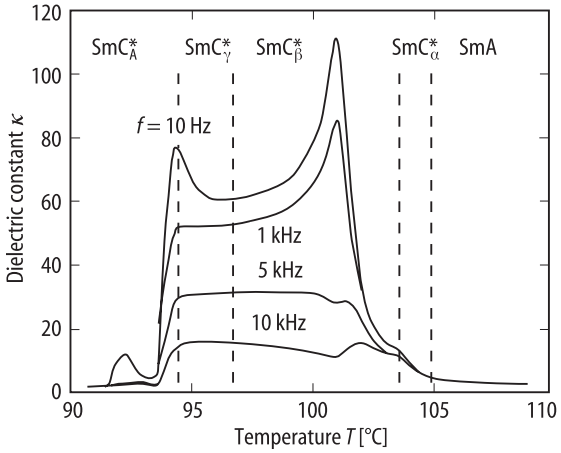

Fig. 71B-8-001. Tolan C8. κ vs. T [93Gis]. Parameter: f. Sample thickness: 23 µm. Cooling (0.5 K min^{-1}).

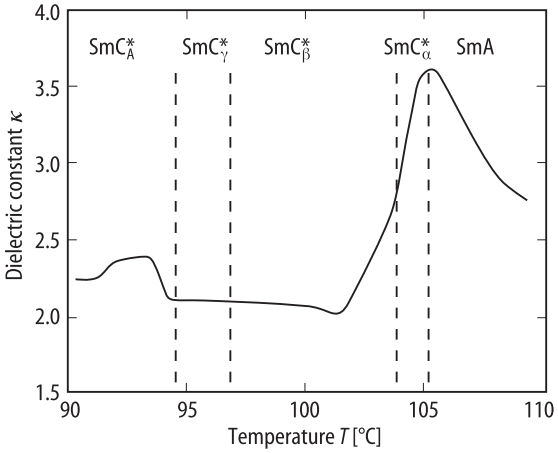

Fig. 71B-8-002. Tolan C8. κ vs. T [93Gis]. f = 100 kHz. Sample thickness: 23 µm. Cooling (0.5 K min^{-1}).

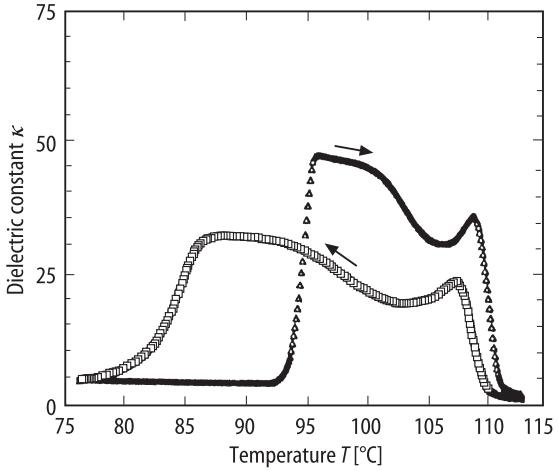

Fig. 71B-8-003. Tolan C10. κ vs. T [93Gis]. f = 10 Hz. Sample thickness: 5 µm. Open square: cooling (0.5 K min^{-1}); open triangle: heating (0.5 K min^{-1}).

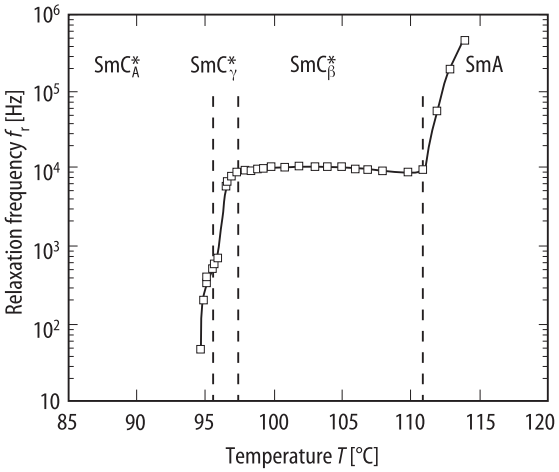

Fig. 71B-8-004. Tolan C10. f_r vs. T [93Gis]. f_r: dielectric relaxation frequency. Sample thickness: 23 μm.

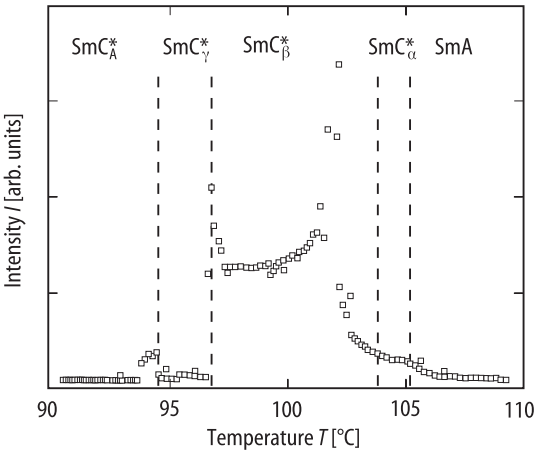

Fig. 71B-8-005. Tolan C8. I vs. T [93Gis]. I: intensity of electrooptic response. f = 10 Hz. Sample thickness: 23 μm. Cooling (0.5 K min^{-1}).

Reference

93Gis Gisse, P., Pavel, J., Nguyen, H.T., Lorman, V.L.: Ferroelectrics **147** (1993) 27.

No. 71B-9 MHTAC

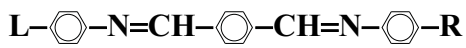

L: $H_{13}C_6CH(CH_3)OCOCH=CH$, R: $CH=CHCOOCH(CH_3)C_6H_{13}$
MHTAC (1-methylheptyl-terephthalidene-bis-aminocinnamate)

1b	phase	III	II	I	I′	93Tak
		crystalline solid	smectic O* (Sm O*)	smectic Q (Sm Q)	isotropic liquid	
	state		(A)	P		
	Θ [°C]	95	130	133		
3b	Tilt angle: Fig. 71B-9-001.					

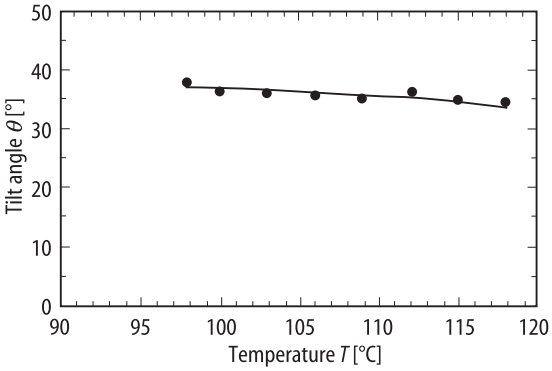

Fig. 71B-9-001. MHTAC. θ vs. T [93Tak]. θ: tilt angle.

Reference

93Tak Takanishi, Y., Takezoe, H., Johno, M., Yui, T., Fukuda, A.: Jpn. J. Appl. Phys. **22** (1993) 4605.